

ABSTRACT

THE SURFACE HEAT BUDGET OF HUDSON BAY

by

ERIC W. DANIELSON, JR.

Meteorology Dept.      M.Sc.

SUMMARY

Monthly mean solar, long wave and turbulent energy fluxes across the Hudson Bay surface are derived, and presented in map form.

After a review of previous studies of Hudson Bay geophysics, and discussion of the heat budget formulae applicable to the problem, monthly mean hydrometeorological data are given, upon which information the heat budget calculations are based. These data include surface air and sea temperatures, ice concentration, cloudiness, wind, atmospheric moisture, ice and water movement figures, and heat storage amounts within Hudson Bay waters.

The calculated heat budget fluxes appear to be consistent with hydrometeorological information such as atmospheric stability, seasonal changes in ice concentration, etc. The computed annual budget is found to balance to within limits of the estimated error.

Title and author, for binding:

THE HEAT BUDGET OF HUDSON BAY  
(title)

DANIELSON  
(author)

THE SURFACE HEAT BUDGET

OF

HUDSON BAY

BY

ERIC W. DANIELSON, JR.

A thesis submitted to the Faculty of Graduate Studies  
and Research in partial fulfillment of the requirements  
for the degree of Master of Science.

Department of Meteorology  
McGill University  
Montréal

February, 1969

TABLE OF CONTENTS

	Page
Abstract . . . . .	vi
Acknowledgements . . . . .	vii
List of Figures . . . . .	viii
List of Tables . . . . .	x
Frontispiece: Place Names . . . . .	xii
CHAPTER I INTRODUCTION	
1.1 The Heat Budget Equation . . . . .	2
1.2 Exploration and Investigation of Hudson Bay Geophysics: an Abstract . . . . .	3
1.3 Statement of the Problem . . . . .	7
CHAPTER II METHODS	
2.1 Time Scales, and the Problem of Variance . . . . .	8
2.2 Computation of Solar Radiation Flux . . . . .	11
2.2.1 Method . . . . .	11
2.2.2 Errors in Solar Radiation Calculations . . . . .	18
2.3 Long Wave Surface and Atmospheric Radiation . . . . .	22
2.3.1 Methods . . . . .	22
2.3.2 Errors in Long Wave Radiation Calculations . . . . .	24
2.4 Turbulent Heat Fluxes: Evaporation and Sensible Heat	27
2.4.1 Discussion and Methods . . . . .	27
2.4.2 Errors in Turbulent Heat Flux Computations . . . . .	29

TABLE OF CONTENTS (cont'd)

	Page
2.5 Heat Storage and Advection . . . . .	33
2.6 Data Requirements . . . . .	37
 CHAPTER III GEOGRAPHICAL AND OCEANOGRAPHIC DATA	
3.1 Boundaries . . . . .	38
3.2 Geographical Setting . . . . .	38
3.3 Local Physiography . . . . .	41
3.4 Circulation and Currents: The Water Budget . . . . .	44
3.5 Vertical Distributions of Temperature and Salinity . . . . .	48
3.6 Sea Surface Temperatures . . . . .	50
3.7 Summer Heat Storage in Hudson Bay Waters . . . . .	53
3.8 Heat Content of Precipitation . . . . .	54
3.9 Runoff . . . . .	55
3.10 Heat Transport by Currents . . . . .	57
 CHAPTER IV ICE CONDITIONS	
4.1 Previous Work . . . . .	60
4.2 Discussion of Existing Data . . . . .	61
4.3 Reduction of Data . . . . .	65
4.4 Presentation of Data . . . . .	66
4.5 Reliability . . . . .	69
4.6 Error Summary for Ice Cover Charts . . . . .	71
4.7 Winter Ice Conditions . . . . .	72

TABLE OF CONTENTS (cont'd)

	Page
4.8	May and June Ice Conditions . . . . . 76
4.9	Break-Up East and West . . . . . 78
4.10	July . . . . . 80
4.11	Influence of Ice on Currents . . . . . 83
4.12	Change-of-Concentration Maps . . . . . 85
4.13	August . . . . . 87
4.14	The Northeast . . . . . 88
4.15	Roes Welcome Sound . . . . . 93
4.16	September, October, November and December . . . . . 93
4.17	Summary of Ice Cover Information . . . . . 95
4.18	The Heat Content of Hudson Bay Ice . . . . . 97
4.19	Ice Export by Currents . . . . . 98
4.20	Ice Import by Currents . . . . . 99
 CHAPTER V METEOROLOGICAL CONDITIONS	
5.1	Introduction . . . . . 102
5.2	Surface Air Temperature . . . . . 104
5.3	Vapour Pressure . . . . . 111
5.4	Surface Wind . . . . . 115
5.5	Temperature and Humidity Aloft . . . . . 120
5.6	Cloudiness . . . . . 121

TABLE OF CONTENTS (cont'd)

	Page
CHAPTER VI THE ENERGY BUDGET	
6.1 Introduction . . . . .	. 136
6.2 Monthly Mean Solar Radiation . . . . .	. 137
6.3 Monthly Mean Long Wave Radiation . . . . .	. 141
6.4 Monthly Mean Radiation Balance . . . . .	. 146
6.5 Monthly Mean Turbulent Heat Fluxes . . . . .	. 150
6.6 Monthly Mean Surface Heat Budget . . . . .	. 155
6.7 Areal Averages of Heat Budget Fluxes . . . . .	. 163
6.8 Comparison of Results With Those of Other Authors . . . . .	. 171
6.9 Summary of Results . . . . .	. 182
 CHAPTER VII CONCLUSION . . . . .	 . 186
 BIBLIOGRAPHY . . . . .	 . 188

## ABSTRACT

Monthly mean solar, long wave, and turbulent energy fluxes across the Hudson Bay surface are derived, and presented in map form.

After a review of previous studies of Hudson Bay geophysics, and discussion of the heat budget formulae applicable to the problem, monthly mean hydrometeorological data are presented, upon which information the heat budget calculations are based. These data include surface air and sea temperatures, ice concentration, cloudiness, wind, atmospheric moisture, ice and water movement, and heat storage amounts within Hudson Bay waters.

The calculated heat budget fluxes appear to be consistent with hydrometeorological information such as atmospheric stability, seasonal changes in ice concentration, etc. The computed annual budget is found to balance to within the limits of the estimated error.

## ACKNOWLEDGMENTS

The author is indebted to a number of people and agencies for their contributions to the present work.

The National Research Council of Canada and the United States Veterans Administration provided financial support.

Dr. Svenn Orvig, the author's advisor, and Dr. E. Vowinckel were constant sources of help and encouragement during all parts of the research. The author will always regard the stimulating discussions with these men as one of the delights of studying at McGill.

The library at The Arctic Institute of North America was an important resource during the research. The author is grateful to the Institute, and especially to the library staff for their skillful and ready assistance.

Donald P. La Salle, director of the Talcott Mountain Science Center for Student Involvement, generously allowed the author time off from work for completion of the thesis, as well as use of the center's office equipment.

To the typists, Mrs. William Delaney and Miss Christine O'Hara, the author is indebted for their careful work.

The most devoted assistance came from my wife, Esther. For her encouragement and enthusiasm in my work, as well as for the hours she spent in preparing all the figures, all the while raising a family of four, I am inexpressibly grateful.

LIST OF FIGURES

Fig.	Title	Page
3-1	Hudson Bay and Surrounding Large-Scale Physiographical Features . . . . .	39
3-2	Hudson Bay Bathymetry and Local Topography . . . . .	43
3-3	Circulation of Hudson Bay Waters . . . . .	45
3-4	Time Cross Sections of Salinity and Temperature Profiles in Northeastern Hudson Bay . . . . .	49
3-5	Monthly Mean Sea Surface Temperatures, Jul.- Oct. . . . .	51
3-6	Runoff Rates for the Hudson Bay Drainage System . . . . .	56
4-1	Mean Ice Concentrations for January through April . . . . .	73
4-2	Mean Ice Concentrations for May and June . . . . .	77
4-3	Mean Ice Concentrations for July and August . . . . .	81
4-4	Late July Ice Concentrations in Relation to Surface Currents . . . . .	84
4-5	Changes with Time of Ice Concentrations During Break-Up . . . . .	86
4-6	Mean Ice Concentrations in Northeast Regions for September and October . . . . .	89
4-7	Changes with Time of Ice Concentrations in Northeast Regions . . . . .	90
4-8	Position of the Ice Pack Boundary during Freeze-Up . . . . .	94
4-9	Areally Averaged Monthly Mean Ice Concentrations. . . . .	96

LIST OF FIGURES (cont'd)

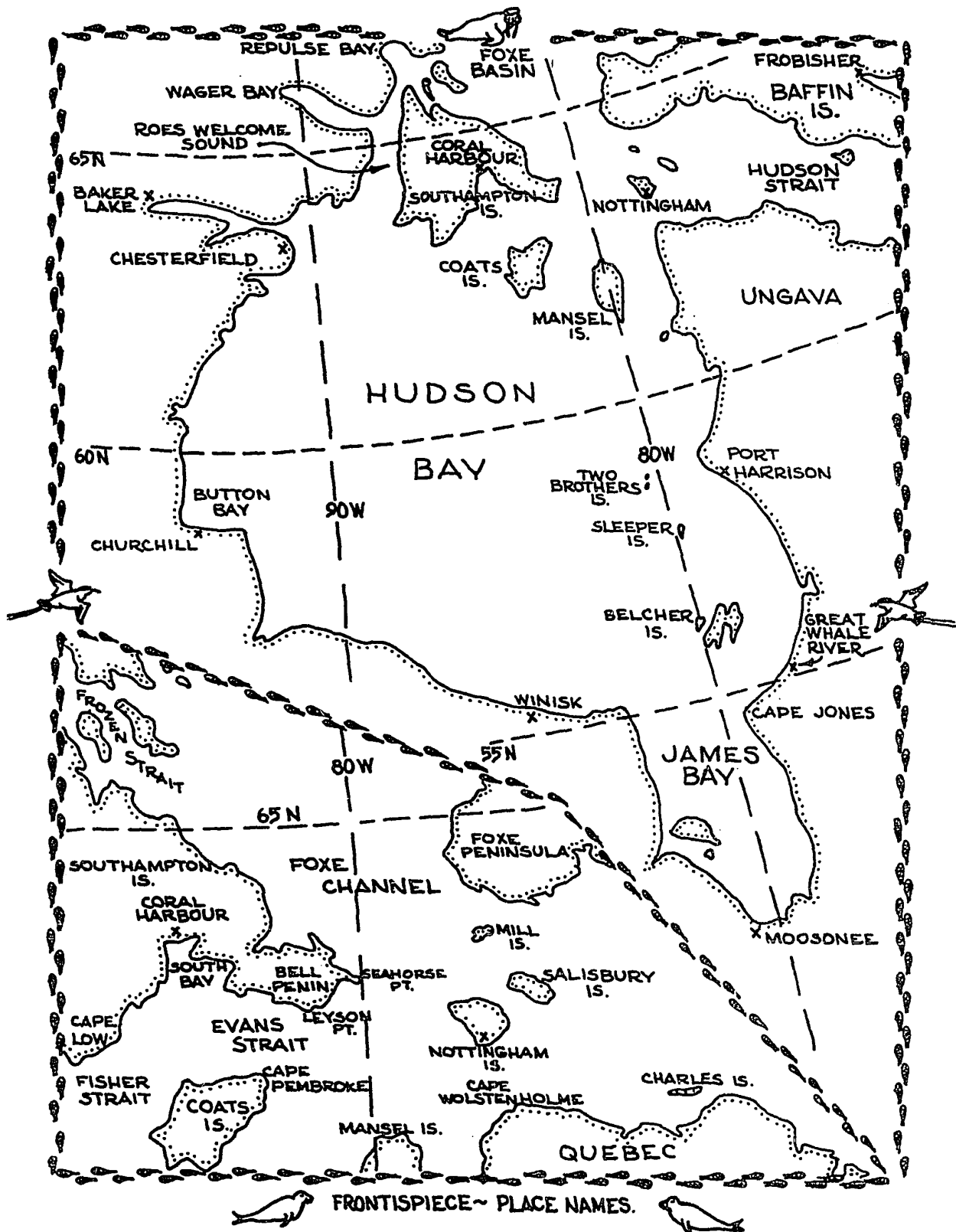
Fig.	Title	Page
5-1	Mean January and July Surface Pressure and 500-mb Contours . . . . .	103
5-2	Monthly Mean Surface Air Temperature . . . . .	.105-107
5-3	Monthly Mean Surface Air Vapour Pressure. . . . .	.113-114
5-4	Monthly Mean Surface Winds: Geostrophic and Observed . . . . .	119
5-5	Monthly Mean Total Cloud Cover . . . . .	.126-128
5-6	Monthly Mean Stratocumulus Cloud Cover: Sep.-Dec. . . . .	129
5-7	Monthly Mean Stratus Cloud Cover . . . . .	.130-132
5-8	Areally Averaged Monthly Mean Cloud Cover . . . . .	134
6-1	Monthly Mean Solar Radiation Absorbed at Surface . . . . .	.138-140
6-2	Monthly Mean Net Long Wave Radiative Flux . . . . .	.142-144
6-3	Monthly Mean Surface Radiation Balance . . . . .	.147-149
6-4	Monthly Mean Evaporative Plus Sensible Heat Fluxes. . . . .	.151-153
6-5	Monthly Mean Surface Heat Budget . . . . .	.156-158
6-6	Annual Mean Heat Budget Components . . . . .	159
6-7	Annual Mean Net Surface Heat Flux . . . . .	162
6-8	Areal Averages of Heat Budget Components (I) . . . . .	164
6-9	Areal Averages of Heat Budget Components (II). . . . .	165
6-10	Areal Mean of Annual Heat Budget Components . . . . .	169

LIST OF TABLES

Table	Title	Page
2-1	Solar Radiation Income with Overcast Cloud Cover, in Percent of Clear Sky Solar Income . . . .	15
2-2	Calculated and Observed Monthly Mean Solar Radiation for Churchill, Man. . . . .	16
2-3	Albedoes for Hudson Bay Surface Conditions . . .	18
2-4	Estimated Errors for Absorbed Solar Radiation . .	22
2-5	Estimated Errors for Upward Long Wave Radiation .	25
2-6	Estimated Errors for Atmospheric Radiation . . .	27
2-7	Estimated Errors for Sensible Heat Flux . . . .	30
2-8	Estimated Errors for Evaporative Heat Flux . . .	33
3-1	Runoff Data . . . . .	56
3-2	Heat Transport by Currents . . . . .	58
4-1	Summary of Monthly and Annual Heat Storage and Advection . . . . .	101
5-1	Monthly Mean Surface Air Temperature by Wind Direction	109
5-2	Monthly Mean Surface Wind Speed over Hudson Bay .	118
5-3	Monthly Mean Low Cloud Coverage at Churchill, Man..	124

LIST OF TABLES (cont'd)

Table	Title	Page
6-1	Computed and Observed Values of Heat Storage plus Advection . . . . .	170
6-2	Comparison of Atmospheric Heat Budget Fluxes of Bryson and Kuhn with Surface Fluxes from Figure 6-9 . . . . .	174
6-3	Evaporative Fluxes Derived from Data of Morrissey compared with Values from Figure 6-9 . . . . .	176
6-4	Monthly Energy Fluxes from Barber compared with Monthly Mean Fluxes from Figures 6-1 to 6-5 . . . . .	180



CHAPTER I  
INTRODUCTION

Hudson Bay is Canada's great inland sea.

For at least two reasons Hudson Bay is worthy of special attention by meteorologists, and geophysicists in general:

(1) From a purely scientific point of view, Hudson Bay is unique. It is the largest body of water in the world to freeze over virtually completely each winter and return to an entirely liquid state each summer. Seasonal air-sea interactions, and variations of surface characteristics and heat storage, would seem to be of special interest.

(2) Due to its central location in Canada and its great size, Hudson Bay's presence and importance are unavoidable. Improved understanding of the physical processes at work there might be helpful to many people, such as Canada's meteorologists who must contend daily with the Bay's air-mass modifying powers, and shippers, who sail the Hudson Bay route to Churchill, Manitoba, when ice conditions permit. At present, Canadians likely think of Hudson Bay as a liability rather than an asset, a great sea which brings the Arctic too far south. By learning more about this sea we may discover ways to realize better its potential as a natural resource.

The present study is an examination of the mean monthly heat fluxes, radiative and turbulent, through the Hudson Bay surface. The interrelation of ice cover and heat fluxes receives special emphasis, since it appears in later chapters that ice cover, itself the result of surface heat losses, is probably the most influential of all hydrometeorological factors affecting Hudson Bay's energy budget.

## 1.1 THE HEAT BUDGET EQUATION

A heat budget, as applied to modern meteorology, is an evaluation of all significant energy fluxes through a given interface or volume. Since energy is neither created nor destroyed, fluxes through a volume must in sum equal zero, or cause a change in the amount of energy stored within the volume. Thus

$$\sum_i F_i = \frac{\partial G}{\partial t} ,$$

where the  $F_i$  are the fluxes and

$\partial G/\partial t$  is the storage change with time.

In a given time  $\Delta t$ ,

$$\sum_i F_i \Delta t = \Delta G , \quad (1-1)$$

where  $\Delta G$  represents the energy change over the period.

The volume considered may be part or all of the atmosphere, ocean, or lithosphere. In the present study it is the water mass of Hudson Bay\*, and a change in storage energy  $\Delta G$  may be a change in water temperature or a change in state (water to ice).

---

\*The unit of volume used in the present study is a water column one  $\text{cm}^2$  in horizontal cross section, extending from the surface to the bottom of Hudson Bay. For brevity, heat fluxes and storage in this unit volume generally will be given "per  $\text{cm}^2$  of surface", the vertical dimension being assumed.

The nature of the flux terms  $F_i$  depends upon the volume under study. For Hudson Bay, the important fluxes are those of absorbed solar radiation (SA), long wave atmospheric radiation (LD), long wave radiation emitted by the water surface (LU), evaporation (E), "sensible" (convective) heating between air and water (H), and advection by currents and runoff (O). Heat fluxes from the earth's interior, organic energy sources and sinks, etc., are assumed to be insignificant by comparison. Equation (1-1) may then be written

$$(SA + LD + LU) + (E + H) = \Delta G - O, \quad (1-2)$$

where now all radiative terms appear in the first brackets, the convective terms in the second brackets, and the hydrographic terms on the right-hand side of the equation.

Equation (1-2) is the energy budget equation in the form used in the present work to study the mean monthly energy fluxes through the Hudson Bay surface.

1.2 EXPLORATION AND INVESTIGATION OF HUDSON BAY GEOPHYSICS:  
AN ABSTRACT

Exploration and scientific investigation of Hudson Bay have had an unusual history. The story of Henry Hudson's voyage in search of a northwest passage is well known. Hudson was totally dedicated to exploration and discovery: so much so that, having already spent one full year in the Bay, including winter on its shore, he fully intended

to remain another year if necessary to finish his investigations. His crew, however, felt no such devotion to duty; in fact the prospect of spending another winter in the Arctic led them to mutiny in June, 1611. Hudson and eight other men were cast adrift in the Bay, never to be seen again.

As a result of this fateful voyage, the world of 1611 knew more of Hudson Bay than about most other parts of Canada. Written reports ( Lambert, 1963 ) and the survivors' verbal descriptions clearly portrayed the bleak terrain and inhospitable weather. Winter spent on the shores of the Bay impressed the men with weather conditions which they could never forget, nor cease to speak of. Thus by early in the 17th century man had learned of Hudson Bay's approximate size, geography, meteorology and ice conditions.

Many arctic regions have remained uninhabited by western man after initial explorations in the 17th or 18th century. In 1670, however, the Hudson Bay Company was chartered in England, and shortly thereafter trading posts appeared along the shores of the Bay. The "factors" at the posts made weather observations, at least casually, and sailors on supply ships doubtless acquired great familiarity with weather and ice conditions on Hudson Bay. Thus, in comparison with other arctic areas, the body of general information about Hudson Bay has had a great many years to grow and become refined. It is curious that, despite its long history under men's eyes, Hudson Bay has given twentieth-century man at least two major surprises. In 1912, R. J. Flaherty showed existing maps of the area to be seriously in error,

by discovering that the "Belcher Islands", depicted on maps as tiny dots west of Great Whale River Post, actually covered thousands of square miles. An even more recent discovery involved ice cover: only since the late 1940's has the nearly complete winter freeze-up of Hudson Bay become a documented, generally accepted fact.

Most scientific study of Hudson Bay, of course, has taken place only in more recent years. Prior to the 1940's, weather reporting stations in north-central Canada were so few in number they could not be considered a "network". Detailed oceanographic exploration began with the Loubyrne expedition of 1930, to which little was added until after World War II. Off-shore ice reports, made by aerial reconnaissance, have become regularly available only in the last ten years. Clearly, the hydrometeorological data are of late appearance. The few existing large-scale studies of Hudson Bay are, necessarily, equally recent.

In 1950, Hare was able to derive the first reliable maps of such basic meteorological information as surface air temperature, precipitation, etc. Burbidge (1949), working with Hare, studied modification of air crossing Hudson Bay. Today these works stand as the only comprehensive studies of Hudson Bay meteorology. In spite of the more severe data limitations at the time, both works have aged well and were found to be of great use in the present study. On the other hand, considering the much greater amount of data now available, it seemed advisable to derive new distributions for many of the parameters required for heat budget computations. In addition, no mean ice cover charts for Hudson Bay have been published. Accordingly, considerable effort was devoted to those ends.

Barber (1967) has assembled much of the oceanographic information related to Hudson Bay. His paper was especially useful because it includes data from the recent, extensive oceanographic surveys in 1961 and 1962. However, publications by Hachey (1954), Dunbar (1951, 1958, 1966), Campbell (1958, 1959) and Grainger (1960) all contain important information on Hudson Bay oceanography. These papers formed the basis for much of the oceanographic information of later chapters.

Several authors have investigated aspects of Hudson Bay's heat budget. Barber (1967) computed the surface heat budget for the year 1961, for the sea in the vicinity of Churchill, Manitoba. (His methods and results, along with those of the following studies, will be discussed in Chapter 6). In a micrometeorological experiment on Button Bay near Churchill, Schwerdtfeger (1962) measured radiative fluxes, ice temperature and thickness, and calculated turbulent fluxes (based on measurements) from January to April, 1961. Bryson and Kuhn (1962) computed heat budget components for air parcels passing from one Canadian radiosonde station to another; the trajectory from Churchill to Port Harrison was used for several calculations. Burbidge (1949) also evaluated air mass changes along the Churchill-to-Port Harrison trajectory. Morrissey (1964) calculated mean atmospheric moisture budgets over Hudson Bay for January, April, July and October 1962.

The works mentioned above contain no comprehensive evaluation of mean heat budget terms for the Hudson Bay surface. The present paper is an effort to determine the monthly mean components, and to show their variations with time (season) and location within the Bay.

1.3      STATEMENT OF THE PROBLEM

The problem now may be described as a threefold one:

(1) To gather mean monthly hydrometeorological data in form appropriate for analysis of meteorological and oceanographic conditions on Hudson Bay;

(2) To use these data in calculating the monthly mean energy budget terms of Equation (1-2);

(3) To study temporal and spatial variations of the energy budget terms and their interactions with ice cover.

## CHAPTER 2

### METHODS

Before gathering and analysing data, it was necessary to decide which energy budget formulae and procedures to adopt. Meteorological literature abounds with different formulae for computing each component of Equation (1-2). Equations range from the theoretically founded to the purely empirical, and from limited to perfectly general applicability. Settling on a method appropriate for the problem at hand requires consideration of several factors, including personal preferences. It was the author's desire that the approach be grounded on physical principles, if possible. In particular, this meant rejecting the basically empirical formulae of some investigators (e.g. Russian workers, typified by Budyko, 1956 ), in favor of methods which dealt more directly with physical processes at work. This latter method was the one employed by Vowinckel and Orvig (1964, 1966) in their arctic heat budget studies.

#### 2.1 TIME SCALES, AND THE PROBLEM OF VARIANCE

Having decided against the use of empirical formulae where possible, a problem of averaging immediately appears. Whereas many empirical formulae are designed to handle climatic data, most procedures based on physical processes apply to short-period measurements of the variables (wind, temperature, etc.), and yield short-period fluxes. ("Short-period" here refers to times of a few hours or less). Most of the functional relationships involve several variables, in non-linear form. Therefore climatic data applied to short-period formulae will not

necessarily give mean fluxes, due to variance and covariance effects.

Thus if  $Q$  is some heat budget term, related to meteorological parameters  $x$ ,  $y$ , and  $z$  by

$$Q = f(x, y, z),$$

then in general

$$\bar{Q} = \overline{f(x, y, z)} \neq f(\bar{x}, \bar{y}, \bar{z}),$$

where bars indicate means.

These considerations indicate that the proper way to compute  $\bar{Q}$  is to compute  $\overline{f(x, y, z)}$ , that is to evaluate  $Q$  for each set of raw meteorological data (e.g. each set of hourly observations), then take the average of the hourly  $Q$ 's to obtain  $\bar{Q}$ .

Unfortunately, it is impossible to follow such a procedure in the present work. The labor involved in determining hourly values of all basic variables at 77 grid-points, for ten or twenty years of data, and in performing the subsequent  $Q$  computations, would be excessive. Furthermore, observations from Hudson Bay itself are rare, mostly confined to the shipping season (July-September), so that hourly charts of surface air temperature, etc., would have to be constructed largely from climatological means derived from all available data for that time of year.

It is doubtful whether hour-by-hour grid point values of temperature, for instance, would be much more than frequent repetitions of monthly mean values. Thus the realities of data coverage and data

volume rule out direct calculation of  $\overline{f(x,y,z)}$ , making it necessary to approach  $\overline{f(x,y,z)}$  through an  $f(\bar{x},\bar{y},\bar{z})$  approximation.

Between the extremes of hourly observations and monthly mean data, a middle ground exists. Synoptic-scale circulation patterns, or air mass types, provide the basis, as follows.

Local air mass properties by definition are supposed to show little variation from local mean values for each air mass. Instead of computing  $f(\bar{x},\bar{y},\bar{z})$  from grand means of  $x$ ,  $y$  and  $z$ , the quantities  $f_1(\bar{x}_1,\bar{y}_1,\bar{z}_1)$ ,  $f_2(\bar{x}_2,\bar{y}_2,\bar{z}_2)$ , . . . .  $f_n(\bar{x}_n,\bar{y}_n,\bar{z}_n)$  may be computed for  $n$  homogeneous sub-populations (air masses). An average of the  $f_i$  weighted according to the frequency of occurrence of each gives the mean heat flux  $\bar{Q}$ .

The approach through air mass characteristics is especially appealing because it allows analysis of the variations from mean heat budget fluxes (see Gagnon, 1964). Furthermore, the investigator may feel confident that he is combining values for meteorological parameters in the heat budget equations which actually occur simultaneously in nature. Such is not always the case when grand means are used.

The feasibility of computing mean heat budget values by resolving observations into air mass or circulation types was investigated by making a tabulation of circulation type frequencies over Hudson Bay. In a preliminary study, eight different synoptic-scale circulation types were found to occur over Hudson Bay with significant regularity. Ten years of daily weather maps from the U. S. Weather Bureau (1958-67) and the Deutscher Wetterdienst (1958-67) were then

studied, and each of four points on Hudson Bay was assigned a circulation type for each day, if possible.

The results were not encouraging. Unless every day is classified in one type or another, it is impossible to arrive at a mean heat budget for all days. As greater effort is made to assign days with nondescript circulation patterns to some type, the variance of temperature, etc., grows. With approximately 20% of days unclassified, already each circulation type had grown to comprise a variety of weather conditions. To keep circulation types more sharply defined would have required a sharp increase in the number of unclassified days.

Due to similar problems, Gagnon (1964, p. 48) stated "It is not possible to calculate monthly means of the energy budget from the known frequency and budget of the weather types" (in his particular study, of the Norwegian Sea). The same appears to be true of Hudson Bay.

For these reasons, it seemed safer to use monthly means, rather than to group days according to circulation type. Discussion of errors arising from variance around mean values (as well as other error sources) will accompany descriptions of computational methods, which follow.

## 2.2 COMPUTATION OF SOLAR RADIATION FLUX

### 2.2.1 METHOD

The method follows that of Houghton(1954), and Vowinckel and Orvig (1964a). Calculations of solar energy received were made for each hour of the day on the 15th day of each month, for each of 77 grid points (the grid points may be seen on the figures in later chapters).

Values thus obtained were assumed to represent mean local conditions for the month.

A mean solar constant of 2.0 langleys (ly) per minute was used. This was corrected by the factor  $(\bar{d}/d)^2$ , where  $\bar{d}$  is the mean earth-sun distance and  $d$  is the distance for the month in question. The factor ranges in value from 1.033 in December and January to 0.971 in June and July.

Unless the sun is in the zenith, solar radiation will be depleted in effect by projection onto the local horizontal. This depletion factor is equal to  $\sin \zeta$ , where  $\zeta$  is the sun's elevation angle above the horizon. Thus SE, the solar energy received on a horizontal surface on earth, in the absence of atmosphere, may be given as

$$SE = 2.0(\bar{d}/d)^2 (\sin \zeta) \quad \text{ly/min} \quad (2-1)$$

$\sin \zeta$  may be evaluated for any time of day, place on earth and time of year by

$$\sin \zeta = (\sin \phi)(\sin \delta) + (\cos \phi)(\cos \delta)(\cos h), \quad (2-2)$$

where  $\phi$  = latitude on earth,  $\delta$  = solar declination, and  $h$  = solar hour angle.

The earth's atmosphere depletes the solar beam in several ways. First, stratospheric ozone absorbs strongly in certain bands. According to Paulin (personal communication), the expression

$$SE' = SE (1 - 0.214 \csc \zeta) \quad (2-3)$$

satisfactorily describes ozone depletion, where SE is the intensity

of the solar beam before and SE' after passage through the ozone. In order that absorption did not reach extreme percentages at low solar elevations, 10% depletion was the maximum permitted.

Dust in the atmosphere both scatters and absorbs solar radiation. Vowinckel and Orvig (1964a, p.358) point out that little is known about arctic dust concentrations, although they must be less than at lower latitudes. Accordingly, they disregarded dust depletion. Mateer (1955) considered dust and haze depletion at Canadian stations, and found it quite small at Churchill for all months except September and October. In view of the uncertainties, it seemed wisest to neglect dust depletion entirely.

Houghton's (1954) curves were used to account for scattering and absorption of sunlight by atmospheric water vapour. From Fritz (1949), moisture content for clear skies was taken at 85% of the mean monthly value, so that the remaining 15% was assumed to be associated with clouds.

Clouds attenuate solar radiation more effectively than any other atmospheric constituent. Vowinckel and Orvig (1962) derived mean monthly solar income values, in percent of clear sky radiation, for various overcast cloud types in the Arctic. These values accounted for the combined effects of reflection, absorption and scattering by clouds, as well as multiple reflection between the earth's surface and cloud base. As they point out, depletion or transmission of solar radiation by a certain cloud type is by no means constant, varying most notably with solar elevation and moisture content (and therefore temperature, since air's capacity for moisture is strongly dependent upon temperature).

Accordingly, their transmission values, derived for 70 to 90 degrees north latitude, could not be applied directly in the present study without adjustment, which was made as follows.

Vowinckel and Orvig's income values for 70 degrees north (70 N) represented conditions along the Arctic Ocean coast, a region geographically similar to Hudson Bay. It was noticed that mean solar elevations and temperatures aloft for February at 70 N were close to January values for Hudson Bay; likewise March at 70 N corresponded to February over Hudson Bay; April to March; May to April; June to May; July at 70 N to August over Hudson Bay; August to September; September to October; October at 70 N to November and December over Hudson Bay. Therefore income percentages for Hudson Bay clouds were taken as those for the analogous months at 70 N. For June and July at Hudson Bay, no analogous conditions existed at 70 N; however, all cloud types showed a monotonic decrease in income values through the summer months at 70 N; thus linear interpolation was used between Hudson Bay values for May and August, giving the June and July figures. As no distinction was made between tabulations of altostratus and altocumulus frequencies in the present study, Vowinckel and Orvig's figures for these two types were averaged. The following table gives the monthly mean transmission values for each cloud type (Stratus (St), Strato-cumulus (Sc), Middle Clouds Altostratus (As) and Altocumulus (Ac), and Cirrus (Ci)).

TABLE 2-1

SOLAR RADIATION INCOME WITH OVERCAST CLOUD COVER,  
IN PER CENT OF CLEAR SKY SOLAR INCOME

	J	F	M	A	M	J	J	A	S	O	N	D
St	38	50	55	56	53	51	51	49	45	40	36	36
Sc	52	56	63	63	57	55	55	53	50	46	45	45
Ac, As	67	71	78	75	67	66	66	65	63	60	59	59
Ci	79	81	92	94	90	89	88	87	84	80	78	78

Solar radiation under cloudy skies (S) was then calculated from the expression

(2-4)

$$S = S_0 \left\{ \left[ (K_{st} \cdot t_{st}) + (K_{sc} \cdot t_{sc}) + (K_{mid} \cdot t_{mid}) + (K_{ci} \cdot t_{ci}) \right] + \left( 1 - \sum_{i=1}^4 K_i \right) \right\},$$

where  $S_0$  is clear sky income, the  $K_s$  are monthly mean coverages of cloud type, and the  $t_s$  are the transmission factors from Table 2-1.

In this manner the mean solar radiation income under conditions of normal cloudiness was obtained. At this point it was necessary to decide whether or not to adjust the calculations to correspond more closely to observed insolation values.

The December, 1967, Monthly Radiation Summary gives mean solar radiation received at Churchill, Manitoba, over an eleven-year period. In Table 2-2, p. 16, these values are compared with those calculated for Churchill following the procedure outlined above.

TABLE 2-2

CALCULATED AND OBSERVED MONTHLY MEAN SOLAR RADIATION (S)  
FOR CHURCHILL, MANITOBA

	J	F	M	A	M	J	J	A	S	O	N	D
Calculated S (ly/day)	51	139	286	448	494	552	539	413	255	121	55	32
Observed S (ly/day)	61	147	305	458	524	538	511	385	221	109	60	35
Std. Dev. of Mo. Obs.	7	12	18	37	35	39	35	48	24	13	8	6
Per Cent Calc. of Observed	84	95	94	98	94	103	105	107	115	111	92	91
Calc. within 1 std. dev.?	No	Yes	No	Yes	Yes	Yes	Yes	Yes	No	Yes	Yes	Yes

It was gratifying to see the generally close correspondence between calculated and observed values. In only three months did the difference between calculated and observed values exceed one standard deviation from the observed monthly mean. On the other hand, deviations of calculated from observed values are obviously non-random in their annual course, with calculated energy too low in winter, too high in summer. Systematic errors almost surely are the cause.

Computationally, the winter errors are of only minor significance, as total income is low and only a small amount of that is actually absorbed. However, computed values for July through October are consistently higher than observed, exceeding one standard deviation from the observed mean in September.

Many factors combine to give the differences between calculated and observed incomes; they will be discussed in detail in the following

section. The normal method of correcting calculated values to observed ones would be to multiply all monthly incomes over Hudson Bay by the ratio (obs./calc.) for that month. The procedure rests on the assumption that the deviation at Churchill is one which applies systematically to income values over all parts of the Bay (as a first approximation), although the physical cause of the deviation is undetermined.

Although this technique doubtless gives a slight improvement to the accuracy of the calculations, it does so only at a price: a step away from physical principles, toward empiricism. Once the step has been taken, it is no longer possible to consider the effects of inaccuracies in this datum or that method, although surely the calculations still fall short of perfection. All errors, involving observation, technique, and theory, have been combined in unknown proportions into a single factor.

Recognizing that solar income calculations thus corrected still would not be error-free, and feeling that the errors implied by Table 2-2 are not unacceptably large, it was decided to use computed radiation values without correction, thereby retaining the essence of the method.

The final step in calculation of the solar energy flux was multiplication of the incoming solar flux  $S$  by an appropriate surface solar absorption factor. If the albedo is designated as  $a$ , then solar energy absorbed,  $SA$ , is given by

$$SA = S(1-a). \quad (2-5)$$

Albedo varies widely with surface characteristics and solar elevation. For snow, Robinson (1966) quotes albedoes from 45% to 95%; for water, 2% with the sun near zenith rising to 60% with low sun. For the present study, 80% was taken for winter snow-covered pack ice. This value agrees with Larsson and Orvig's (1962) values for the same condition. Following Robinson, and Munn (1966), albedo of open water at Hudson Bay latitudes was taken to be 10%, and ice cover in an advanced state of decay (July and August), 40%. May and June ice albedoes were interpolated from April and July values. Results are summarized in Table 2-3.

TABLE 2-3

ALBEDOES (%) FOR HUDSON BAY SURFACE CONDITIONS

Month	J	F	M	A	M	J	J	A	S	O	N	D
Open Water	10	10	10	10	10	10	10	10	10	10	10	10
Ice/Snow	80	80	80	80	65	50	40	40	-	80	80	80
Ice/snow for James Bay, if diff. from Line 2.						55	45					

2.2.2 ERRORS IN SOLAR RADIATION CALCULATIONS

The above procedure contains many uncertainties and errors. The solar "constant" is known to vary in time (Sellers, 1965, p. 11), and the mean value of 2.0 ly/min. may be in error by 2-3%. This would cause solar energy received at the surface to be in error by about the same percentage.

The maximum allowed ozone depletion of 10% may well be incorrect, but the effect is of little importance due to the small amount of energy received at low solar elevations. Changing the cutoff figure to 5% would increase the amount of solar energy absorbed at the surface in January by 0.5 ly/day, in July by 1.9 ly/day. This is probably within the accuracy of the formula itself, and insignificant compared to other errors.

Using hourly solar elevations on the 15th day of each month to represent conditions for the whole month is of course only an approximation. As a test, calculations were made at 59 N seven times in each month, on dates whose mean fell at mid-month (e.g. on the 1st, 6th, 11th, 16th, 21st, 26th and 31st of the month). The resultant changes in absorbed radiation ranged from +1 ly/day in January to -3 ly/day in August; thus the mid-month approximation seems justified. Approximating each hour's mean solar elevation by the value at the half hour was computational convenience; a series of comparisons with mean values of  $\sin \zeta$  integrated over the hour indicated an error of less than 0.3%, which is less than 1.5 ly per day for conditions in Hudson Bay.

Omission of dust depletion causes an over-estimate of solar income in the snow free months. As an upper-limit estimate for this error, the traditional mid-latitude depletion factor of  $0.95^m$ , where  $m$  = air mass (Houghton, 1954), was used. The correction amounts to the following changes in energy absorbed:

MONTH	JUNE	JULY	AUGUST	SEPT.	OCT.
LY/DAY	- 24	- 30	- 35	- 29	- 15

Clearly if dust depletion over Hudson Bay is as important as in mid-latitudes, the errors due to its omission are significant.

Houghton's scattering and absorption curves have been used successfully in many situations. There is no reason to doubt their general validity. They are probably accurate to within 15 ly/day of absorbed radiation in June and July, and more accurate in other months.

Fritz's (1949) reduction factor of 15% for mean moisture content to describe cloudless conditions may be too small for Hudson Bay latitudes. As Vowinckel and Orvig (1964 a, p.360) point out, cloudless days are less frequent in the Arctic than in the U.S.A., where the figure of 15% was derived; therefore moisture on cloudless days may be less than 85% of the mean monthly value. Furthermore, the mean monthly moisture figures cannot be expected to be exact, although they should be within 15% of the actual figures. An error of 15% in cloudless sky water content would alter absorbed solar radiation by about 3%; thus  $\pm 12$  ly/day in July, as a maximum.

Energy depletion by cloudiness introduces several sources of error. Both the cloud transmissivities modified from Vowinckel and Orvig and mean monthly amounts of each cloud type doubtless contain significant errors. The resultant total depletions by clouds may therefore be in error by  $\pm 15\%$  of their mean values. This would result in the following errors in mean monthly absorbed solar energy:

MONTH	J	F	M	A	M	J	J	A	S	O	N	D
LY/DAY	1	4	8	12	22	27	49	36	21	9	4	2
(+)												

These possible errors, like those for dust depletion, are of definite significance during the warmer months.

Albedo uncertainties constitute a final important source of error for absorbed solar radiation. The values extracted from Robinson, Munn, and Larsson and Orvig seemed to lie in the middle of the range of albedoes which may be found in the literature for each condition (ice, snow, slush, water). Likely errors range from  $\pm 0.04$  for September's open water, to  $\pm 0.1$  in the transition months of May, June, and November, and  $\pm 0.2$  for December. The associated energy uncertainties are:

MONTH	J	F	M	A	M	J	J	A	S	O	N	D
LY/DAY	1	2	4	8	21	34	39	21	9	5	4	3
(+)												

Variance and co-variance of moisture content, cloud type and amount, and solar elevation also give rise to errors. Solar radiation income varies slowly with water vapour content, making mean moisture content a satisfactory estimator of the varying conditions. Most weather reporting stations show a distinct correlation of cloud amount and solar elevation (time of day), a result of surface heating causing instability cloud formation. However, over large water bodies the diurnal sea surface temperature variation is very small, certainly less than 1 C (Sverdrup, Johnson and Fleming, 1942. p. 133); with the mechanism for diurnal instability variations removed, it appears unlikely that diurnal cloud variation over Hudson Bay is large. Variance and covariance errors related to mean solar income were

therefore assumed to be of secondary importance to those arising from dust depletion, and cloudiness and albedo calculations.

Employing traditional error propagation methods, the square root of the sum of the squares of the errors for dust, cloudiness and albedo uncertainties gives the following rough probable error estimates for absorbed solar radiation:

TABLE 2-4

ESTIMATED ERRORS FOR ABSORBED SOLAR RADIATION (LY/DAY)

MONTH	J	F	M	A	M	J	J	A	S	O	N	D
ERROR	±1	±5	±9	±14	±30	+50 to <sub>43</sub>	+70 to <sub>63</sub>	+54 to <sub>42</sub>	+37 to <sub>23</sub>	+18 to <sub>10</sub>	±6	±4
% OF CALCULATED	±10	±16	±14	±14	±15	+15 to <sub>13</sub>	+17 to <sub>14</sub>	+15 to <sub>12</sub>	+16 to <sub>10</sub>	+17 to <sub>9</sub>	±16	±30

### 2.3 LONG WAVE SURFACE AND ATMOSPHERIC RADIATION

#### 2.3.1 METHODS

Long wave radiation emitted upward from the surface, LU, may be calculated from the Stefan-Boltzmann law for black body radiation:

$$LU = \sigma T_s^4, \quad (2-6)$$

where  $T_s$  is the sea surface temperature (deg. K), and  $\sigma$  is the Boltzmann constant. For LU in ly/day,  $\sigma = 1.171 \times 10^{-7}$  deg.  $K^{-4}$  day $^{-1}$  ly $^+1$ . Equation (2-6) was evaluated for each month at each grid point, using for  $T_s$  the local monthly mean sea surface temperature.

Long wave atmospheric radiation was computed using the Elsasser radiation chart. Optical depth and mean temperature for layers between the surface, 850, 700, 500, and 300 mb were the input data. In the months of April, July, and August, significant variations

in mean low-level temperatures appeared, which would have been obscured by a mean level from the surface to 850 mb; therefore, a 950 mb level was used as well for these months.

Increments of optical depth  $\Delta u_i$  were computed from the expression

$$\Delta u_i = \frac{1000}{g} \left( \frac{\bar{P}_i}{1000} \right) \bar{q}_i \Delta P_i \quad (2-7)$$

Here  $g$  = gravity (c.g.s. units)

$\bar{P}_i$  = mean pressure (in mb) for the layer  $i$

$\Delta P_i$  = layer thickness (mb)

$\bar{q}_i$  = mean specific humidity in the layer  $i$ .

$\Delta u_i$  is then expressed in  $gm/cm^2$ , the mass of absorbing matter (water vapour) per  $cm^2$  column normal to the radiation.

As in the case of solar radiation, clear-sky downward long wave radiation computations were made with 85% of mean moisture. Clouds, accounting for the remaining 15%, were inserted at the following altitudes:

Stratus	1000 mb	500 ft. m.s.l.
Stratocumulus	925 mb	2300 ft. m.s.l.
Middle clouds	700 mb	9500 ft. m.s.l.
Cirrus	400 mb	23000 ft. m.s.l.

All clouds were assumed to radiate at black body rates except for cirrus, for which, following Vowinckel and Orvig (1964b, p.460-1), 50% of black body was taken.

Atmospheric radiation, first for clear skies and then for mean

cloud frequencies, was computed in this manner for each month at each of twenty grid points evenly spaced across Hudson Bay. The number of grid points was reduced for this component in order to diminish the very large amount of computational effort required. The loss of accuracy involved in this reduction is believed to be insignificant; of all heat budget components, atmospheric radiation is probably least affected by local hydrometeorological variations.

### 2.3.2 ERRORS IN LONG WAVE RADIATION CALCULATIONS

Equation (2-6) is designed for use with discrete temperatures, not monthly means. In this case the error in approximating  $\overline{T^4}$  by  $(\bar{T})^4$  may be directly evaluated, as follows.

$$\begin{aligned} \overline{T^4} &= \frac{1}{n} \sum_{i=1}^n (\bar{T} - \Delta T_i)^4 \\ &= \frac{1}{n} \sum_{i=1}^n \left\{ (\bar{T})^4 - 4(\bar{T})^3 \Delta T_i + 6(\bar{T})^2 \Delta T_i^2 - 4\bar{T} \Delta T_i^3 + \Delta T_i^4 \right\} \end{aligned} \quad (2-8)$$

where  $\bar{T}$  = mean temperature of n discrete observations

and  $\Delta T_i$  = the deviation of the i<sup>th</sup> observation from  $\bar{T}$ .

Now the term  $\frac{1}{n} \sum_{i=1}^n -4(\bar{T})^3 \Delta T_i = -\frac{4(\bar{T})^3}{n} \sum_{i=1}^n \Delta T_i = 0$ .

Furthermore,  $\bar{T}$  is more than one order of magnitude larger than  $\Delta T$  for local monthly surface temperatures in Hudson Bay; thus the  $\Delta T_i^3$  and  $\Delta T_i^4$  terms will be small in comparison to the  $\Delta T_i^2$  term. Therefore, (2-8) may be written

$$\overline{T^4} \approx (\bar{T})^4 + \frac{6(\bar{T})^2}{n} \sum_{i=1}^n (\Delta T_i)^2 \quad (2-9)$$

But  $\frac{1}{n} \sum_{i=1}^n \Delta T_i^2$  is just the variance ( $\sigma^2$ ) of a normal distribution; thus

$$\overline{T^4} \approx (\bar{T})^4 + 6 (\bar{T})^2 \sigma^2. \quad (2-10)$$

Sea surface temperature information indicates that  $\sigma^2$  will be less than 100 deg. K<sup>2</sup> at all times in Hudson Bay, from which it follows that

$$\frac{\overline{T^4} - (\bar{T})^4}{\bar{T}^4} \leq \frac{600 (\bar{T})^2}{\bar{T}^4} \leq 1\% \quad (2-11)$$

The maximum percentage error occurs in winter, with small T and large  $\sigma$  over the ice surface. At that time, errors of just over 2 ly/day are possible. In summer,  $\sigma^2$  is much smaller than 100 and T larger than in winter, so that percentage errors from equation (2-11) are approximately 0.2% or 1.4 ly/day. Compared to uncertainties in the surface temperatures themselves, these errors are insignificant.

Probable error for surface temperatures was estimated to be  $\pm 1$  deg. C from January through June and  $\pm 1.5$  deg. C from July through December. Table 2-5 shows the associated errors.

TABLE 2-5

ESTIMATED ERRORS FOR UPWARD LONG WAVE RADIATION

MONTH	J	F	M	A	M	J	J	A	S	O	N	D
LY/DAY	$\pm 7$	$\pm 7$	$\pm 8$	$\pm 9$	$\pm 9$	$\pm 9$	$\pm 15$	$\pm 15$	$\pm 15$	$\pm 15$	$\pm 14$	$\pm 13$
% OF CALCULATED	2	2	2	2	1	1	2	2	2	2	2	2

Rodgers and Walshaw (1966) studied errors resulting from computing mean atmospheric radiation using time-measured temperature and humidity data,

rather than actual soundings. They found, for a wide variety of temperature and humidity profiles, that it made little difference whether means were taken before or after the radiation computations. Under cloudless skies this component appears to be insensitive to variance considerations.

Atmospheric radiation is also rather unaffected by minor changes in moisture content. The 15% uncertainty in moisture content referred to in Section 2.2.2 implies an error of from 4 to 6 ly/day, with higher values in summer. A systematic error of 2 deg. C in mean temperatures aloft will alter local radiation received at the surface by 8 ly/day in winter, and as much as 15 ly/day in summer.

Additional uncertainties are associated with clouds. It is likely (see Vowinckel and Orvig, 1964b, p. 463) that stratus appears with temperatures generally warmer than the monthly mean for its altitude; a temperature error of as much as 3 deg. C is conceivable for this cloud type, in which case radiation received at the ground would be increased by up to 4 ly/day in May, the month with greatest stratus cover. Temperature errors have less effect on radiation from higher clouds; total error due to cloud temperatures is probably less than 10 ly/day for any month.

Cloud amounts present more serious problems. Due to uncertainties in total cloud amounts as well as in partitioning amounts to each cloud type, the radiation from clouds may be in error by up to 20%, or from  $\pm 12$  ly/day in January and February to  $\pm 25$  ly/day in October.

All of the errors associated with atmospheric radiation are

combined in Table 2-6.

TABLE 2-6

ESTIMATED ERRORS FOR ATMOSPHERIC RADIATION (ly/day)												
MONTH	J	F	M	A	M	J	J	A	S	O	N	D
ERROR	±14	14	16	20	26	27	25	28	29	30	28	22
% OF CALCULATED	4	4	4	4	5	4	4	4	5	5	5	5

#### 2.4 TURBULENT HEAT FLUXES: EVAPORATION AND SENSIBLE HEAT

##### 2.4.1 DISCUSSION AND METHODS

A wide variety of formulae for computing turbulent fluxes may be found in the literature. Matheson (1967) provides an excellent review of these formulae. His reasoning and decision to use Malkus' (1962) evaporation formula and the Shuleikin (1957) sensible heat exchange formulae for winter conditions over the Gulf of St. Lawrence apply equally well to Hudson Bay. This procedure, with only slight modifications of the evaporation formula, has been employed in several studies of arctic waters, e.g. those of Walmsley (1966), and Vowinckel and Taylor (1965).

The formulae are as follows:

For evaporation,

$$E = -3.88(1 + 0.07V)(e_s - e_a)V, \quad (2-12)$$

where E = evaporative heat flux in ly/day (negative upward);

V = wind speed in m/s;

$e_s, e_a$  = sea surface and air vapour pressures in mb.

For sensible heat transfer, the expression depends upon the direction of the temperature gradient. If the surface sea temperature  $T_s$  is less than the surface air temperature  $T_a$ , then (for downward fluxes positive)

$$H = -0.432 (T_s - T_a)V \quad (1y/day) \quad (2-13)$$

If  $T_s > T_a$ ,

$$H = -30.24 (T_s - T_a) \quad (1y/day) \quad (2-14)$$

The empirical Shuleikin formulae were derived for arctic ice and water conditions, and reflect the importance of stability on energy transfer. For a given  $|T_s - T_a|$ , an upward flux, aided by buoyancy, is likely to give a much larger energy transfer than a downward flux. Malkus' formula was derived for slightly unstable conditions, and therefore would likely over-estimate a downward evaporative flux (condensation), which must operate without the help of instability. In addition, there may be some doubt as to whether the heat of condensation on a sea surface actually enters the sea or the atmosphere (Dr. E. Vowinckel, personal communication). Thus, in view of the probably small magnitude of downward fluxes, their uncertain predictability by Formula (2-12), and the indeterminate disposition of the associated energy, all downward evaporative fluxes were taken to be zero.

Monthly mean evaporative and sensible heat exchange rates were computed for each month at each grid point, using local mean values of temperature and vapour pressure. As will be explained in Chapter 5, a single wind speed appropriate to all points was used for each month.

#### 2.4.2 ERRORS IN TURBULENT HEAT FLUX COMPUTATIONS

It might be said that the greatest uncertainty in the turbulent flux calculations lies in the very suitability of the formulae for application to Hudson Bay's weather conditions. Very little is known about the conditions under which the Shuleikin formulae were derived, beyond the fact that the surface was mixed ice and water, and the location was arctic. In particular, the range of fluxes for which his formulae are valid is unknown. Malkus' evaporation equation is theoretically sound under slightly unstable conditions typical of the tropics; its applicability to Hudson Bay, where lapse rates often are far from adiabatic, is very questionable. Of course, the generally successful application of these formulae by other arctic workers is some evidence for their validity in these regions. In the following error discussion, the suitability of the formulae for the task at hand is assumed. One must remember, however, that the formulae's possible inapplicability is an additional source of uncertainty, above and beyond the usual data-based error sources.

Variance around mean values is not an important cause of error for sensible heat flux since only one variable (temperature) appears in linear form as a factor in the formula for unstable conditions; furthermore, fluxes under stable conditions are so small that no likely correlation of temperature and wind speed would give significant differences for means taken before or after computation.

Probable errors in air-sea temperature differences give large uncertainties in sensible heat calculations for some months. Maximum

probable errors appear in November, when mid-Bay temperature differences may be incorrect by  $\pm 3$  deg. C, implying an energy uncertainty in that region of  $\pm 91$  ly/day. Generally the uncertainty is less, but even a 1 deg. C error amounts to 30 ly/day.

The estimated error in wind speed is  $\pm 1.5$  m/sec, for average Bay conditions. Locally the error may be higher. Wind speed error has relevance to sensible heat fluxes only in months of downward flux, of course.

Table 2-7 gives sensible heat flux uncertainties, averaged across the Bay.

TABLE 2-7

ESTIMATED ERRORS FOR SENSIBLE HEAT FLUX (ly/day)

MONTH	J	F	M	A	M	J	J	A	S	O	N	D
	+3	+3	+3									
ERROR	$\pm 30$	$\pm 30$	$\pm 30$	$\pm 21$	$\pm 17$	$\pm 5$	$\pm 6$	$\pm 4$	$\pm 24$	$\pm 45$	$\pm 60$	$\pm 45$
% OF CALCULATED	-	-	-	49	77	71	65	90	69	55	63	44

Errors in evaporation calculations arise from three main sources: (1) the method of computing mean vapour pressure from mean relative humidity; (2) covariance of  $V$  and  $e$ ; and (3) errors in the magnitudes of  $(e_s - e_a)$  and  $V$ .

Mean monthly vapour pressure  $\bar{e}$  for stations surrounding Hudson Bay was found from the expression

$$\bar{e} = \bar{r} e_{\text{sat}}(\bar{T}) \quad (2-15)$$

where  $e_{\text{sat}}(\bar{T})$  is saturation vapour pressure at the station's monthly mean air temperature  $\bar{T}$ , and  $\bar{r}$  is monthly mean relative humidity.

Equation (2-15) is not exact. The factor  $(P - e_{\text{sat}})/(P - e)$  (where  $P$  = atmospheric pressure) should be included on the right-hand side of the equation; over Hudson Bay's surface, however, it never differs from unity by more than 0.002. Therefore it may be safely disregarded. Applying mean temperature and relative humidity observations to the expression gives an incorrect value for mean vapour pressure even if covariance of temperature and humidity is zero. This is because saturation vapour pressure increases exponentially with temperature, and a mid-range value (from  $\bar{T}$ ) will underestimate the true mean vapour pressure. Since the short-period (e.g. daily) variations of  $e_a$  are generally larger than those of  $e_s$ , the underestimate will have greater effect on  $e_a$ , and will result in evaporation estimates slightly higher than reality. Greatest errors of this sort appear in October through December, when rather warm, open-water temperatures and large variations from the mean occur. In these months the error may reach 15 ly/day. In other months it will be considerably smaller.

Covariance of  $V$  and  $(e_a - e_s) = \Delta e$  may bias results from equation (2-12) when mean values are used. If  $\Delta e$  and  $V$  are positively correlated, mean values of each will underestimate evaporation. Local  $e_a$  generally varies much more than  $e_s$ , and  $e_a$  is strongly dependent upon surface temperature so that  $\Delta e$  is large when  $T$  is low. Thus it may be said that a positive  $T, V$  correlation (negative  $\Delta e, V$  correlation) will cause Eq.(2-12) to overestimate evaporation.

Land stations generally experience positive  $T, V$  correlations.

Coldest temperatures usually occur under light winds. Linear correlation coefficients,  $cc$ , computed from data listed in Temperature and Wind Frequency Tables for North America and Greenland (1960) showed:

for Chesterfield Inlet in November:  $cc(T,V) = +0.17$

for Port Harrison in November :  $cc(T,V) = +0.22$

for Port Harrison in December :  $cc(T,V) = +0.38$

Over open water, however, the situation may be different.

Without wind to maintain a supply of unmodified air, the air-surface gradients of temperature and vapour pressure would soon decrease. Thus a negative T,V correlation may be more common over water. The problem is one which must be solved by local observation, as local circulation patterns may be important. Thus Kraus and Morrison (1966), Morrissey (1965) and Vowinckel (1965) present conflicting evidence for the sign of  $cc(T,V)$  over open water, largely perhaps because of differing local climatologies in the regions studied. The determination of the actual correlation is of clear significance, since Kraus and Morrison, and Vowinckel show evaporation errors of 15 to 25% (up to 25 ly/day) resulting from T,V correlations. For the error estimate appearing below, uncertainty due to this effect was taken to be  $\pm 25$  ly/day for open water in October through December, less in other months.

Greatest evaporation errors arise from uncertainties in estimating  $\Delta e$  over the Bay. As will be discussed in Chapter 5, humidity information at hand from Hudson Bay is minimal, and a hopefully reasonable extrapolation from land stations is the only method available. Errors resulting from this technique may reach values of  $\pm 1$  mb locally in

November and December, implying a local evaporation error of 50 ly/day.

Table 2-8 gives monthly estimates of evaporation uncertainties caused by all the factors described on the previous pages.

TABLE 2-8

ESTIMATED ERRORS FOR EVAPORATIVE HEAT FLUX (ly/day)

MONTH	J	F	M	A	M	J	J	A	S	O	N	D
ERROR	±3	3	3	15	26	10	10	19	31	42	41	37
% OF CALCULATED	50	60	75	58	69	-	-	73	33	35	40	62

2.5 HEAT STORAGE AND ADVECTION

The residual of radiative and turbulent fluxes must appear as a change in heat stored in Hudson Bay, or must be compensated for by advection. Since the water's heat storage changes are the important quantities, the point of zero heat storage is arbitrary. In this study it was taken to be liquid phase at -1.6 deg C (the freezing temperature of water at Hudson Bay salinities).

Heat storage in the water is given by

$$G_w = dc (T+1.6) \rho, \quad (2-16)$$

where  $G_w$  is the heat storage, in calories, in a column of  $1\text{cm}^2$  cross section;  $d$  is the depth of the column, in cm;  $T$  is the temperature in deg. C;  $c$  is the specific heat of water; and  $\rho$  is the density. For temperatures and salinities typical of Hudson Bay,  $c = 0.945$  (Sverdrup et al., 1942, p.61), and  $\rho \approx 1$  (ibid, p.56ff).

The presence of ice represents a storage deficit, since heat is required to change the phase to liquid. Furthermore, during winter months the ice generally is colder than  $-1.6$  deg. C., and therefore carries an additional storage deficit.

The latent heat of freezing ( $L$ ) is a function of the water's salinity ( $s$ ). A unit cross-section of ice,  $h$  cm thick, of density  $\rho'$ , will have a heat deficit ( $G_f$ ) given by

$$G_f = -\rho' h L(s). \quad (2-17)$$

$G_f$  represents only the heat required to change phase. The heat required to alter the temperature depends on the heat capacity which itself is a function of temperature and salinity. Untersteiner (1964) gives an approximate expression for the heat  $G_t$  (calories/cm<sup>3</sup> of ice) required to change sea ice of salinity  $s'$  (o/oo) from an initial temperature  $T_1$  deg. C. to a final temperature  $T_2$  deg. C.:

$$G_t = 0.9(T_2 - T_1) \left( 0.5 + \frac{4.1s'}{T_1 T_2} \right). \quad (2-18)$$

The total heat deficit in ice ( $G_I$ ), therefore, is

$$G_I = G_f + G_t h. \quad (2-19)$$

Because observations of ice thickness, ice temperature and sub-surface water temperature are non-existent for many parts of Hudson Bay for much of the year, it was not possible to compute directly the storage changes from month to month, or from point to point across the Bay. However, mean annual maximum and minimum heat storage could be

estimated from the data available. Thus it was possible to find the range of heat storage values for the year, giving an important check on the accuracy of the other heat budget components.

Advection consists of four terms. First is water exchange with other oceanic sources. This advective flux ( $O_w$ ) may be given by

$$O_w = -m_o c_o (T_o + 1.6) + m_i c_i (T_i + 1.6), \quad (2-20)$$

where  $m_o$  and  $m_i$  are outflowing and inflowing masses of water,  $c_o$  and  $c_i$  are their specific heats, and  $T_o$  and  $T_i$  are their temperatures.

Runoff of fresh water constitutes a heat gain, since it is always warmer than  $-1.6$  deg. C. Runoff heat ( $O_r$ ) is given by

$$O_r = m_r (T_r + 1.6), \quad (2-21)$$

where  $m_r$  and  $T_r$  are runoff mass and temperature.

A third advective term arises from the import and export of ice by currents. The heat ( $O_i$ ) involved in this process is

$$O_i = m'_o b_o w_o v_o - m'_i b_i w_i v_i. \quad (2-22)$$

Here  $m'_o$  and  $m'_i$  are ice concentrations (from 0.0 to 1.0) in the outgoing and incoming currents,  $b_o$  and  $b_i$  are the heat contents per  $\text{cm}^2$  of ice surface,  $w_o$  and  $w_i$  are the current widths, and  $v_o$  and  $v_i$  are the current speeds. If ice concentrations are high,  $v$  must be reduced in Equation (2-22), as ice will move more slowly than the current.

Finally, precipitation may be regarded as an advective term, bringing heat (positive or negative) by arriving on the surface at

temperatures other than -1.6 deg. C, and by the deposit of snow which requires melting. The heat involved, per unit area of surface, is

$$O_p = (T + 1.6) \cdot (P_s \cdot C_s + P_r \cdot C_r) - 80P_s, \quad (2-23)$$

where  $P_r$  = grams of rain  
 $P_s$  = grams of solid precipitation, which requires 80 calories of energy per gram of water for the phase change,  
 $C_r$  = specific heat of rain (water)  
 $C_s$  = specific heat of snow  
 $T$  = temperature of the precipitation as it strikes the surface.

Of course, snow may not melt in the month during which it falls. In this case it appears in the monthly budget as an unbalanced deficit, and requires no compensatory heat flux until the month of melting.

The sum of all advective terms (O) may be written

$$O = O_w + O_r + O_i + O_p. \quad (2-24)$$

Little is known of current rates within Hudson Bay; thus the advective terms could not be directly evaluated at every grid point. Instead, this term was computed each month for the Bay as a whole.

Errors and uncertainties related to storage and advection will be discussed in the following chapter with the associated data, as data coverage forms by far the greatest source of error.

3.6      DATA REQUIREMENTS

For the calculations outlined on the previous pages, the following hydrometeorological information was needed: surface air temperature, vapour pressure and wind; temperature and atmospheric moisture content aloft, and cloud coverage; sea surface temperature and ice coverage; and oceanographic storage and advection data. The next three chapters are devoted to presenting this material.

## CHAPTER 3

### GEOGRAPHICAL AND OCEANOGRAPHIC DATA

#### 3.1 BOUNDARIES

Hudson Bay is a saltwater sea which forms the major indentation on the boundary of the North American continent. Its areal coverage is approximately one quarter of a million square miles.

Foxe Basin and James Bay are northward and southward extensions of the Hudson Bay basin. However Southampton Island tends to isolate Foxe Basin from Hudson Bay both oceanographically and climatically, whereas James Bay is an obvious limb. Therefore James Bay is, and Foxe Basin is not, included within "Hudson Bay" boundaries. For purposes of this study, Hudson Bay comprises the region outlined in Figure 3-1.

#### 3.2 GEOGRAPHICAL SETTING

Important large-scale geographical aspects of Hudson Bay's situation are illustrated in Figure 3-1. Noteworthy are:

(1) Hudson Bay's continental surroundings. Only in a north-east direction do significant amounts of open water appear nearby.

(2) The Cordillera to the far west, which acts as an effective barrier to air masses from the Pacific Ocean. The mountains not only hinder the movement of maritime air inland, but also greatly modify any air mass which does cross the divide, most notably by removing moisture. Because of the mountains, pure Pacific air masses are more remote from Hudson Bay than the distance alone suggests.

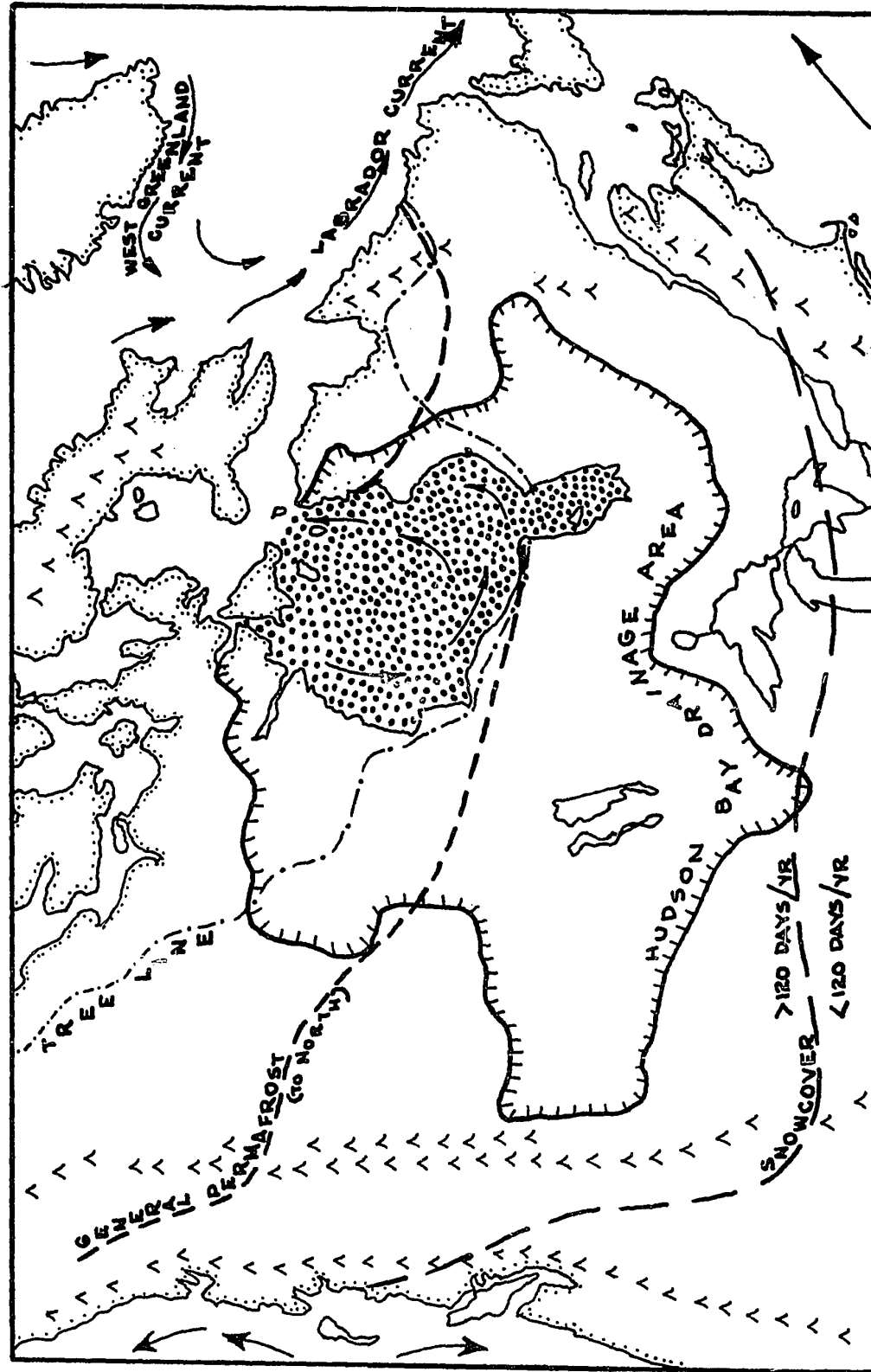


Figure 3-1. Hudson Bay and surrounding large-scale physiographical features.

(3) In contrast to (2), the lack of important relief to the northwest or north. As a result, Hudson Bay lies exposed to arctic air masses from the Archipelago or the Polar Ocean. In fact, airflow from northwest and north is by far the most common over the Bay.

(4) Mountains in Baffin Island, Quebec, Labrador, and the northeastern U.S.A. Although much less imposing than the Rockies, these ranges act as a buffer between Hudson Bay and Atlantic Ocean air masses.

(5) The vast continental plain, comprising the whole interior of the continent, up to the borders of Hudson Bay itself. Relief generally is slight, and air encounters few obstacles to free flow. The surface varies greatly in character. Much of the Canadian plain is moist to the point of swampiness during the warm months, with vegetation ranging from tundra to boreal forest. Southward, in the forest and prairie areas of the U.S.A., the surface is much drier. Superimposed on these rather permanent features is an important seasonally varying property, the snow cover.

(6) The broad-scale pattern of ocean currents. The Gulf Stream, brushing the east coast of the United States with warm water, passes seaward south of the Maritime Provinces. The coast north of the Maritimes lies under the influence of the Labrador Current, a cold and often ice-laden stream. Maritime air reaching Hudson Bay from the eastern U.S.A. will be far warmer than air from the Labrador Sea: warmer than merely the difference in latitude would imply. Ice formation in the northern waters during winter magnifies this effect, since ice cover transforms the water surface to essentially a continental one.

In concert, these large-scale features explain much of Hudson Bay's climatology relative to its surroundings. In winter months (January through April), Hudson Bay's remoteness from regions with different surface characteristics is extreme. Frozen, snow-covered ground (or ice), just like that of the Bay itself, extends far in all directions. The western Cordillera, and the mean downwind location of the Atlantic, accentuate isolation from mild open water surfaces. Winter conditions over Hudson Bay are little different from those generally in north-central North America. In other months, however, surfaces of widely differing nature lie close to Hudson Bay. Arctic ice fields, open water, swamp, tundra, forest and semi-arid plain all are relatively nearby. In non-winter months, therefore, Hudson Bay's presence and influence are much more conspicuous.

### 3.3 LOCAL PHYSIOGRAPHY

The most notable local topographic feature is the flatness of the lands bordering Hudson Bay. The only exceptions are the sheer cliffs at Wolstenholme in the extreme northeast, and the rather sharp relief of the coast from Port Harrison to Cape Jones. These are the only significant local barriers to free air flow. Nearly the entire west and south coasts, from Chesterfield Inlet to Cape Jones, are the epitome of terrestrial flatness. Manning (ca. 1950) says that two or three clusters of sandhills, thirty to fifty feet high, constitute the major relief along the south coast. He estimates the average slope west and south from the coast to be less than two feet per mile.

The relatively short interval since de-glaciation (10,000 years) and the presence of permafrost influence the local terrain. Glaciers scraped away any previous soils, laying bare the Pre-Cambrian shield granites (or Paleozoic rock, along the south coast). Subsequent erosion, and organic growth and decay, have not had time to develop an adequate base for a rich plant community. In addition, glacial action easily disrupted drainage systems in the flat country. Permafrost contributes to drainage problems by prohibiting seepage. As a result, swampiness is a permanent warm-season feature of the Hudson Bay flatlands. From the point of view of available moisture, there is little contrast from "land" to the Bay itself along western and southern shores. Of course the shallow and rather stagnant swamp water responds much more sharply to temperature changes than does Hudson Bay itself, so that earlier freezing and melting, and higher summer surface temperatures, may be expected over "land".

Considering next the bottom topography of Hudson Bay (Figure 3-2), the most striking fact (besides the general shallowness) is that the submarine relief is similar to that of the surrounding land. Western portions are flat, featureless and less deep, whereas the eastern bottom is rugged, with a 300-foot deep channel quite near shore, and many off-shore islands. The islands may be thought of as constituting a loose chain off much of the eastern shore; in the next chapter it will be seen that they seem to influence local ice conditions.

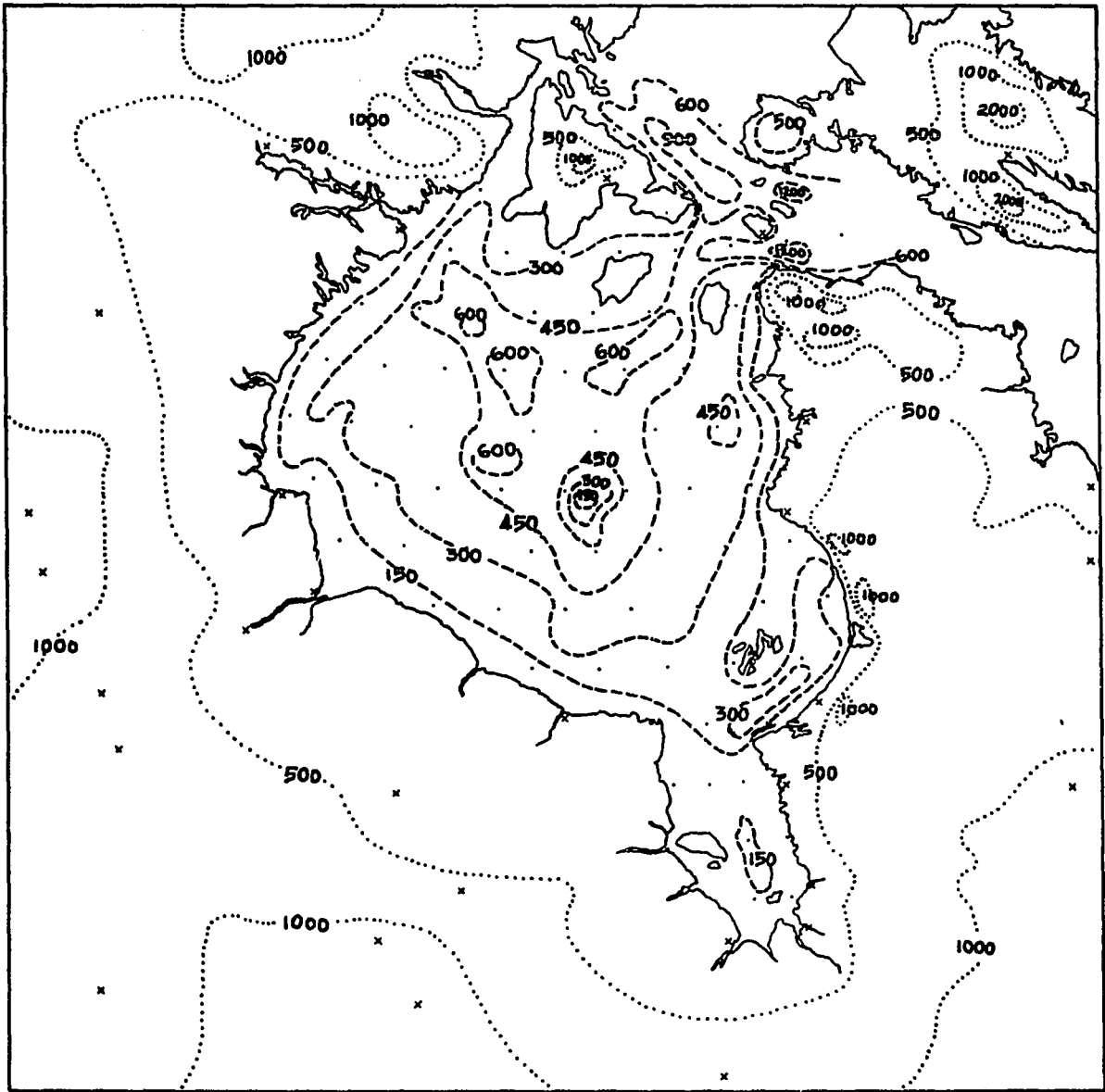


Figure 3-2. Hudson Bay bathymetry and local topography. All data in feet below or above mean sea level.

In the northeastern and north central parts of Hudson Bay is an area of deep waters, over 600 feet, which connects with the still deeper channels of Hudson Strait. There is no "limiting depth", or submarine barrier, to restrict the free flow of water between Bay and Strait. Figure 3-2 shows that a limiting depth of about 600 feet restricts the movement of deep waters between Nottingham Island and Bell Peninsula (Southampton Island). Barber (1967) quotes limiting depths of 160 feet for Roes Welcome Sound, and 180 feet for Fury and Helca Strait. These two figures are important because they imply that water moving into Hudson Bay via these channels must be surface, rather than deep, water. Due to its overall shallowness compared with Hudson Bay, James Bay has no limiting depth as such. Greatest depths, about 300 feet, occur at its mouth.

#### 3.4 CIRCULATION AND CURRENTS: THE WATER BUDGET

Hudson Bay waters circulate in a large-scale version of an estuarine system (Figure 3-3). The driving power is the large volume of fresh water runoff, which enters the Bay through innumerable rivers, rivulets and brooks, and leaves the Bay by way of Hudson Strait, thence to the Atlantic. Coriolis deflects the outflowing waters to the right of the direction of motion, resulting in a counter-clockwise rotation of water in Hudson Bay, and outward flow along the south side of Hudson Strait. Great tidal variations (values approaching 50 feet have been observed in Hudson Strait; at Churchill, the range is up to 17 feet) help to mix the fresh and salt waters, especially in Hudson Strait; but

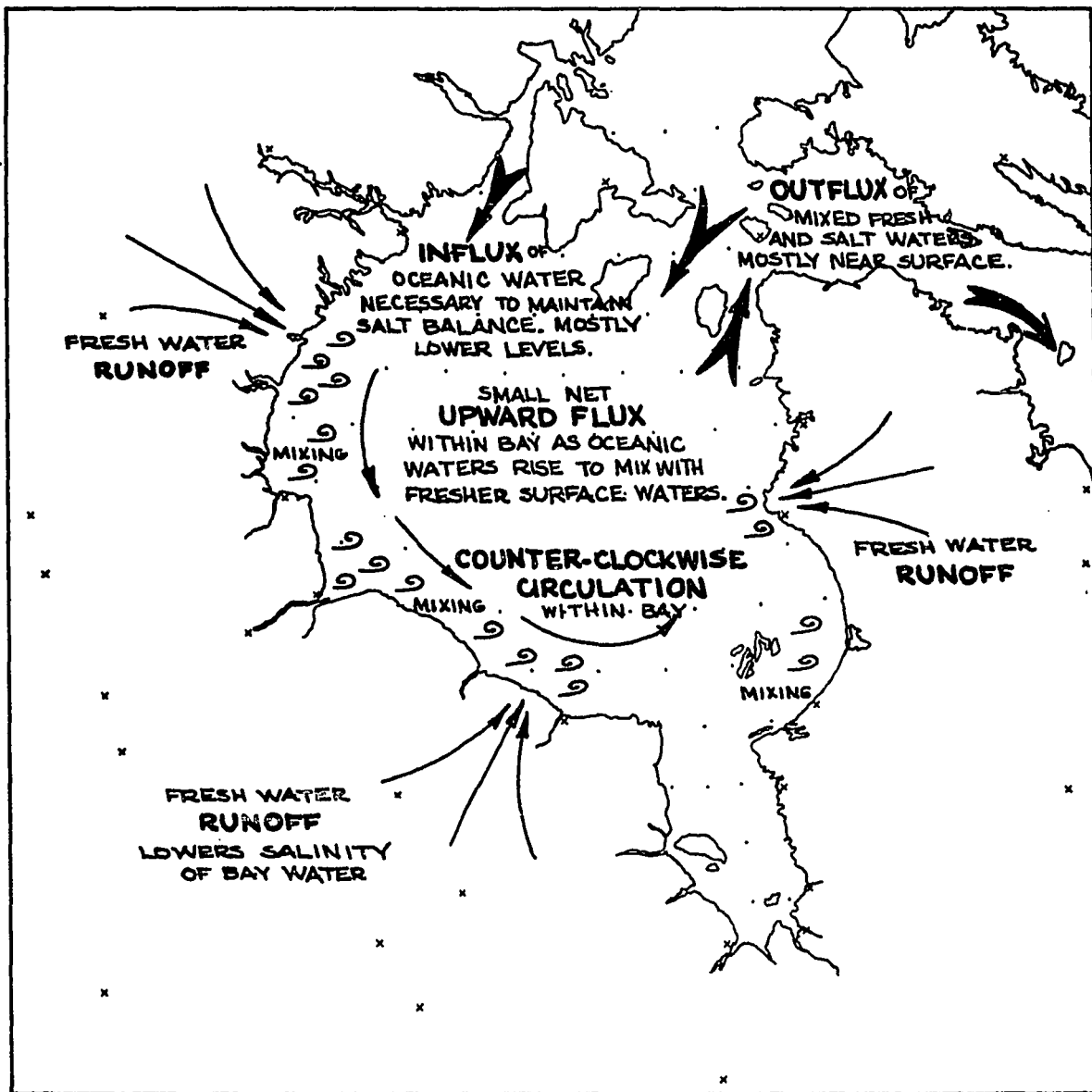


Figure 3-3. Circulation of Hudson Bay waters and elements of estuarine flow.

some stratification remains, as less dense, warm, fresh runoff water overrides the colder saline deep waters of the Bay. Since Hudson Bay receives no salt through runoff, but loses salt in the mixed fresh and saltwater outflow, the Bay must have a source of salt in order to maintain salinity at a constant level. In-flowing oceanic waters provide the salt necessary for balance. Mixing of salt and fresh waters may be assisted by a slight upward flux of the underlying oceanic water, replacing a mostly surface outflux of fresher waters. Barber (1967) shows that a net upward flux as small as  $0.4 \times 10^{-4}$  cm/sec would account for the observed degree of mixing.

The Hudson Bay drainage system (Figure 3-1) covers an area of  $3.92 \times 10^6$  km<sup>2</sup>. Mean annual precipitation over this region (from Atlas of Canada, 1957, map 25) is 18.2 inches, or, in total volume,  $1.81 \times 10^{12}$  m<sup>3</sup>/year ( $5.76 \times 10^4$  m<sup>3</sup>/sec.). This rate represents an upper limit to the mean fresh water runoff from the Hudson Bay system, since evaporation will diminish the volume. The amount of runoff lost to evaporation depends on many factors (rainfall, temperature, wind, ground cover, etc.), so that large-scale evaluations are necessarily rough estimates. Vowinckel (1967) found annual evaporation ranges from nearly 50% of the annual precipitation in the James Bay Basin to over 80% in the Canadian prairies. Cavadias' (1961) evaporation rates for the Hudson Bay drainage system vary from about 40% to 80%, with lowest also for the rainiest southeastern regions. Because the southeast contributes most to runoff due to greater precipitation, and because rain falling onto Hudson Bay

itself suffers no evaporative loss in transit, an evaporation: precipitation ratio of 50% was used for the entire drainage system. The resultant mean annual runoff rate was found to be  $2.88 \times 10^4 \text{ m}^3/\text{sec}$ . ( $0.90 \times 10^{18} \text{ cm}^3/\text{year}$ ).

With this estimate for the volume of fresh water input, the volume of oceanic water entering and mixed water leaving may be determined, if the incoming and outgoing salinities are known. Barber (1967, p. 30) suggests that  $33\text{‰}$  and  $30\text{‰}$  are representative for the purpose. Thus incoming oceanic water is diluted by 10% within Hudson Bay by the fresh-water runoff. The oceanic inflow then must be ten times the fresh water runoff, or  $29 \times 10^4 \text{ m}^3/\text{sec}$ . Total outflow must equal the sum of the fresh and saltwater inflows. Therefore:

$$\begin{array}{rcl}
 \text{Fresh Water Runoff} & = & 2.9 \times 10^4 \text{ m}^3/\text{sec}. \\
 + \text{ Oceanic Inflow} & = & 29 \times 10^4 \text{ m}^3/\text{sec}. \\
 \hline
 \text{Total Outflow} & = & 31.9 \times 10^4 \text{ m}^3/\text{sec}. \\
 & & \text{on an annual average}
 \end{array}$$

Figure 3-3 indicates that outflow occurs past Mansel Island, south of Nottingham Island, and eastward along the south coast of Hudson Strait. Outflow is mostly in the upper levels. Much less certainty exists with respect to the inflowing salt water, however. Although its existence is necessary to achieve salt and water balance, observational evidence is incomplete, perhaps even contradictory. Barber (1967), Dunbar (1966, 1958), Collin (1966) and Campbell (1959) all discuss aspects of the problem. For the present purpose the situation may be summarized by saying that Atlantic and Arctic waters, in undetermined proportions,

enter Hudson Bay through Roes Welcome Sound and, after considerable tidal mixing, between Southampton Island and Quebec.

### 3.5 VERTICAL DISTRIBUTIONS OF TEMPERATURE AND SALINITY

As discussed in the previous section, oceanic inflow offsets dilution by fresh water runoff, allowing salinity to remain constant except for seasonal variations. The annual processes of ice formation greatly affect the distribution of salinity and temperature within the Bay, both vertically and horizontally. As sea water freezes it rejects approximately 90% of the salt (Pounder, 1965, p. 12). By winter's end, the Hudson Bay ice cover typically is about 1.5 m thick (see Section 4.18). Therefore, as melting progresses, surface waters are diluted by nearly 1.5 m of almost salt-free water. The resulting stratification of salinity is hydrostatically stable, since less saline waters are less dense. Summer surface heating adds to the stability. Turbulent mixing of surface and near-surface waters helps to make upper levels uniform, with sharp gradients of temperature (the thermocline) and salinity (the halocline) separating surface and deep waters. As mixing continues the thermocline and halocline are forced to greater depths and weaken in intensity. With autumnal surface cooling, hydrostatic mixing begins, which increases the vertical homogeneity of the waters. Release of salts during freezing further decreases stability so that winter waters are vertically homogeneous.

Figure 3-4, taken from Barber (1967, p.29), illustrates clearly the seasonal variations of salinity and temperature at a point about

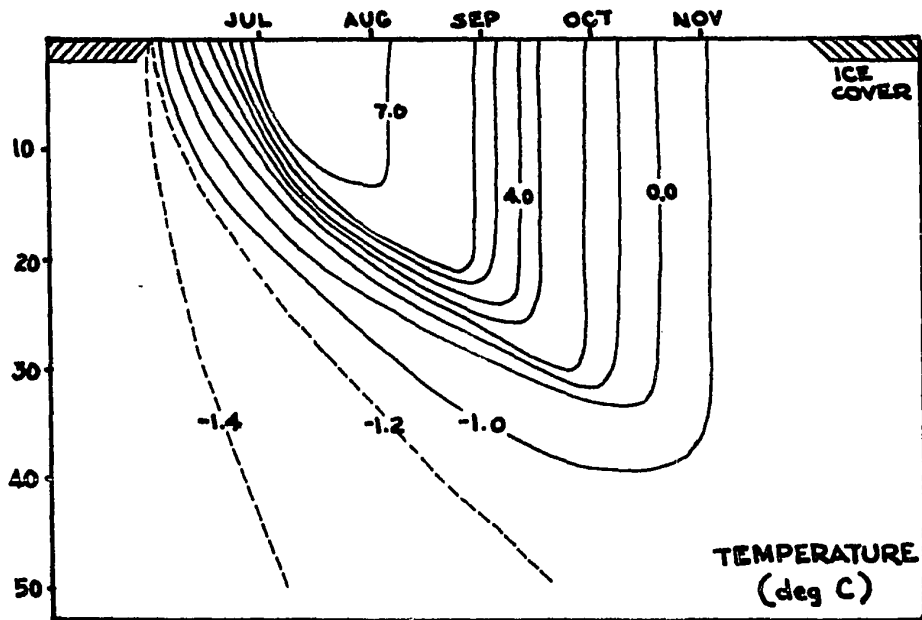
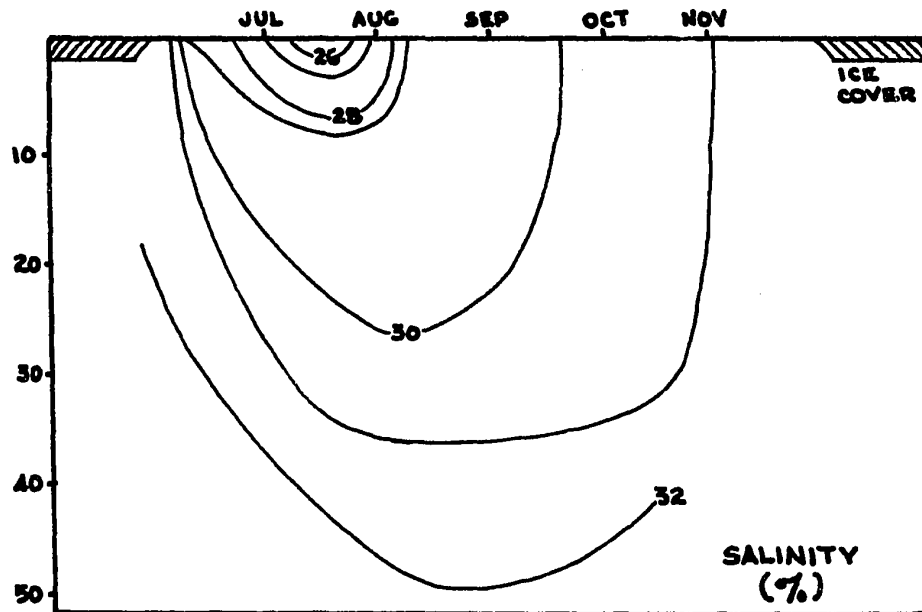


Figure 3-4. Time cross sections of the vertical distributions of salinity and temperature in northeastern Hudson Bay. From Barber, 1967, p.29.

60 miles southwest of Mansel Island. The figure is based on observations in months of July, September and October. The sharp seasonal variations of surface properties in response to ice-cover are evident, as is the thermocline. The halocline is less well-defined.

### 3.6 SEA SURFACE TEMPERATURES

Sea surface temperatures for open-water months are presented in Figure 3-5. In other months, surface ice (or snow) temperatures are simple modifications of surface air temperatures, and are not included here in chart form.

No pre-existing sea surface temperature charts supplied the data in the form or detail required, so Figure 3-5 was constructed from all available information. This included earlier maps by Dunbar (1951, 1958), Barber (1967), Grainger (1960), Campbell (1959) and Wendland et al. (1966, 1967), as well as several hundred sea surface temperature reports by oceanographic ships and ships traveling the Hudson Bay shipping route. In addition, ice conditions were studied (and reported on in the next chapter); the resulting mean ice cover charts were a great aid in sea surface isotherm construction.

The charts show that mean annual maximum temperatures over most of Hudson Bay are around +7 deg. C. Low temperatures in the southwest part of the Bay result from the usually late dissipation of ice cover there. This feature is in opposition to earlier charts (e.g. Dunbar, 1951) based largely on the Loubyrne expedition data of 1930. Ice concentrations in the southwestern part of Hudson Bay must have been abnormally light that

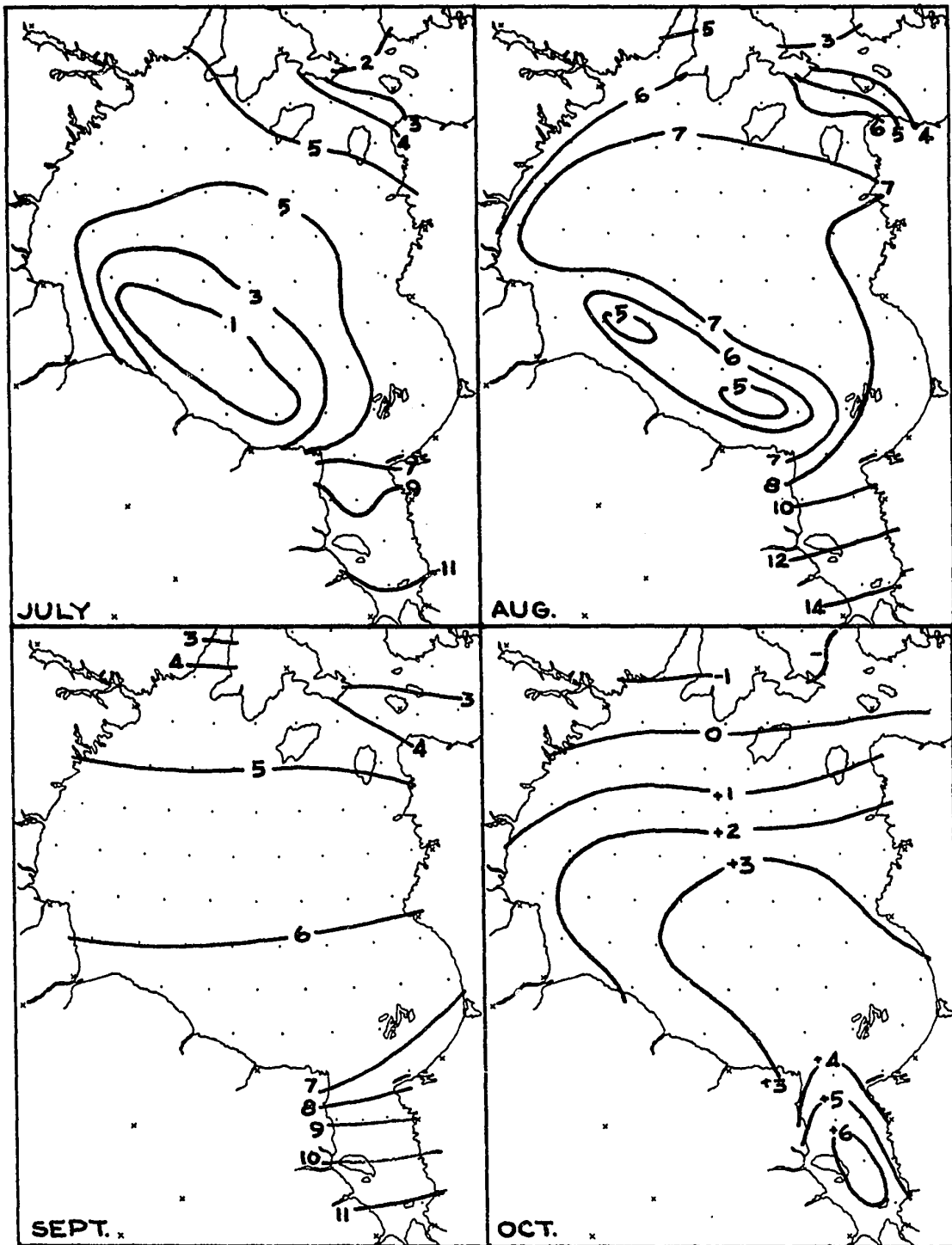


Figure 3-5. Monthly mean sea (or ice) surface temperatures, July through October (degrees Centigrade).

year, because temperatures over 9 deg. C. were recorded, the warmest anywhere in the Bay. Barber's (1967) charts were the first to show generally colder temperatures in the southwestern parts.

Indirect methods were resorted to for determining surface water or ice temperatures at other times of year. Water temperatures as freeze-up approached were derived by interpolating between the last period for which observations existed, and a freeze-up temperature of -1.6 deg. C. Surface ice temperature for the month of freeze-up was taken to be 1 deg. C. warmer than the surface air temperature; for the remainder of the winter (through March), the air-to-sea temperature difference was assumed to be zero. These adjustments from surface air temperature differ from those of Vowinckel and Orvig (1964 b, p. 456), who, using Russian "North Pole 2" data, took surface ice temperature to be 1 to 2 deg. C. colder than surface air temperatures during the winter months. The reasons for a warmer Hudson Bay surface are as follows:

(1) Hudson Bay is south of the Arctic Circle, so that even in January, and certainly in February and March, significant amounts of solar radiation are absorbed at the surface.

(2) Hudson Bay ice cover is much thinner than "North Pole 2", especially in January. Heat from the water below will reach the surface more easily.

(3) Schwerdtfeger (1962) measured energy fluxes over the Hudson Bay surface from January to April, 1961. His measurements indicated that from January through March the surface was on the average slightly warmer (less than 1 deg. C.) than the air.

In April and May, "North Pole 2" observations indicated a surface temperature 1 deg. C. warmer than that of the air. In these months, Hudson Bay conditions are similar to those at "North Pole 2". Hudson Bay winter ice formation is nearly over in April, implying that heat conduction upwards through the ice is small. Also like "North Pole 2", the Hudson Bay surface receives ever larger amounts of solar radiation in spring, which suggests that the surface becomes increasingly warmer than the overlying air. Thus, although the air-to-surface temperature gradient for "North Pole 2" in April and May probably is not exactly correct for Hudson Bay, it appeared to be the best information available, and was applied over Hudson Bay in April and May, wherever the air temperature was less than -1 deg. C.

When monthly mean air temperatures over Hudson Bay rose above -1 deg. C., the ice surface was assumed to remain at 0 deg. C. until 50% of the local ice cover had disappeared. Interpolation supplied temperatures for the period between the time of 50% ice cover and the first oceanographic observations.

### 3.7 SUMMER HEAT STORAGE IN HUDSON BAY WATERS

Data for summer heating of Hudson Bay waters came from the 1948 Haida expedition (Dunbar, 1959), the Calanus in 1958 and 1959 (Grainger, 1960), the Theta and Calanus in 1961 (Canadian Oceanographic Data Center, 1964). In all, 201 soundings from the months of July to October were plotted and analyzed.

From each sounding a rough integration was made of the "deg. C. grams" of water above the zero heat storage point (-1.6 deg. C.). Multiplication by the specific heat (Equation (2-16)) gave the quantity of heat in storage. The data were grouped according to time of year and location in Hudson Bay. The likely effect of abnormal ice conditions was considered when it seemed of importance.

This analysis gave the following information: the time of maximum heat storage, averaged over Hudson Bay, is early September, with a mean value at this time of 20,000 cal/cm<sup>2</sup> (or ly) of surface. Data were too sparse to allow maps of local storage variations to be drawn, beyond the fact that the southwest quarter of the Bay showed minimum early September values, of perhaps 15,000 ly, while southern James Bay had greatest storage, at nearly 25,000 ly.

Uncertainty in the mean annual maximum storage figure of 20,000 ly is estimated to be ±3,000 ly.

### 3.8 HEAT CONTENT OF PRECIPITATION

Snow falling onto the Hudson Bay surface generally represents a heat deficit in two ways. Usually the snow reaches the surface at a temperature below the zero heat-content level of -1.6 deg. C., and eventually the snow must be melted, which requires 80 calories per gram of snow.

The first factor is very small. November is the month when it reaches its maximum: mean snowfall for the month over Hudson Bay is about 38 cm (from Potter, 1965), or about 3.8 gm, and the snow temperature as

it reaches the surface is about -8 deg. C. For a specific heat of 0.5 for snow, the heat required to raise the snow to -1.6 deg. C. amounts to 12 calories (per month per cm<sup>2</sup>), or less than 0.5 cal/day. This term plainly may be neglected.

Mean annual snowfall for Hudson Bay is approximately 67 inches (from Potter, 1965), or 170 cm. The standard 10:1 snow-to-water equivalence gives 17.0 gm or cm of snow melted. All of this snow which is not sublimated must eventually be melted. Looking ahead briefly to Chapter 6, mean wintertime evaporation heat loss over snow and ice is found to be 1480 calories, or, dividing by the heat of sublimation (673 cal/gm), 2.2 gm of ice. Thus 17.0-2.2, or 14.8 gm of snow, must be melted in Hudson Bay, at the rate of 80 calories per gram for fresh-water ice. Total heat required therefore is about 1180 calories per cm<sup>2</sup> of surface per year. This figure is probably accurate to  $\pm 200$  ly/year.

The heat content of liquid precipitation is included in the runoff data considered in the following section.

### 3.9 RUNOFF

MacKay (1966) discussed seasonal variations in runoff rates for various Canadian watersheds. From his paper the following runoff rates were obtained:

10%	of the annual runoff into Hudson Bay occurs in Dec-Feb;
40%	" " " " March-May;
35%	" " " " June-Aug;
15%	" " " " Sept-Nov.

Each three-monthly rate was divided by three to represent mean monthly rates, and plotted as a three months long bar (Figure 3-6).

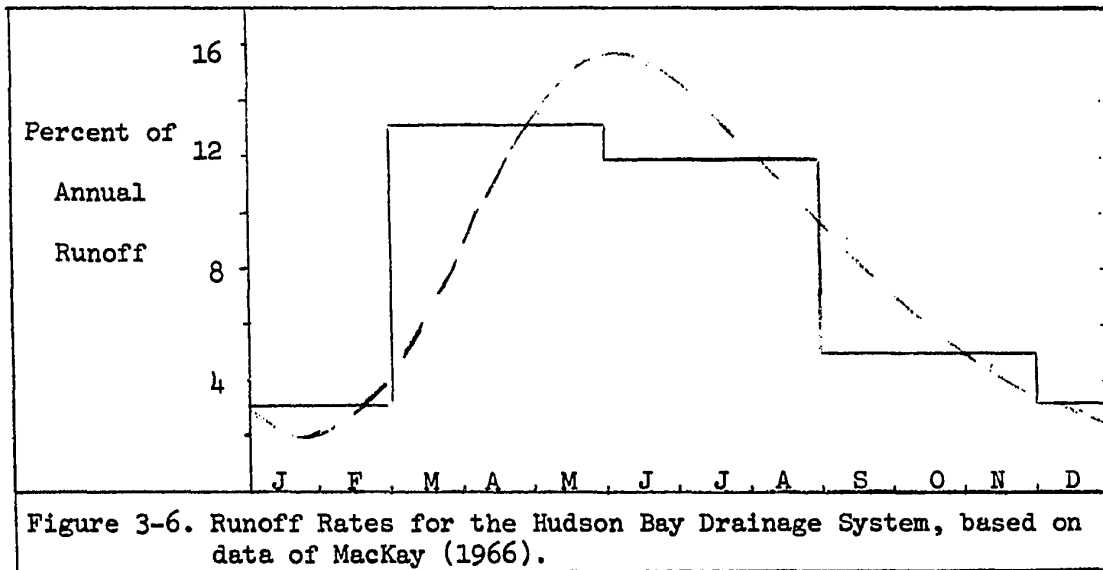


Figure 3-6. Runoff Rates for the Hudson Bay Drainage System, based on data of MacKay (1966).

Then a smooth curve was constructed which satisfied the histogram. This smooth curve gave monthly runoff rates, as a percentage of annual runoff.

In Section 3-4, runoff was seen to be  $0.90 \times 10^{18} \text{ cm}^3/\text{year}$ .

From this and Figure 3-6, mean monthly runoff masses were calculated.

The results appear in line 2 of table 3-1.

TABLE 3-1

RUNOFF DATA

	J	F	M	A	M	J	J	A	S	O	N	D
% of annual runoff	2	2	6	10	14	15	14	12	9	7	5	3
gm runoff per month, $\times 10^{16}$	1.8	1.8	5.4	9.0	12.6	13.5	12.6	10.8	8.1	6.3	4.5	2.7
temp of runoff (deg. C.)	0.5	0.5	0.5	0.5	1.5	5.5	12.5	12.5	8.5	2.5	1.5	0.5
cal/cm <sup>2</sup> /month	6	6	19	29	60	150	266	240	129	40	21	9

Mean temperature of runoff water was determined from surface air temperature charts and considerations of ground heating (less in spring, more in fall). Line 4 gives the amount of heat added to Hudson Bay by runoff each month, per  $\text{cm}^2$  of Bay area. Maximum values, in July, reach about 9 calories per  $\text{cm}^2$  of surface per day. Total annual heat gain by runoff, per  $\text{cm}^2$  of surface, is 975 calories. As will be seen in the following section, much of this heat gain does not become available for use within the Bay, as currents remove it into Hudson Strait.

Uncertainty in the heat fluxes associated with runoff is estimated to be  $\pm 25\%$ .

### 3.10 HEAT TRANSPORT BY CURRENTS

This term is subject to the greatest of uncertainties, due to lack of definite knowledge about current speeds, and even directions, in some locations.

As described in Section 3.4, the outward-flowing wedge of warm, low-salinity water is clearly marked between Mansel Island and the Quebec coast. Campbell (1959) computed northward volume transport through this strait to be  $0.5 \times 10^6 \text{ m}^3/\text{sec.}$ , for October 1955 and July 1956. At this rate, approximately 2.2% of the volume of water in Hudson Bay passes through the channel in a month. If the current speed is assumed to increase linearly with height from zero at the bottom (about 100 meters), then surface currents are 0.15 m/s or 0.3 kts, a useful estimation for future calculations.

Figure 3-4, p. 49, was used as the basis of heat export computations . The heat contained in each ten-meter interval was taken to be transported by a current speed for that interval, based upon the surface current and the linear decrease of speed with depth mentioned in the last paragraph. The resultant export figures, given as heat losses per  $\text{cm}^2$  of Hudson Bay surface per month, appear in Table 3-2, below. For other months, the outward flowing water was assumed to be at the zero storage temperature of  $-1.6$  deg. C.

TABLE 3-2

HEAT TRANSPORT BY CURRENTS  
(Cal per  $\text{cm}^2$  of surface per month)

Month	JUL	AUG	SEP	OCT	ANNUAL (per year)
Export (-)	-309	-565	-592	-238	-1704
Import (+)	+ 23	+129	+208	+129	+ 489
Net	-286	-436	-384	-109	-1215

For heat transport by inward flowing oceanic water, volume inflow (including runoff) was assumed to be equal to the outflow between Mansel Island and the mainland. This is likely an overestimate of the inward oceanic transport, as runoff forces the outward flow, but probably does not immediately affect the inward oceanic flow. Temperature data for the inflowing water were constructed from Campbell's (1959) data for northwestern Hudson Strait, and from Barber's (1967) charts.

The transport figures must be regarded as order-of-magnitude estimates at best. If current directions are not in error, the values are likely correct to within a factor of three. Fortunately, due to the small magnitude of these advection figures when averaged across the Bay, even an error of a factor of three will not seriously influence final results.

All storage and advection data are condensed and presented in Table 4-1, along with ice storage and advection information, on p.101.

## CHAPTER 4

### ICE CONDITIONS

Ice cover is a basic hydrometeorological variable in Hudson Bay. Perhaps it should be called the most basic of all, because it influences all other conditions on the Bay so decisively. Since little information exists on average ice conditions in Hudson Bay, this chapter contains a detailed study of the subject.

#### 4.1 PREVIOUS WORK

Knowledge of just the very fundamental aspects of Hudson Bay's ice cover, namely that it freezes over virtually completely each winter and melts completely each summer, came relatively recently. Previous to the 1940's, the accepted view was that extensive shore ice formed each winter in the Bay, up to sixty or seventy miles off-shore in places (United States Hydrographic Office, 1946), but that the central portions were open all winter, except for a few fields of drifting ice. This ice was reported to melt during the summer.

The first real evidence contrary to this winter open-water belief came from airplane pilots flying across the Bay during World War II. They reported the Bay quite generally ice-covered in winter. After the war study of the situation was intensified through investigations in which observational and climatological data were gathered and evaluated.

The evidence, presented by Hare and Montgomery (1949), Lamont (1949), Montgomery (1950), Burbidge (1949), and Hare (1950), was indisputable.

Photo and visual reconnaissance showed a virtually uninterrupted ice cover across the Bay from January to April. Temperature, precipitation and cloudiness data all clearly indicated that open water in November became ice by early January. Thus it was 1950 before the basic facts of Hudson Bay ice cover came to light.

Since knowledge of Hudson Bay ice conditions was so slow in coming, it is not surprising that an adequate description of the month-to-month ice changes is non-existent. In fact, to the author's knowledge, only one study has been attempted, that of Forward (1956). Gathering data from all sources, but mostly from ship reports, he portrayed ice conditions along and north of the Hudson Bay shipping route, for intervals ranging from five days to two weeks, for the months July through November. Forward's study was found to be of little use for the purpose at hand, however, since the Bay south of a line from Churchill to Cape Smith is not considered, and because his criteria for ice coverage, namely "main ice areas most favorable years", etc., are very difficult to convert to tenths of ice coverage. Since Forward's data consisted mostly of ship observations, in which ice usually is described as "scattered", "very heavy", or in other qualitative terms, rather than in percentages of ice cover, the results of his study were bound to show the same degree of imprecision as the data.

#### 4.2 DISCUSSION OF EXISTING DATA

Information on ice cover can be divided into four distinct categories, based upon the observer's location: on land, ship, aircraft or satellite. All four types of observations exist for Hudson Bay; a brief

discussion of their relative merits follows .

Observations from land are limited by the observer's horizon. Conditions on and near shore often are not typical of those further seaward, so extrapolation of these land-based observations outside the immediate vicinity of the observer is hazardous. Such mis-application of shore-based observations was largely responsible for the winter open-water beliefs about Hudson Bay. Shore-based observers reported arctic sea-smoke visible beyond the shore fast ice many winter days, which was correctly attributed to the presence of open water off-shore. Extrapolating these results toward the center of the Bay gave the incorrect result that the center of Hudson Bay did not freeze. In reality a coastal singularity, the shore-lead, was the source of the sea smoke.

Ice observations from ships suffer the same defect as land-based observations, although to a lesser extent. Ship reports come from all parts of the Bay, making them considerably more useful for an ice survey than reports from shore. However, the range of view from a ship's bridge is limited, so each ship report is in effect a point, or at best a line, observation. Ship reports from Hudson Bay simply are not numerous enough to compensate for the small areal coverage of a single observation. In addition, ship reports suffer a serious bias: ships generally avoid the heavy ice areas, thereby exaggerating frequencies of lower concentrations. Reports from areas of 90-100% ice cover would not occur.

Another problem is common to both ship-based and land-based reports: although some reports go back dozens or even hundreds of years,

only a few of the most recent (notably the Ice Thickness Data for Selected Canadian Stations, published annually by the Meteorological Branch of the Department of Transport) are standardized in format, content or location. Reports such as "heavy ice", "frozen over", "very little ice" are not easily rendered into quantitative terms. Sometimes even the main intent is unclear. For instance: "The Eskimo said that Frozen Strait and Roes Welcome Sound as a rule did not freeze over in winter . . ." (Mathiasson, 1931, p. 55) sounds as if little ice forms in these channels. The fact is that winter ice cover there is well in excess of 90%. A lead twenty feet wide will prohibit travel across these waters, so to the foot traveller they have not "frozen over", although their ice cover may be over 99%.

It is dangerous to rely on the accuracy of these reports when ice observation is not the reporter's main job. Contradictions abound. For example, from the literature we may read that Roes Welcome Sound freezes over so that travel is possible from Southampton Island to the mainland "occasionally, perhaps every ten years or so" (Mathiasson, 1931, p. 55), "only exceptionally" (K. Birket-Smith, 1931, p. 74), "every other year" (H. T. Munn, 1919, p. 52), and "two years out of three" (P. M. Bennett, 1940, p. 111).

Meteorological satellites are now giving us useful information about ice cover. The main drawbacks at present are lack of sufficiently long records and difficulties connected with cloudiness. At best, five years' data are available, 1963-1967. Cloudiness makes a further restriction in two ways. First is the difficulty in distinguishing clouds from

ice. Secondly, with extensive cloudiness so prevalent in the arctic summer, only a small percentage of the pictures yield ice information. Of the eleven days in July 1963 that Tiros satellites scanned Hudson Bay, cloud conditions on six days were completely overcast.

Fortunately the rather bleak picture described so far brightens immeasurably when we turn to aerially gathered data. In several ways observations made from aircraft are ideal for ice surveys. The airplane travels high enough and fast enough for the observer to report on great areas in a single day. Unlike the seagoing observer, the airborne observer may fully explore areas of heavy ice concentrations. In addition, clouds do not present nearly the problem they do to satellite observations.

Since 1958 the Meteorological Branch of the Department of Transport has conducted annual aerial surveys of ice break-up and formation in Hudson Bay, primarily in support of shipping along the Hudson Bay Route. Flights are frequent, and, most important, reporting procedures are standardized and quantitative in nature, so that reports from different years and different observers may be compared. The Meteorological Branch has published these observations in various Circulars (Cir. 4432, 4509, 3569, 3710, 3896, 3951).

In order to preserve the uniformity of the data, information other than the aerially gathered data was used as little as possible. In the absence of aerial observations, recourse to land and shore based reports which seemed especially reliable, and to climatic data, was

occasionally necessary. In particular, very little direct observational evidence exists for December, so ice pack positions are mostly smooth interpolations between November and January values.

#### 4.3 REDUCTION OF DATA

Ice conditions in Hudson Bay fall into four seasonal categories:

- (1) "Winter": January--April, when ice cover is nearly 100%;
- (2) "Spring": May--mid-August, when ice cover is dissipating;
- (3) "Summer": late August--early October, when ice cover is nearly zero;
- (4) "Fall": early October--late December, when ice cover is forming.

Winter and summer are static situations for the most part. Ice concentrations were taken to be 10/10 and 0/10, except for fringe areas described below. Climatic data provided the date of onset of winter (i.e., nearly totally frozen conditions); other dates came directly from aerial data.

Fall and spring concentrations were determined as follows:

The seventy-seven grid points employed in this study appear on each map as small dots. In general they are all odd-odd and even-even intersections of degrees of longitude west of 75 W and latitude south of 65 N, except where these coordinates fell on islands. Each grid point, then, represents 2 degrees of longitude by 1 degree of latitude or about 3600 square nautical miles of surface.

The Circulars mentioned above provided the data for 1958-1964. For 1965 and 1966 data came directly from (the photostat copies of) the ice observers' charts, on file at the Library of the Arctic Institute of North America. Ice amounts (10<sup>ths</sup> of coverage) were read for each grid point covered on each flight. These were combined into semi-monthly averages at each point for each year. Observation dates ranged from late April to late November, with the greatest number falling in July and August.

Averages were then taken for each grid point and half-month, over however many years' observations were present. Very few points had observations for all nine years for any semi-month. It was necessary to standardize the data to the full 9-year period in order to reduce bias arising from the small number (statistically speaking) of observations. A combination of interpolation, extrapolation and graphical subtraction supplied missing data. In certain regions, notably the southeast and the extreme northwest, observations were lacking over large areas for long periods of time. In such cases no attempt was made to supply the missing data number-for-number, so these regions represent less than nine years' data and are therefore less reliable.

#### 4.4 PRESENTATION OF DATA

Presentation of the data is in the form of semi-monthly maps showing isolines of 10<sup>ths</sup> of ice concentration.

Except where noted below, the values at the grid points are nine-year means for the semi-month, areally averaged over the domain of each grid point. This results in considerable smoothing of the picture along the coasts. Before the fast ice has left the shore in spring, for instance, concentrations at the shore quite generally will be 10/10<sup>ths</sup>, will drop to 0/10 at the ever-widening shore lead, and then rise to 9/10 or more as the central pack is reached. This widespread coastal condition may be described by a series of 6/10 and 7/10 observations at the coastal grid points, which obscures the fact that the concentrations are highest on the immediate shore. Isolines of concentration were drawn for the grid points, generally without considering the smaller patterns.

For the autumn months the presentation is slightly different from that for the other seasons, because of the behaviour of the ice cover in the autumn months. On any given date near the average freeze-up time at a particular location, the distribution of ice concentrations observed over the years will be sharply bi-modal. Concentrations of 0/10 and over 9/10 will occur almost to the exclusion of intermediate values. This is due to the fact that the Hudson Bay ice forms over large areas simultaneously; when cooled by large-scale invasions of very cold air from the northwest the ice locally, except for a very short transition period, covers either all or none of the surface.

This process of ice formation (and later decay also) is so closely analogous to that of formation of the cirro-stratus alto-stratus cloud deck of a warm front that comparison may be useful. In both cases

gradual cooling takes place until the critical temperature is reached; with additional cooling a rather sudden change of state occurs simultaneously over large areas, resulting in an overcast. The break-up of pack-ice, like the dissipation of a stratiform cloud deck, is somewhat more gradual. The edges of the ice pack melt into smaller floes surrounded by open water just as the edge of the cloud deck breaks up into cells (alto-cumulus) surrounded by "clear" air. Concentrations other than 0/10 or 10/10 are to be expected near the dissipating boundaries.

Since autumn conditions are so clearly bi-modal, the map for these months (October and November) depicts modal, rather than mean values (except in and near Hudson Strait, where the currents keep the ice broken up and moving until a late date--all winter in places--and intermediate concentrations occur). The median position of the ice pack boundary appears on the fall maps, with 0/10 concentration of ice southeast of the boundary, over 9/10 northwest.

In spring the frequency distribution at many points tends to favor extreme conditions also, because (as the analogy suggests) intermediate concentrations are common only along the boundary of the ice pack. (The local variability of melting dates is greater than the average time taken for the local concentration to drop from 10/10 to 0/10.) For instance, late July concentrations examined in the southwest parts of the Bay, where mean concentrations were 4 to 5/10, showed that only 1/3 of the actually observed values were 2, 3, 4, 5, or 6/10. Thus in melting as well as in freezing, the middle concentrations are less common.

"Once it starts, the ice disappears very rapidly." (Dunbar, 1954, p. 16). The spring case is not so extreme as in the fall, however, and the only safe way to deal with the spring charts was to use mean values.

#### 4.5 RELIABILITY

Reliability of the results varies considerably by region and season. From late June through late August, the period of best over-all coverage by aerial reconnaissance, over 3000 grid point observations form the basis of the maps; this is about 600 observations per semi-month. For other months the coverage is thinner, and drops to almost nothing for most areas from September through mid-May. This is not so very serious however, for the ice reconnaissance flights are by no means randomly scheduled. They operate when and where ice conditions are changing. Thus a nearly complete lack of data for September in the southern 3/4 of the Bay is not a serious handicap, since it is clear from August reports, and climatic considerations, that no ice is to be expected. On the other hand, September coverage of northeast Hudson Bay and Hudson Strait, where ice does exist, is nearly perfect. Thus the ice reconnaissance flights give more information than a simple tally of the number of observations would imply.

Flying to pre-selected areas cuts down on the chances of discovering the unexpected, of course; perhaps very small ice concentrations do usually linger in the southwest Bay into September. Such very local phenomena, however, are beyond the intent of this study.

As plentiful as these nine years of aerial observations appear by comparison with earlier data, nonetheless nine years is not a sufficiently long time for positive conclusions to be drawn. This is particularly true because year-to-year variations are very large, on the coastal regions if not in the central parts. Hudson Bay temperature anomalies for the years 1958-1966 were examined in an effort to check on the climatic representativeness of these years compared with long-period averages. From the temperature anomaly map in each Monthly Record for the nine years under study, monthly departures for northwest, northeast, southwest and southeast parts of Hudson Bay were recorded.

January through March are the months of ice thickness growth everywhere across the Bay. January and February were generally warmer than normal, March definitely colder. Combining the effects of these three months gives 48 months warmer than average, 49 colder and 11 normal ones, so the months of ice thickness increase appear to have been, on the average, quite typical.

Small but frequent June (negative) and July (positive) temperature departures in the eastern regions appeared to be the only variants from more or less normal conditions over the years 1958-1966. Determination of a correction factor to adjust for these departures would be highly arbitrary. It is hoped, therefore, that the effects are small, and no correction has been attempted.

Temperature is just one factor having an important bearing on changes of ice amounts. Perhaps even more important, especially for

break-up, is wind, both direction in regard to ice transport, and speed, for physical break-up of the ice and mixing with the water. There is no simple way to compare wind conditions over the nine years with average, so no attempt was made; but it may be argued that persistently anomolous wind conditions would be reflected in the temperature departure data, which have just been examined.

A possible source of bias lay in the distribution of observations around the mean time for a period, e.g. late July. If the bulk of late July observations for one grid point came late in the period 17-31 July, it would reflect an incorrectly low ice concentration value. The likelihood of this is especially high for points with few observations. Accordingly, observation dates were examined at points with scanty coverage; minor adjustments were made where appropriate. Construction of maps showing concentration change from semi-month to semi-month aided in this process.

#### 4.6 ERROR SUMMARY FOR ICE COVER CHARTS

It is difficult to estimate a likely numerical error, due to the complexity of the influencing factors mentioned (anomalous weather, interpolation and presentation procedures, non-random flight paths, etc.). It is believed that the results generally portray average conditions to within 1/10 of concentration, except for June through early August in the southeast and extreme northwest. Averages there usually are based on less than seven years' data and may be off by 2-3/10; even the general

patterns should be accepted with caution in these regions. In the fall months the position of the ice pack boundary is probably accurate to within 40 miles through early November, but the December positions are highly uncertain, and could conceivably be off by 100 miles in places.

#### 4.7 WINTER ICE CONDITIONS

From January through April (Figure 4-1) ice coverage of 10/10 is the rule everywhere except near the Belcher Islands, along the coasts, and in Hudson Strait.

Precipitation, cloudiness and temperature data for January at Great Whale River all indicate significantly more open water upwind of that station than later in the winter. Hare (1950, p. 129) suggests late December or early January as the time of final ice formation. Accordingly, the region just west of the Belcher Islands was assumed to be open water on the average through January 5<sup>th</sup>, then ice covered.

A shore lead, of five miles width in the west and two miles on the east coast, was assumed to exist through these months. Assuming the shore lead to be open water, and averaging this 0/10 cover with 10/10 cover for the rest of the coastal regions, gave winter values of 9/10 for the west coast, 9.6/10 for the east.

The choice of seven miles (five on the west coast, two on the east) for the width of the shore lead was rather arbitrary, but was based on the following considerations. Observers have noted that after a period of persistent winds from a certain direction, a shore lead will

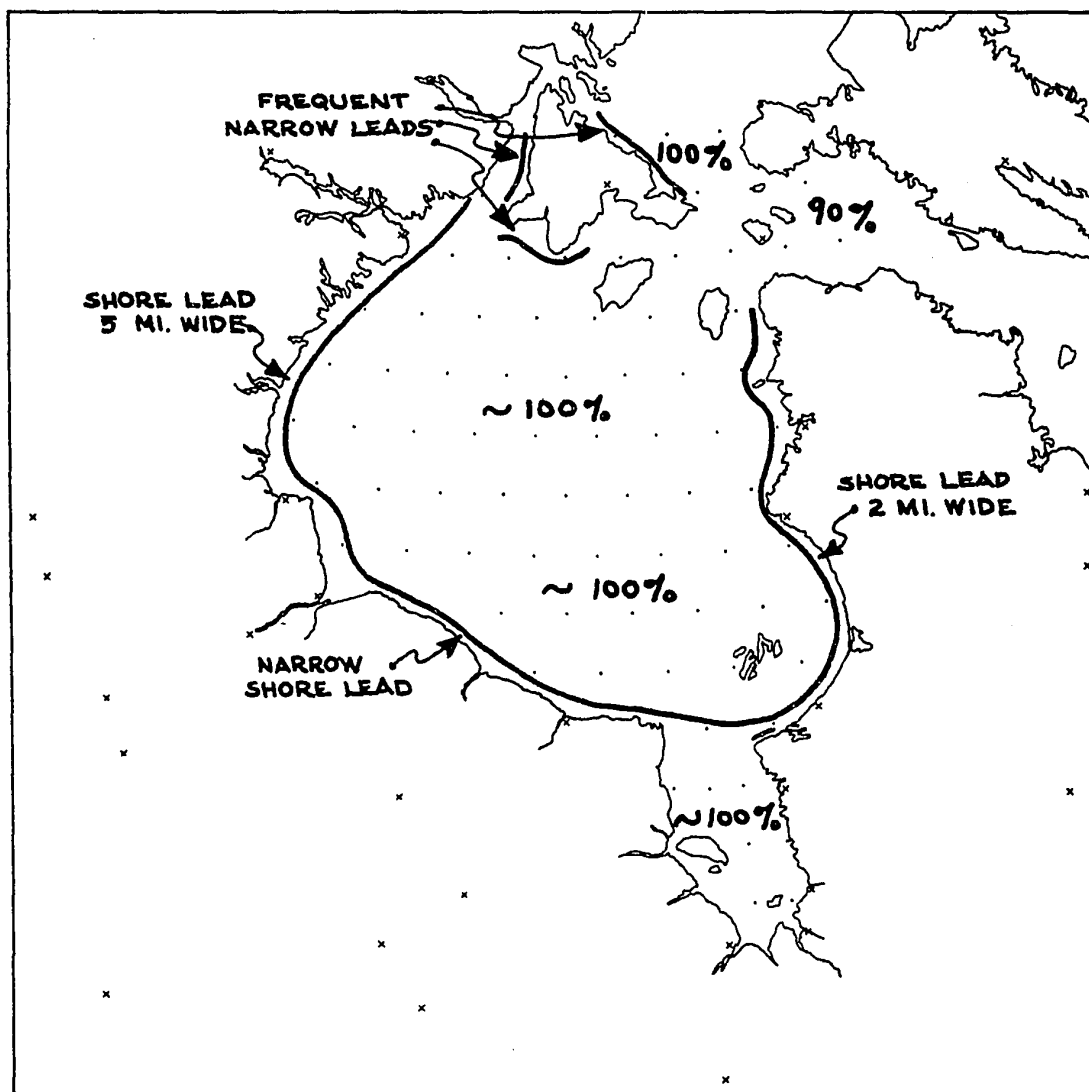


Figure 4-1. Mean ice concentration for January through April.

develop along the off-shore coast. Donovan (1957, p. 3) says that at Churchill this lead is about 10 miles wide after southerly winds have persisted for several days, a value which Barber (1967) accepts. Such a lead is larger than a mean value, since with a steady wind rafting takes place as the lead downwind closes; also, with less wind (and hence with less ice floe movement), the small leads freeze. For these reasons a value less than 10 miles was adopted; 7 was chosen as hopefully representative. Five miles were assigned to the west shore, 2 to the east, because of the prevalence of westerly over easterly winds. In reality, the shore lead is rarely present on both sides of the Bay simultaneously.

The "shore lead" does not occur directly at the shore, but some distance seaward. Fast ice along the shore is a permanent winter feature, regardless of wind direction. About the location of the shore lead, Lamont (1948, p. 2) reported ". . . the shore lead varies in distance from the shore from a few yards up to several miles. Its width varies from almost nil to up to 10 miles and more depending to a considerable extent on the wind direction."

The location of the winter shore lead on the eastern side may vary much more than on the west coast. In some years at least the fast ice extends off-shore to the Ottawa and Belcher Islands (Hare, 1950, p. 120-129); Eskimos living on these islands visit the Hudson Bay Company posts on the mainland in winter, according to Flaherty (1918, p. 453). At these times the "shore lead" perhaps appears just west of this loose chain of islands. Hare and Montgomery (1949, p. 160) say "This possibility

is further strengthened by the observation of R. J. Flaherty (quoted in the Arctic Pilot) that 'The climate of the islands differs widely from that of the opposite mainland. Compared with weather reports from Great Whale River for the same period . . . [the islands had] a far greater proportion of overcast skies and fogs, stronger and more constant winds, but higher and more equable temperatures'."

Winter observations still are insufficient to confirm this interesting possibility, however, so the winter maps show the lead in its more traditional position close to the mainland.

A lead was assumed at the mouth of James Bay, with mean coverage of 9.6/10 at 55 deg. N 81 deg. W. This is based on the observation of Montgomery (1950, p. 42-3) that a lead seems to persist between the Hudson Bay and James Bay packs.

Ice cover even in mid-winter in the center of the Bay will not be exactly 100%, but slightly less due to occasional small leads. In a March 1949 flight over central portions of the Bay, Merrill (1949) counted the number of leads flown across in a given time and estimated the average lead width, which allowed an estimate of ice cover over a region Merrill said was typical in appearance of conditions over the central Bay. The ice cover thus determined was 99.44%. To use a value of 10/10 then seems to be quite justified.

Values of 9/10 for Hudson Strait represent an average from several sources. Raw data for winter being so scarce, it was impossible to be precise in evaluating the freezing effects of the very low temperatures

versus the break-up effects of the large tidal changes and strong currents. Hare and Montgomery (1949, p. 154) say winter coverage in Hudson Strait "usually averages at least 80-85%". A coverage of 9/10 was taken to be a reasonable value.

Foxe Channel concentrations are 10/10. The only debatable region here is along the east coast of Southampton Island, where small shore leads have been reported through the winter (U.S.H.O. 1946, p. 370).

#### 4.8 MAY AND JUNE ICE CONDITIONS

During May and June (Figure 4-2) no significant decrease in concentration, from over 9/10, occurs in central or southwest Hudson Bay, but along the west, north and east coasts concentrations are down to 5-6/10 by the late June chart. James Bay ice decreases greatly in this period, with late June values near zero in the extreme south, but still 7/10 in the north central parts. Hudson Strait ice has decreased considerably with average amounts near 5/10 by late June. However all but the very southernmost parts of Foxe Channel are nearly unchanged, with coverage still over 9/10.

As mentioned above, isolines of ice cover are drawn for the grid points, which are areal average conditions. If instead one concentrated all the open water into one single shore lead, by late May the shore lead would be 26 miles wide on the west coast, 29 miles on the east.

Low values of 3-4/10 appear by late June just southwest of Southampton Island, showing the importance of the wind in ice distribution; for although this region has the lowest air temperatures of all the Bay

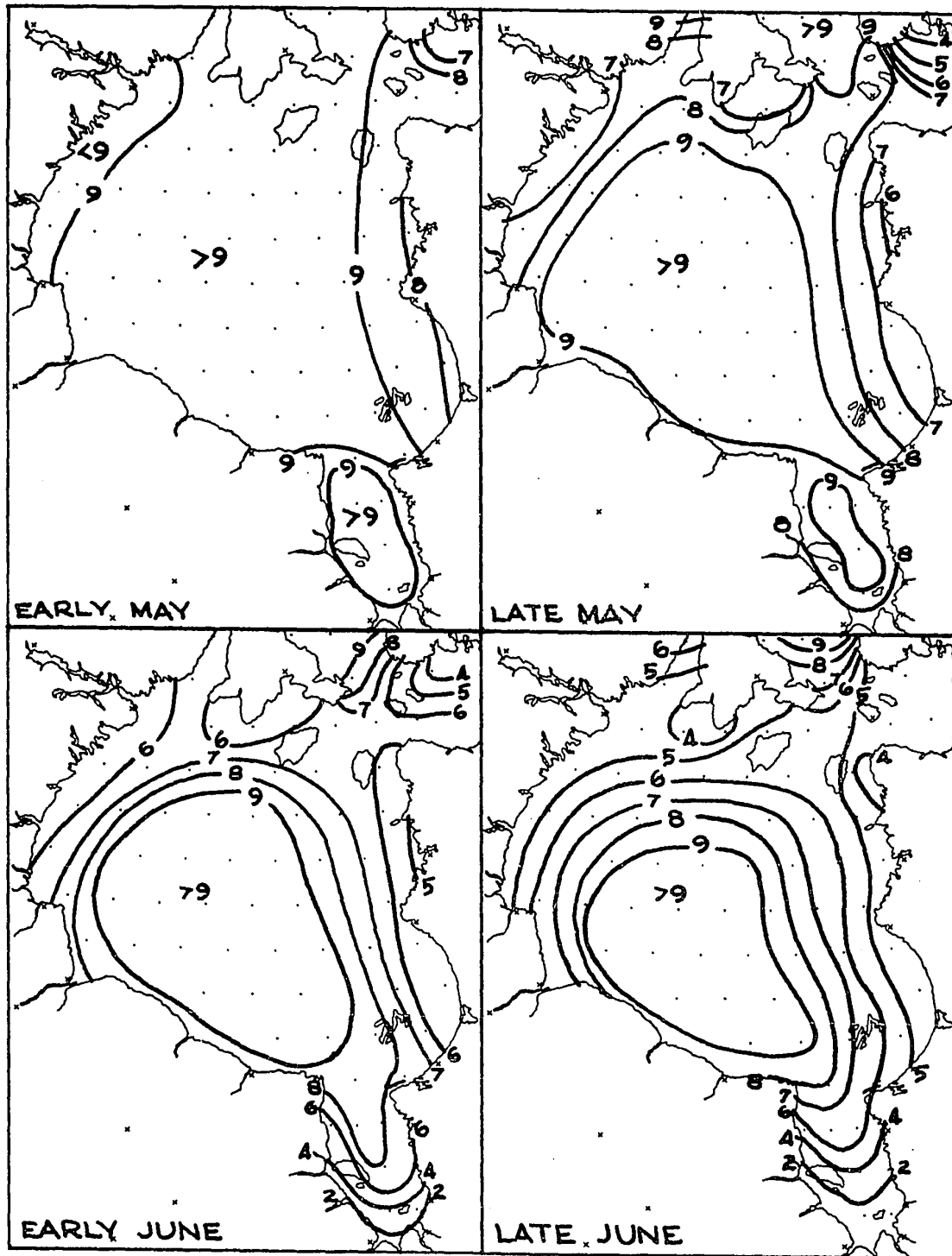


Figure 4-2. Mean ice concentration for May and June (tenths of coverage).

at this time of year, it is among the first regions to lose its ice cover. Due to the persistence of the north winds, ice from the north moves southwards to melt in the southern parts of the Bay. (The large tidal ranges and strong tidal currents undoubtedly aid in this process along Southampton Island by fracturing and loosening the ice, thus facilitating transport.) In Hudson Bay the local decrease with time of ice cover is no indication of the amount of heat used locally for melting for the period. The curious fact is that melting in the southern parts of the Bay causes open water in the north, for as the southern ice softens and melts it becomes more compressible and allows more ice to be pushed down from the north. Thus there is a direct relationship between the rate of melting in the south and the rate of clearing of ice from the northern waters. Wind stress and water currents, both of which generally move ice southward in western Hudson Bay, are also necessary for the process, but not sufficient by themselves; for no amount of north winds in the winter months can clear the northern parts of the Bay of ice.

This melting pattern, a product of the geographical and climatological setting, causes a distinct imbalance in the heat budget of Hudson Bay, with the southern portions being forced to melt many times more ice than the northern areas.

#### 4.9 BREAK-UP EAST VS. WEST

With prevailing winds from the northwest, one would think that ice coverage would decrease faster on the western coast than in the east, but the opposite is the case. Through the entire thaw period, May to

August, ice coverage decreases faster in the east than in the west. Several factors contribute to this condition: the northward-running current along the east coast, persistent and relatively strong especially between Mansel Island and Quebec, certainly carries some ice out of the Bay, into Hudson Strait. Although only a small percentage of the Bay ice is likely to be removed by this current (see Section 4.19), the volume may be large enough to cause lower concentrations locally, i.e. along the east coast.

The geography of the east side of the Bay may assist in this process. The off-shore islands, from Mansel Island in the north through the Ottawas, the Two Brothers, Farmer Island, the Sleepers and the Belchers, constitute a loose chain which has two effects. First, it acts as a partial buffer to ice from the west, so that under west winds the ice cannot jam solidly into the eastern half of the Bay. (This effect is quite apparent on the late July and early August maps.) Secondly, during spring the ice between the islands and the east coast develops a coastal lead with either east or west winds, the lead with east winds being along the east coast of the Bay, with west winds along the east coasts of the islands. Thus leads are forming nearly all the time during thawing, resulting in a general loosening of the pack ice in this protected body between the islands and the east shore. Early break-up of ice into smaller floes hastens both melting and export.

It seems, then, that the off-shore islands may partially isolate the eastern portions from the rest of the Bay, from the point of view of

ice break-up. The occurrence of complete fast ice cover, some years at least, and earlier break-up, are typical of conditions on a smaller body of water at the same latitudes as Hudson Bay (see McFadden, 1965). If one imagined the east coast of Hudson Bay to lie along the chain of islands instead of in its actual location, the ice concentrations in these spring months would reflect a more reasonable amount of west-wind bias toward high concentrations in the east.

Freeze-up dates in the east lag behind those in the west by as much as a month. It would seem, then, that western ice would be considerably thicker than eastern ice by the end of winter (and slower to melt in spring). However, heat transport through an ice cover decreases with increasing ice thickness; ice tends to insulate itself against further growth. As a result, the difference between eastern and western thicknesses diminishes as the winter advances. Thus an early freeze-up date may not in itself imply an especially thick ice cover by the arrival of spring.

#### 4.10 JULY

July (see the upper half of Figure 4-3) is the month that sees the greatest decrease in Hudson Bay ice coverage. At the beginning of the month mean concentrations at most points are greater than 5/10; by the first of August the greatest value anywhere in the Bay is 4/10, and most points are at or close to zero. The pattern established earlier is continued with lowest concentrations in the north, and east of the Ottawa . Belcher chain; higher values retreat to the central and southwest parts, and later just the southwest areas offshore from Churchill to the Belchers.

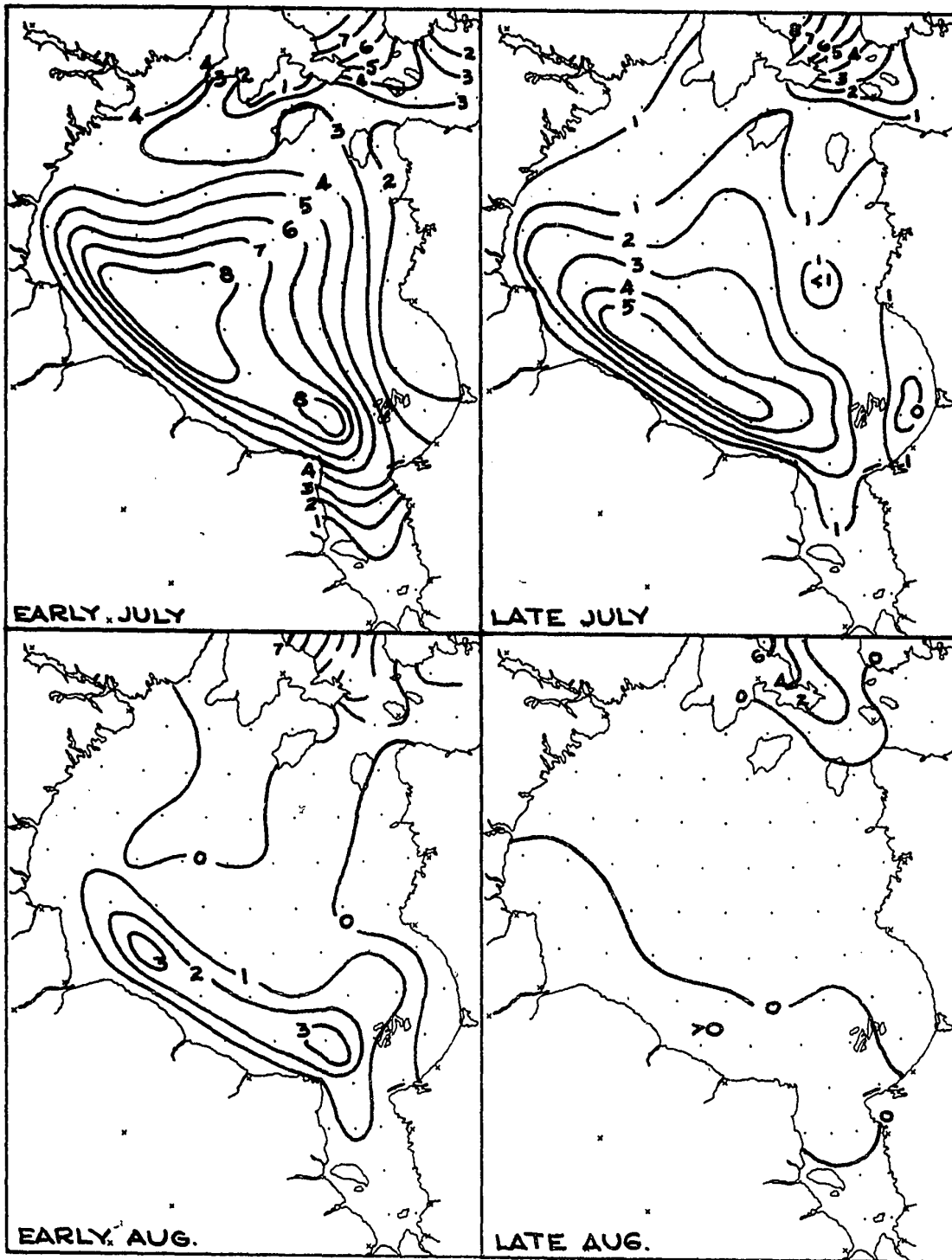


Fig. 4-3. Mean ice concentrations for July and August (tenths of coverage).

An interesting feature of the July maps is the trough of lower concentrations which extends southwest from Southampton Island for a distance of about 300 miles. Observational coverage in this region was rather complete, allowing confidence in the trough's reality to be relatively high. The location is noteworthy, for it falls along the southwestward flowing current from near Southampton to east of Churchill (see Figure 3-3). The current could cause such a trough in several ways:

(1) Simply by physical transport of low concentrations, the current would dilute the concentrations.

(2) Being relatively ice-free, the surface water would have a temperature above the melting point: thus the current may advect warmer water.

(3) With less ice concentration, the albedo of the surface would be lower near the current than outside it, allowing increased solar radiation absorption; then the lowering of albedo, increased absorption, decrease of ice cover cycle has a head start on surrounding regions.

A similar but less pronounced trough appears on the eastern side of the main July ice mass. This indentation, like the one in the northwest, lies close to a main current: in this case, the northeastward moving one, which leaves the Bay by Mansel Island. It seems possible that export of ice is the cause of this trough. Since data coverage consists of only 6-7 years in these parts, the feature should be accepted only with caution.

#### 4.11 INFLUENCE OF ICE ON CURRENTS

Surface currents in Hudson Bay are known to flow generally cyclonically (Figure 3-3), but the July ice cover charts hint at a possible variation. When the current from the north reaches 60 N, it pushes into relatively high ice concentrations, encountering greater and greater resistance to its path of flow. Passing from 61 N to 59.5 N the ice concentration in early July rises from less than 3/10 to more than 8/10; this is a decrease in the amount of open water by about a factor of 3. As just mentioned, this advection of open water seems to aid in causing a depletion of ice cover near 60 N. The surface current meets more and more ice, however, and this ice must eventually act like a dam, to the top meter of water, at least. Unable to proceed southward, the surface current may diverge to the left and right of its normal course. The result would be the eddy circulation pattern shown in Figure 4-4.

Figure 4-4 indicates that currents off Churchill at this time of year would be northwestward. This idea is supported by the lingering of higher ice concentrations northeast and east of Churchill, as seen on the charts for early July through early August. The possibility of a northward-moving current in this region has been suggested several times in the annual Ice Summaries. Markham (1962, p. 7) says "During the summer of 1960 there was good evidence of wind-driven water currents off Churchill which ran counter to drift-bottle findings. It has also been noted that southward drift of ice off Cape Churchill is often lower than expected which can only be explained by water movements." Of the 1963

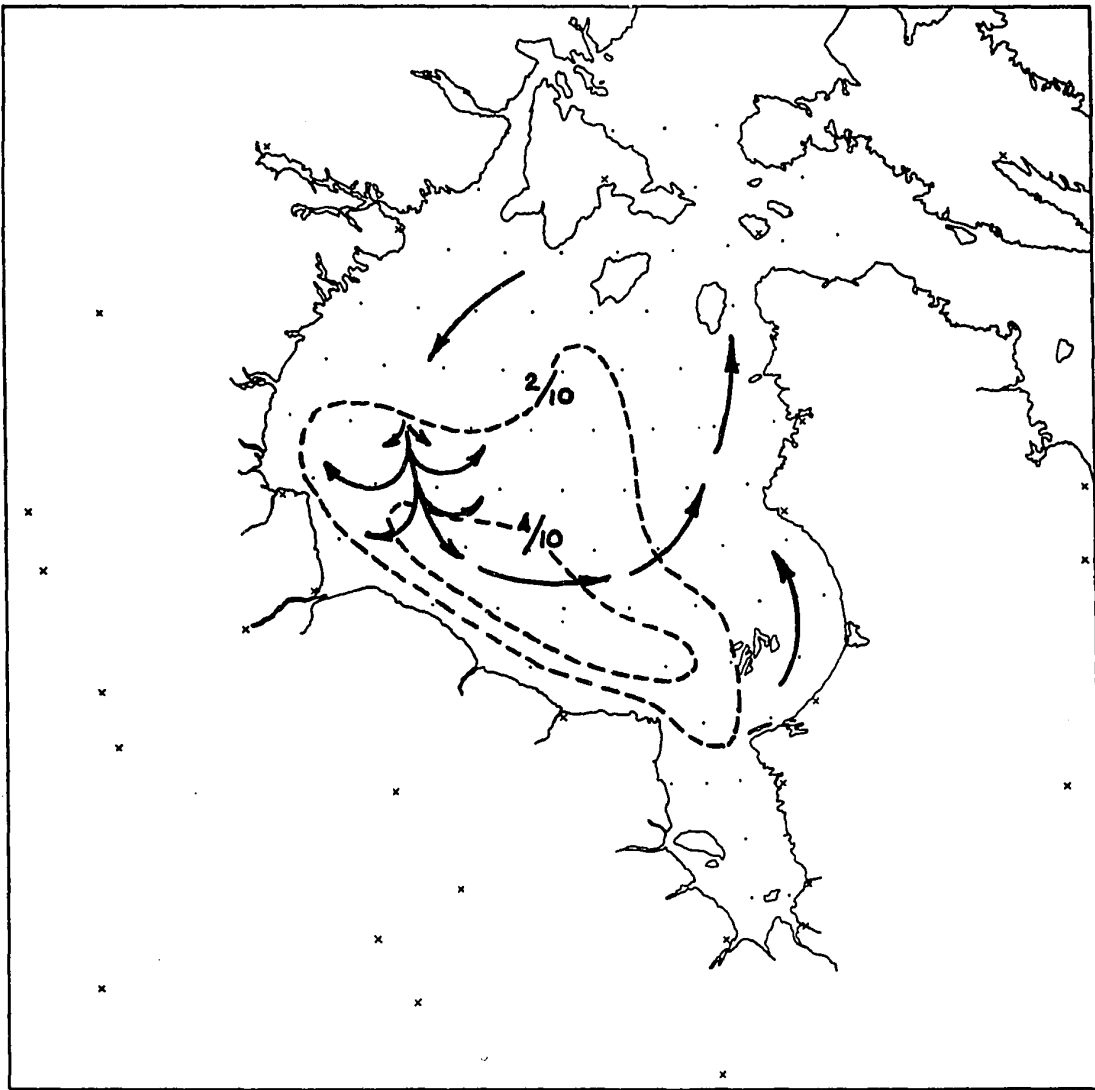


Figure 4-4. Late July ice concentrations (dashed lines) in relation to surface currents (arrows).

season Beaton and Markham (1963, p. 5) remark:

"It is apparent from the motion of the lingering ice east of Cape Churchill in August that the current drift must have opposed the wind drift for the net motion in one week is negligible despite northerly winds of about 10 knots in the week 6-13 August and northwest winds of 15 knots in the interval 13-20 August . . . . This same behaviour was also noticed in 1960 . . . . It is suggested on this basis that wind driven currents are often established in the bay and that they are relatively persistent once they are established."

Rather than being wind-induced, perhaps such northward moving currents are simply the result of the positions of the ice pack and the main current from Southampton Island, and exist only during ice break-up.

#### 4.12 CHANGE OF CONCENTRATION MAPS

Maps of change in ice concentration from period to period were prepared, starting with the change from early to late June (see Figure 4-5). These charts show the area of maximum ice dissipation proceeding southwestward with time along the northwest parts of the Bay (again, in the vicinity of the southwestward moving current). A second maximum of change moves northward from James Bay. (Unlike Hudson Bay, James Bay ice clears generally from the south. Because of James Bay's much greater length than width, only wind from precisely the right direction, due north, will drive ice into the southernmost parts of James Bay. Thus the southern waters usually can clear first, and the ice boundary retreats northwards. Northernmost parts of James Bay receive ice from Hudson Bay when the wind is anywhere from west, northwest or north, which makes final clearing here very late.)

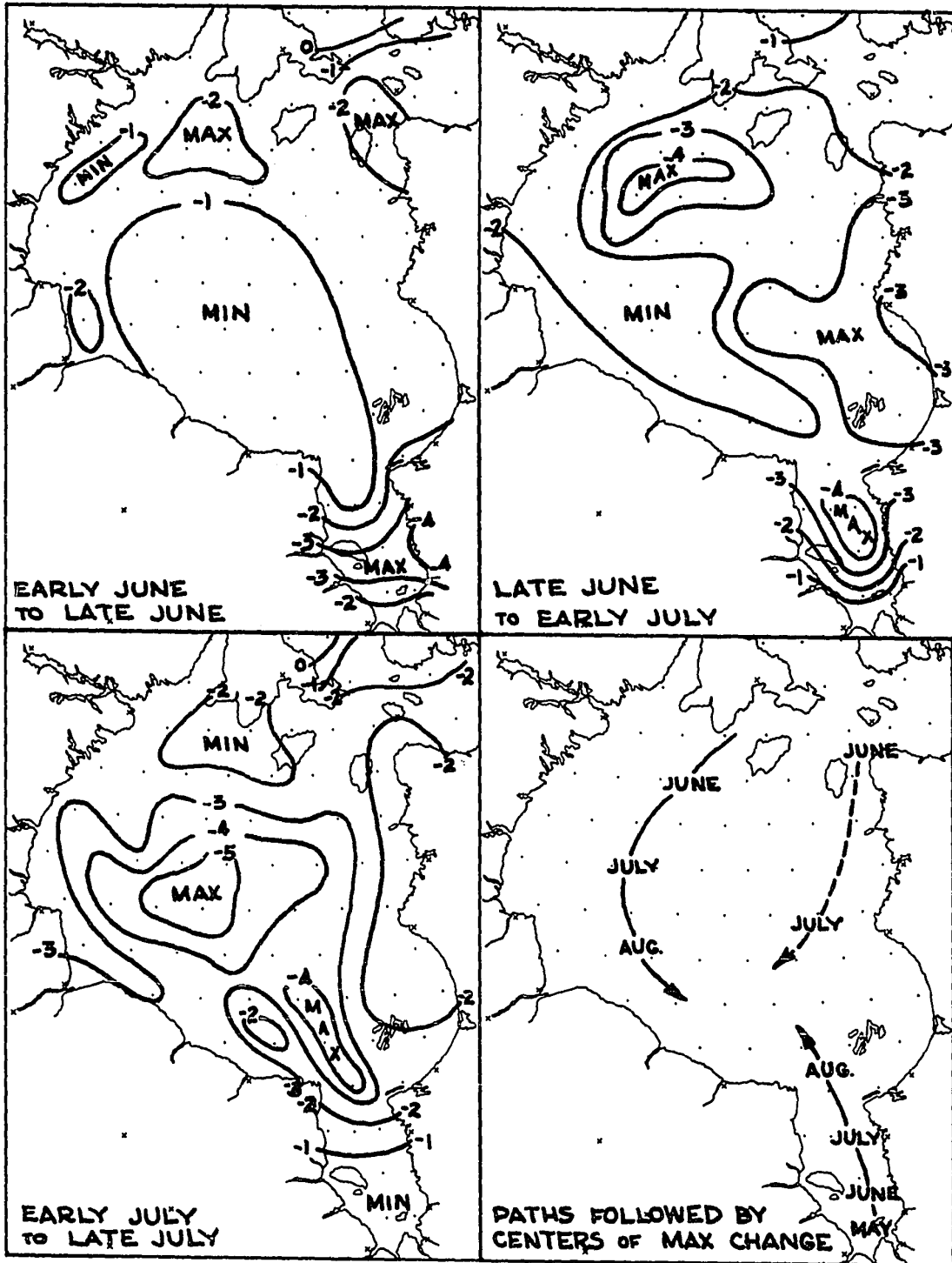


Figure 4-5. Changes with time of ice concentrations during break-up.

It is tempting to say that a third center of maximum change, near Mansel Island in mid-June, moves southward, although evidence for this is rather scanty. The lower right-hand map on Figure 4-5 shows the paths followed during break up by these maximum change centers. The fact that they all converge to the southwest parts of the Bay is evidence that melting takes place mostly on the edges of a single large ice mass, rather than here and there in small random patterns. The paths also tell of the ice dissipation forces at work in Hudson Bay. Besides the general influence of solar heating during summer which affects all areas, there is:

(1) clearing in the northwest due to ice transport southward, driven by both water and air;

(2) a hint of ice export from the northeastern areas by the northward-moving current (assisted by local geography in breaking up the ice); and

(3) the summer heat source (as compared with ice cover) of southern James Bay, whose higher air and water temperatures work at melting the southeastern boundary of the ice.

#### 4.13 AUGUST

By early August (Figure 4-3) the only ice of significance typically lies off the southwest shore from east of Churchill to the Belchers. Concentrations here average about 3/10, even at this late date. Elsewhere in the Bay, concentrations most years are zero, although ice occasionally survives nearly the whole summer in places

where wind flow, air temperature and cloudiness anomalies retard melting. Thus ice may be reported at any time of year from any part of the Bay. By early August, however, most points have seen their last ice of the season. Of the 61 grid points within the Bay, just 6 in the southwest have early August median ice concentrations other than zero. In James Bay all but the northernmost parts have usually lost all ice by mid-July.

The line of zero ice concentration, which appears on August and later maps, shows regions where ice never was observed over the 9 years for the month in question. It does not imply, of course, that August ice never will be observed in these regions.

#### 4.14 THE NORTHEAST

In Hudson Strait and Foxe Channel, late summer ice is more persistent than in Hudson Bay. Figures 4-6 and 4-7 depict the situation in this region. Along the eastern shore of Southampton Island and around Bell Peninsula, summer ice coverage never is typically zero. Early August modal values in western Hudson Strait are zero, although small quantities linger later to the danger of shipping.

The occurrence of ice all season long near the east coast of Southampton Island is due to discharge of Foxe Basin ice, which thaws, loosens and begins to move south relatively late in the season. The late onset of break-up probably reflects Foxe Basin's more northerly location.

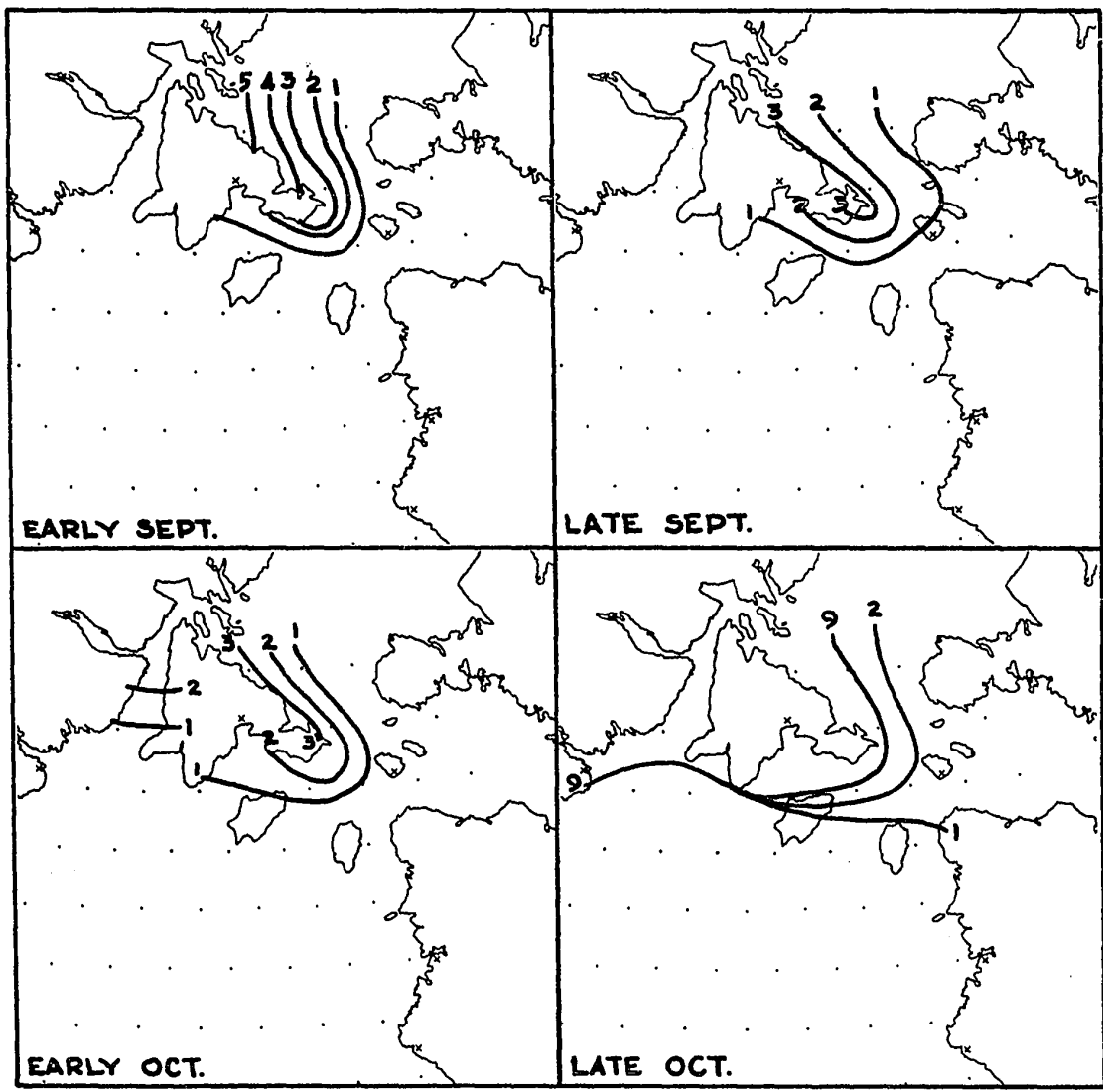


Figure 4-6. Mean ice concentrations in northeast regions for September and October (tenths of coverage).

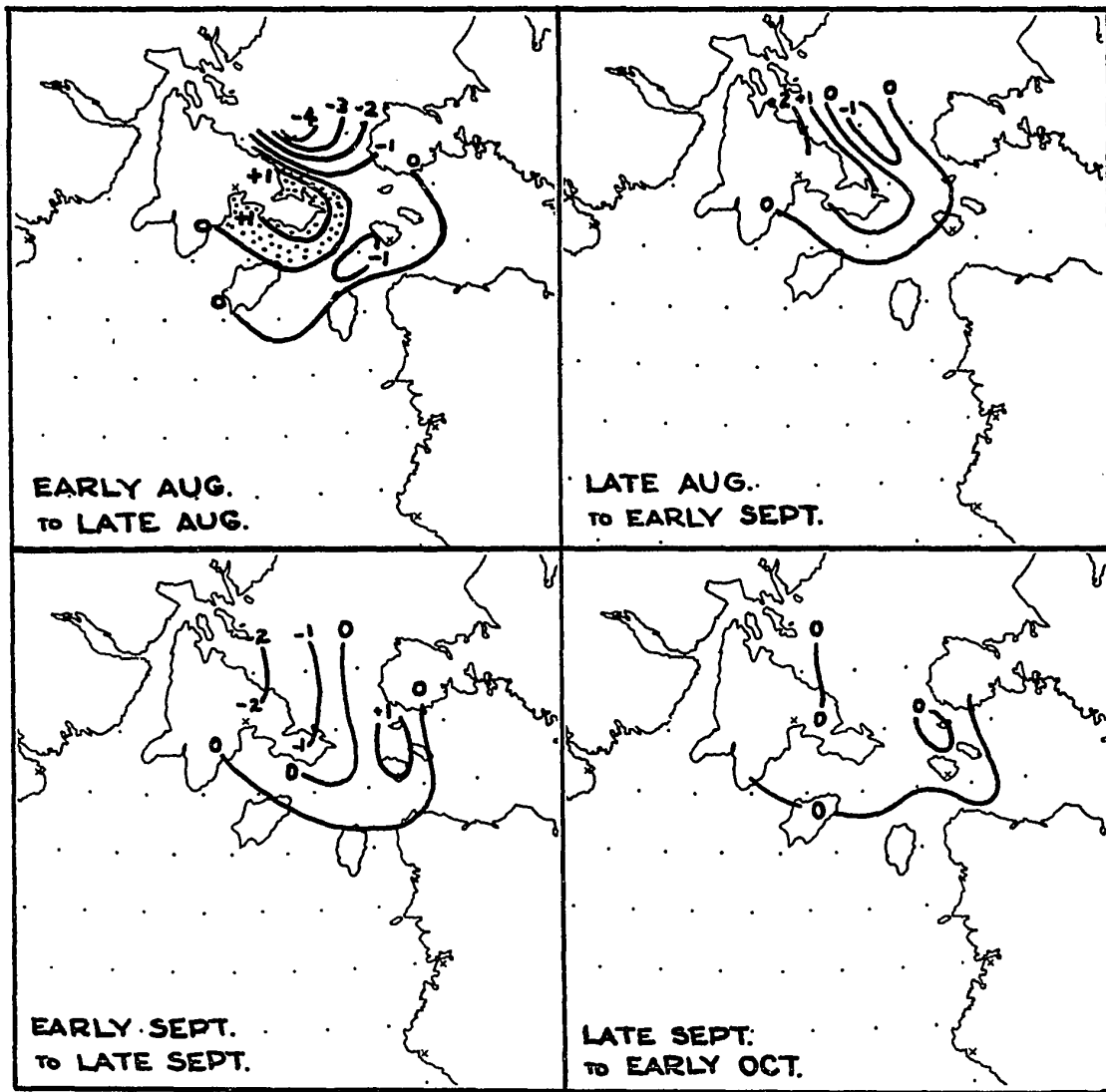


Figure 4-7. Changes with time of ice concentrations in northeast regions.

Bell Peninsula and Foxe Peninsula create a bottleneck at the southern end of Foxe Channel, which likely retards export; also ice enters Foxe Basin from the north through Fury and Helca Strait. As a result of these factors, Foxe Basin and Channel usually contain some ice all year long. Foxe Basin ice moves southward with the current along Southampton Island into Hudson Strait all year, except for the winter months when ice is so extensive that movement is difficult.

As the Foxe Basin ice moves south of 64°N it may take either of two courses: continuing southeastwards, sometimes it proceeds towards the Atlantic along the south side of Hudson Strait; or it may round Bell Peninsula and move south or southwestward into the extreme northeastern parts of Hudson Bay. Variations in wind direction may determine the path taken. In either case it melts steadily in the progressively warmer late summer waters.

Passage of Foxe Basin ice into Evans Strait is well substantiated, (Bennett, 1940, p. 113; Manning, 1943, p. 228) especially under conditions of easterly wind flow in July, August and September. During these months it usually melts before reaching Nottingham Island in the east, or Fisher Strait in the west (Hanson, 1949, p. 14).

By the end of October, however, it is increasing in volume and spreading farther south. By early November it has effectively sealed the west end of Hudson Strait. Since loose ice moves so readily in response to wind, and since the currents between Coats and Mansel Islands are light, some Foxe Basin ice undoubtedly enters Hudson Bay by

this route under northeast winds. The Captain of a Canadian ice patrol vessel reported on 24 September 1931 "35 miles south of Cape Pembroke, Coats Island. Sighted ice field extending north. This is the loose tail end of the ice field off Southampton Island" (Dept. of Marine, 1931, p. 33)

It is apparent then that waters of extreme northeast Hudson Bay are forced to expend some heat in summer and fall, melting ice which originated in Foxe Channel. Although easterly air flow, which probably is necessary for extensive ice transport into the Bay, is not the usual one, it occurs often enough to be significant. An order-of-magnitude computation of the quantity of ice transport appears in Section 4.20.

The ice change maps in late summer and early fall (Figure 4-7) show an interesting feature in northeastern parts. From early to late August ice amounts surrounding Bell Peninsula indicate a slight increase, due apparently to increasing discharge from Foxe Basin. From late August to early September this region of ice increase has moved into central Foxe Channel and away from the coast of Bell Peninsula, with decreasing concentrations again along the east coast of Southampton Island. From early to late September this increasing area is still clearly defined, and farther yet from its source. Increases are general from late September to early October, signifying the start of the winter freeze-up in these regions. Apparently then a wave of higher ice concentrations from Foxe Basin, followed by decreasing values before freeze-up is a regular late summer feature of these regions.

4.15 ROES WELCOME SOUND

Roes Welcome Sound, which has a southward running current, presents another possible route for ice import to Hudson Bay. Aircraft-observed data from the Sound are not plentiful, but seem to indicate that no Foxe Basin ice is carried into Hudson Bay by this route. The Sound clears of ice at about the same time as the northwestern parts of the Bay, and remains ice-free until the October freeze-up. Ice usually persists all summer in Frozen Strait, but it cannot pass the northern point of Southampton Island to move south in important quantities. Some ice may enter the Sound from Repulse Bay in late summer, but it is unlikely that this ice reaches Hudson Bay proper before melting.

4.16 SEPTEMBER, OCTOBER, NOVEMBER, AND DECEMBER

Hudson Bay sees its last ice in August, and remains ice-free through September, except for Foxe Channel ice in the extreme northeast, and rare small patches elsewhere. Summer is short, however, and ice begins re-forming in October. It starts early in the month along the coast (see Figure 4-8) of Southampton Island and on the shores of Roes Welcome Sound, and gradually spreads southwards along the west coast. By the end of October the southern edge of a continuous ice sheet passes through Foxe Channel, southeast of Bell Peninsula by 30 miles or so, just north of Coats Island, close to Cape Kendall, and then to the west shore of the Bay, extending south to Churchill but only a short distance off-shore.

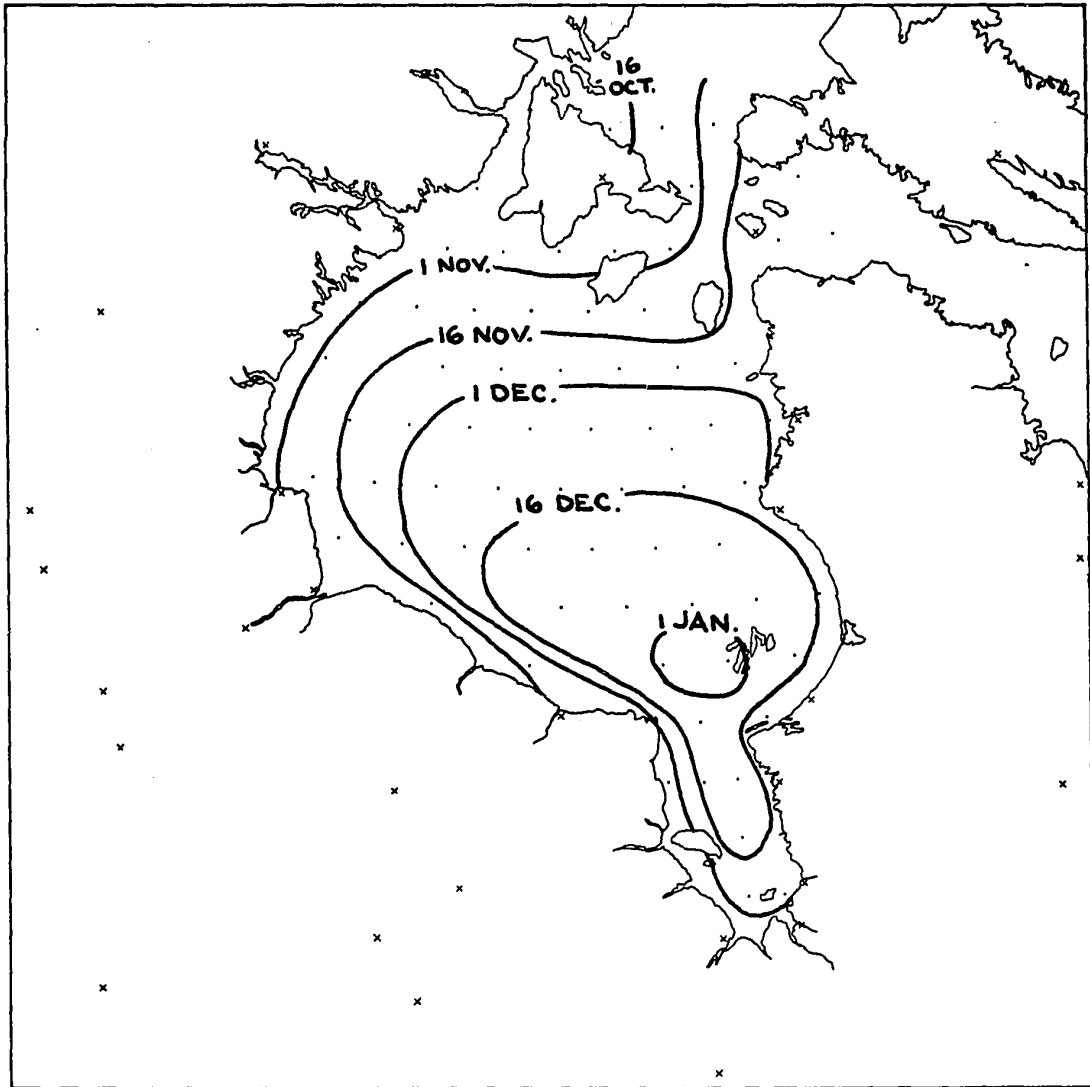


Figure 4-8. Position of the ice pack boundary during freeze-up. Ice concentration is nearly 100% to the northward or coast-side of the position for each date.

By early November the ice extends roughly 50 miles off-shore from Southampton Island to Churchill, and has formed along shore from Churchill to Winisk. Coastal ice is forming locally elsewhere as well, but by far the greatest part of the Bay is open water. The pack ice continues to grow most rapidly from the northwest, although extensive shore ice rings the entire Bay by early December. Observational and climatological evidence indicate that freeze-up is nearly complete by the end of December, with significant amounts of open water (apart from shore leads) only in the extreme southeast. Except for the ever-present shore leads, the surface is entirely ice-covered by early January.

#### 4.17 SUMMARY OF ICE COVER INFORMATION

Figure 4-9 shows mean monthly ice coverage for Hudson Bay as a whole. Mean annual coverage is 57.1%. The great width of the winter maximum seems to emphasize the unalterable reality of Hudson Bay's ice cover. It would appear that no modest climatic variation, natural or man-made, will prevent formation of a complete winter ice surface. On the other hand, the summer's effort to effect open water conditions barely achieves its goal in September before autumn's freeze-up takes over. Thus open water in Hudson Bay appears to be a more tenuous condition than that of ice cover.

This large annual oscillation suggests sizeable variations in heat stored within the Bay. Estimates of these heat storages appear in the following sections.

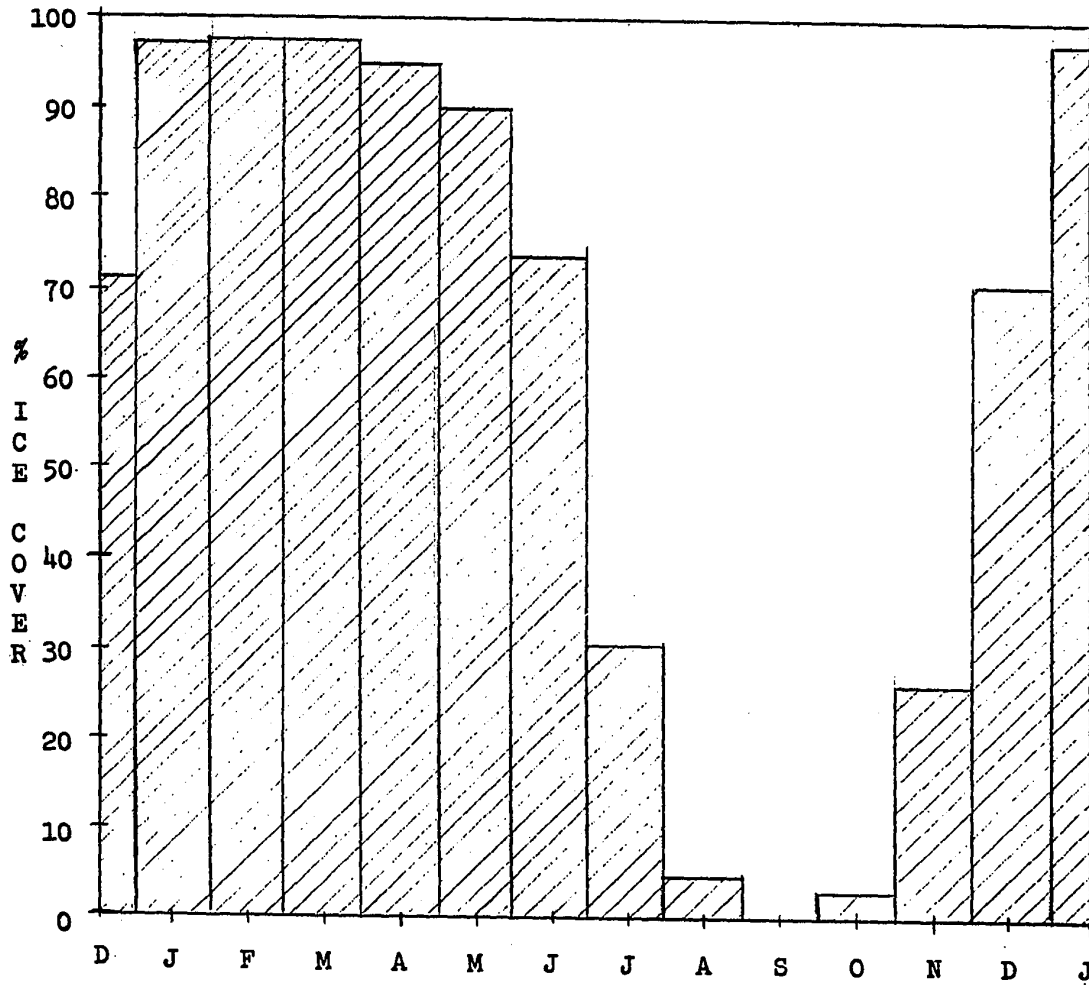


Figure 4-9. Areal Average Monthly Mean Ice Concentrations.

4.18 HEAT CONTENT OF HUDSON BAY ICE

In order to determine the heat deficit implied by Hudson Bay's ice cover, the thickness, temperature, and salinity of the ice must be known, as discussed in Section 2-5.

Ice thickness information was taken from the annual Ice Thickness Data Circulars published by the Department of Transport; from Kniskern and Potocsky (1965), and from Schwerdtfeger (1962). These data allowed an estimate of mean annual maximum ice thickness of 1.8m around the Hudson Bay perimeter. Time of maximum ice thickness, on the average, was early April.

It is quite likely that ice thickness measurements made within a few hundred yards of shore will yield higher figures than what is typical in mid-Bay. The reason is that the shallower waters near shore have less heat stored at depth from the previous summer, and do not freely circulate with deeper waters. In addition, excessive cooling over open shore leads probably assists in thickening the ice pack. Hence, the figure of 1.8m is probably too large for average Bay conditions. A rather arbitrary reduction factor of 0.3m was applied, giving a mean maximum ice thickness of 1.5 meters, occurring in early April. MacKay (1952) also assumed 1.5m to be typical maximum thickness for Hudson Bay ice. Clearly, considerable uncertainty exists in this important figure.

Schwerdtfeger (1962) measured Hudson Bay ice temperatures and salinities off the coast of Churchill in 1961. His data for mean ice

salinity (5 o/oo), density ( $0.90 \text{ gm/cm}^3$ ), and ice temperature in early April (-4 deg. C.) were accepted as mean figures for the Bay.

The latent heat of fusion for ice at 5 o/oo salinity is 68.1 calories per gram of ice (Schwerdtfeger, 1963). Applying this and the values above to Equations 2-17 and 2-18, the heat deficit of 150 cm of ice is found to be

$$\begin{array}{r} -593 \text{ calories due to temperature below freezing point} \\ -9194 \text{ calories in heat of fusion} \\ \hline \text{Total} = -9787 \text{ calories/cm}^2 \text{ of pack ice surface} \end{array}$$

Due mainly to inadequate knowledge of ice thickness, for which the mean maximum figure of 1.5 m may be in error by  $\pm 0.3$  m, the uncertainty in the mean minimum storage figure is estimated at  $\pm 2000 \text{ cal/cm}^2$ .

#### 4.19 ICE EXPORT BY CURRENTS

In Section 3.10, an estimate of 0.3 kts was made for the surface current flowing northward between Mansel Island and Quebec during summer. As no other quantitative estimate of this parameter could be found, the figure was adopted for ice export calculations. As discussed in Section 3.4, this current is the only clearly defined one passing out of Hudson Bay.

Significant amounts of ice export are likely to occur only from late May through July. In other months ice is either too congested or too scarce for export to be important. The ice was assumed to move at half the speed of the current during late May and June, when congestion

probably hampers free movement, and at the full current speed in July. Areal ice coverage for each semi-month for the 35-mile wide channel was taken from Figures 4-2 and 4-3.

The outward moving ice was assumed to be 1.5 meters thick, at a temperature of  $-1.6$  deg C. Thus its heat content was  $-9200$  calories per  $\text{cm}^2$  of ice surface. Application of Equation 2-22 then yielded the following values of heat storage gain due to ice export:

May	June	July
72	92	38 calories/ $\text{cm}^2$ of Hudson Bay surface per month

#### 4.20 ICE IMPORT BY CURRENTS

In Section 4-14 it was mentioned that ice from Foxe Basin enters northeastern Hudson Bay in late summer and fall. (Before that time, Foxe Basin ice is too consolidated for significant southward movement. It may be restrained also by the summer surge of effluxing waters from Hudson Bay (Dept. of Marine, 1931, p. 33)). A knowledge of current speeds and ice concentrations would allow a calculation of the type described in the previous section.

Unfortunately, no estimate of the current speed between Southampton and Nottingham Islands is available. General agreement among oceanographers as to its southward direction (Dunbar, 1958, p. 179; Hachey, 1954, p. 20; Campbell, 1958, p. 47) suggests it must be significant, however. In order to proceed with an order-of-magnitude estimate of transport, an average surface speed of 0.3kts was assumed across the 63-mile wide passage.

Ice concentrations in the region during September and October (Figure 4-6) are approximately 20%. Half of this ice was taken to enter and melt in Hudson Bay, the other half proceeding eastward to Hudson Strait.

Foxe Basin ice is often described as "heavy" and "thick" compared to Hudson Bay ice (Wakeham, 1898, p. 21; U.S.H.O., 1946, p. 373) Binney (1929, p. 7) describes it in late summer as "reaching to a depth of 15 feet or more." Foxe Basin's more northerly latitude also implies the likelihood of greater ice thickness. On the basis of this information, a mean thickness in autumn of 2.5 m was adopted, implying a heat content of  $-15,500$  calories/cm<sup>2</sup> of surface.

Substitution of this information into Equation 2-22 yielded the following very rough estimate of heat deficit imported by Foxe Basin ice:

September	October
58	120 calories/cm <sup>2</sup> of Hudson Bay surface per month

Like the advection figures derived in Chapter 3, the ice transport values are highly uncertain. They are probably within a factor of three of the correct values.

Table 4-1 on page 101 summarizes all storage and advection information, including estimated errors.

TABLE 4-1

SUMMARY OF MONTHLY AND ANNUAL MEAN HEAT STORAGE AND ADVECTION

Units: calories per cm<sup>2</sup> of Hudson Bay surface per month (year)

	J	F	M	A	M	J	J	A	S	O	N	D	ANNUAL TOTAL	ANNUAL UNCER- TAINTY
Maximum Storage													20000	±3000
Minimum Storage													-9787	±2000
Runoff	6	6	19	29	60	150	266	240	129	40	21	9	975	± 240
Snow													-1160	± 200
Water Advection							-286	-436	-384	-109			-1215	to -3645 +405
Ice Advection					72	92	38		-58	-120			24	± 600
Total Advection													-1376	to -3700 +780

## CHAPTER 5

### METEOROLOGICAL CONDITIONS OVER HUDSON BAY

#### 5.1 INTRODUCTION

"Keewatin" means "land of the north wind" in Eskimo. The name is a fitting one for the District bordering Hudson Bay on the northwest: at Chesterfield Inlet, Keewatin's oldest weather reporting station, January surface winds blow from northwest or north 76% of the time (Climatic Summaries, V. II 1959). With winds of such persistence bringing Arctic Ocean air to Hudson Bay, the region is understandably cold. Only on the Aleutian Islands and the Labrador Coast do the conventional limits of "the Arctic" (Hare, 1951 p. 956) extend as far south as they do into Hudson Bay.

Nor is the surface the only level of persistent northerly winds. Maps of mean monthly geostrophic wind speed for 850 through 300 mb over Hudson Bay (Titus, 1967) show not a single exception to cyclonic flow with a northerly component.

The center of action for this northwesterly flow is the western extension of the Icelandic Low, which, depending on pressure level and season, may be found over Baffin Bay or the eastern Canadian Archipelago. In addition, a weak mean high pressure cell appears at the surface during winter months over Mackenzie District (Figure 5-1), which amplifies the gradient across Hudson Bay.

Cyclone tracks lie well south and east of Hudson Bay, except during summer, when high zonal-index "Alberta Lows" frequently skirt

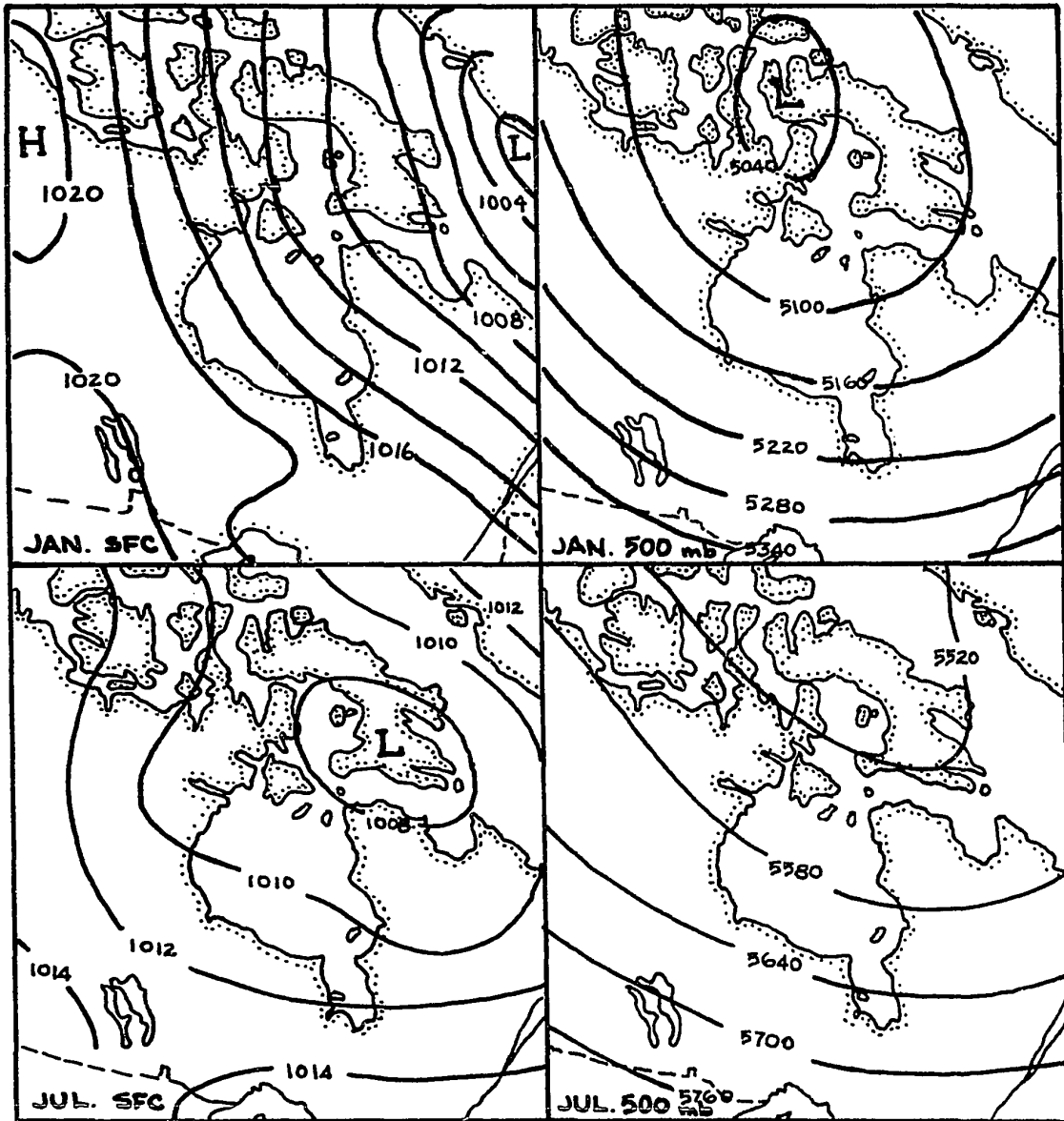


Figure 5-1. Mean January and July surface pressure (in millibars) and 500-millibar (in geopotential meters) contours. Surface data from Atlas of Canada, 1957; 500-mb data from Titus, 1967.

the southern edge of the Bay. The study of weather circulation types referred to in Section 2.1 revealed that the most common daily circulation pattern was a close copy of the monthly mean sea level pressure chart, with low pressure over Davis Strait or Baffin Bay controlling the circulation. The resemblance of daily and mean surface pressure charts for a region is by no means a meteorological necessity; its occurrence over Hudson Bay lends credence to the use of mean surface pressure charts as a description of mean surface wind flow.

The study indicated that low pressure travelling northward into Keewatin District is an especially uncommon occurrence, implying that periods of southerly winds are uncommon. Maritime arctic air from the Labrador Sea occasionally reaches the Bay under easterly flow; in fact this pattern seems to give Hudson Bay its greatest positive winter temperature anomalies.

With these general ideas in mind, attention is turned to methods used in determining local meteorological parameters over Hudson Bay, and the significance of the data obtained.

## 5.2 SURFACE AIR TEMPERATURE

Surface air temperature charts (Figures 5-2) are based on the following data:

(1) monthly mean temperatures were obtained for the years 1942 to 1966 for twenty-seven stations located on the shores of or near Hudson Bay. Corrections to the full 25-year period were made for stations

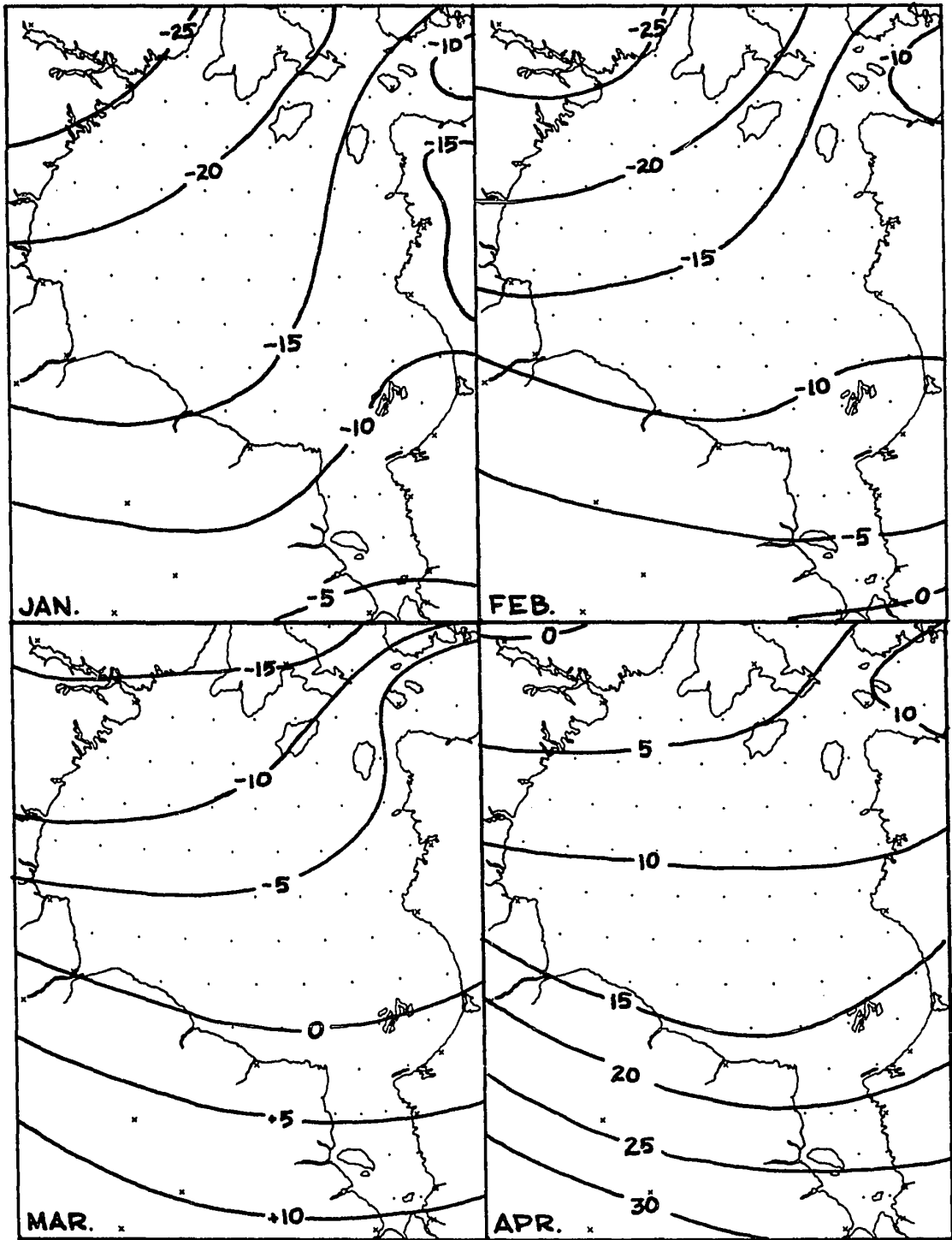


Figure 5-2. Monthly mean surface air temperature (degrees Fahrenheit).

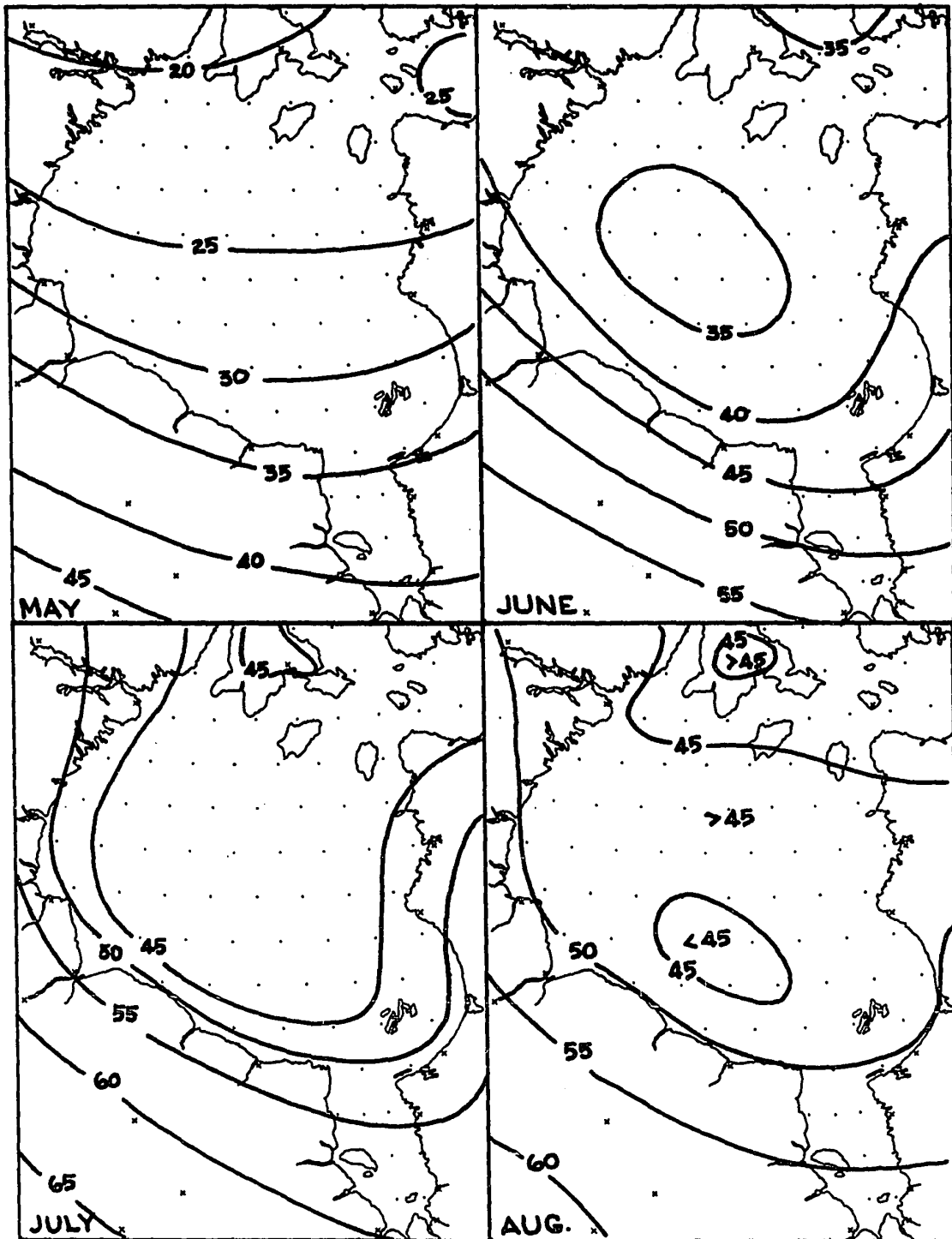


Fig.5-2 cont'd. Monthly mean surface air temperature (degrees Fahrenheit).

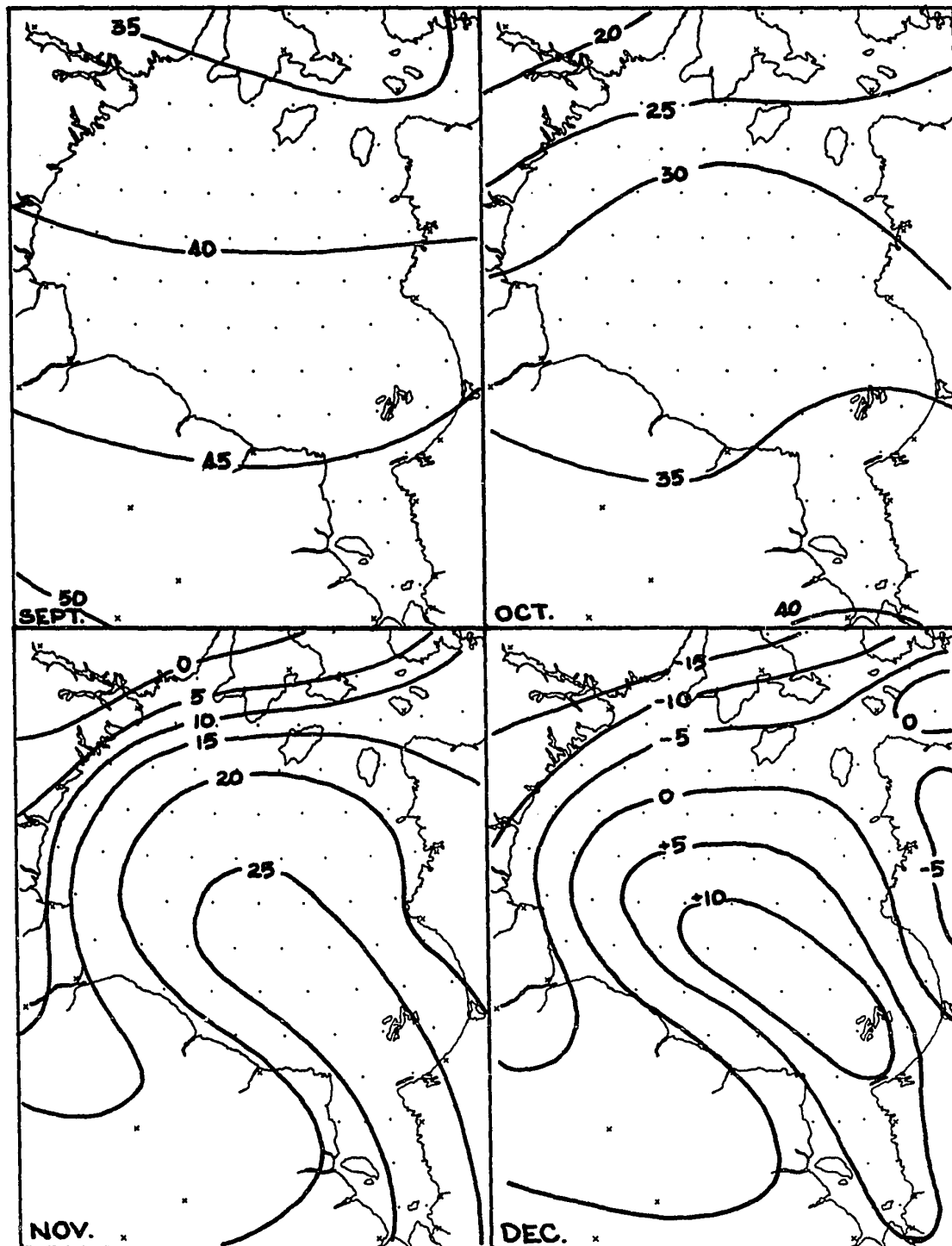


Fig. 5-2 cont'd. Monthly mean surface air temperature (degrees Fahrenheit).

with incomplete data. Data was extracted from The Monthly Record, World Weather Records, and Thompson (1965).

(2) Ship reports from Hudson Bay were also studied and used. In particular, for the months July through September, 248 synoptic weather reports made by oceanographic ships, and weather reports from icebreakers and merchant vessels sailing the Hudson Bay shipping route, were plotted and incorporated.

(3) Data from the U. S. Navy Climatic Atlas of the World, Vol. VI (1963) were also extracted and utilized (Table 5-1). This information relates local air temperature and wind direction, for Churchill, Chesterfield, and Port Harrison. Especially during months when ship reports were lacking, these temperatures provided useful guides in isotherm construction.

(4) Air modification determinations made by Burbridge (1949, p. 102-104) gave much useful information about air-sea temperature differences.

(5) Ice charts discussed in the previous chapter served as general guides.

The resultant charts appear in Figure 5-2 as monthly mean maps. Noteworthy features are described below.

The January chart shows eastern parts of the Bay decidedly warmer than the western regions. Port Harrison's temperature of -12.1 deg. F is over 5 deg. F warmer than Churchill's. As discussed

TABLE 5-1

## MONTHLY MEAN SURFACE AIR TEMPERATURE (deg. F) BY WIND DIRECTION.

Data extracted from Marine Climatic Atlas, Vol. VI.

"w" and "c" indicate warmest and coldest temperatures,

respectively, for each month.

JAN FEB MAR APR MAY JUN JUL AUG SEP OCT NOV DEC

CHESTERFIELD INLET:

NE	-10	-15	-5	8	23	36	44	46	36	22	6	-7
E	-6w	-9	2w	15w	27	34	43	45	38	26	14	5
SE	-6w	-5w	-2	15w	26	33c	42c	44c	39w	30	21w	0
S	-8	-6	-1	14	26	35	43	45	38	32w	18	2
SW	-11	-11	1	10	28w	36	51	48	39w	28	11	6w
W	-21	-25	-11	3	22	37w	52w	50w	38	18	1	-13
NW	-29	-30c	-19c	-2c	15c	36	51	49	37	16c	-10c	-21
N	-30c	-29	-15	0	19	37w	50	49	35c	18	-5	-22c

CHURCHILL:

NE	-10	-9	5w	16	28	39	49	50	41	33w	22w	5w
E	-12	-10	5w	20w	30	42	52	52	41	31	21	5w
SE	-8w	-8w	1	19	31	47	56	53	42	33w	18	1
S	-16	-8w	5w	19	37w	49	58	55	44	32	14	-2
SW	-20	-14	-2	17	36	52w	59w	57w	46w	30	11	-12
W	-24c	-21c	-11c	8c	23c	42	53	54	42	27	4	-15c
NW	-19	-15	-9	10	24	37c	49	49	41	26c	8c	-9
N	-9	-8w	3	15	27	37c	47c	48c	40c	31	20	1

PORT HARRISON:

NE	-13	-12	1	16	29	46	53	52	41	27c	11c	2
E	1w	-5	8	21	36w	49w	55w	54w	44w	31	18	7
SE	-1	1w	9w	23w	35	43	51	50	44w	35	25	9w
S	-11	-9	1	18	32	42	46	48	44w	37w	29w	7
SW	-15c	-14	-1	19	28	36c	45c	45c	41	34	25	4
W	-13	-15c	-2c	11c	27	38	47	46	41	32	22	-2
NW	-6	-10	0	18	25c	38	47	47	39c	29	15	4
N	-12	-9	-2c	11c	28	41	51	48	40	28	13	-4c

JAN FEB MAR APR MAY JUN JUL AUG SEP OCT NOV DEC

in Chapter 4, part of the relative mildness of Great Whale River's temperature (-8.8 deg. F) is accounted for by the presence of open water to the north during the early days of the month. The remainder of this general west-to-east warming trend must occur by way of heat fluxes through leads and the as yet thin ice cover. This idea gains credit as charts for February, March, and April are examined. The east-west temperature gradient declines as the ice thickness increases, so that by April Port Harrison and Churchill show a difference of only 0.4 deg. F. Earlier charts (e.g. Hare, 1950), drawn with considerably fewer data, showed the January and February east-west gradient much less clearly.

From May through July, Hudson Bay develops and intensifies its role as a cooling agent. Most extreme conditions appear in July, with mid-Bay temperatures more than 10 deg. F colder than on the western shore. Coldest air is associated with the dwindling pack ice in the southwest, but in all regions the Bay is colder than the surrounding land. Table 5-1 shows that from June to August the lowest temperatures at Port Harrison, Churchill, and Great Whale River come with wind off the Bay. Baker Lake, Northwest Territories, and Great Whale River, Quebec, although separated by 9 degrees of latitude, have equal July mean temperatures.

September shows little contrast between air and water temperatures. From October through December Hudson Bay supplies the

air with vast amounts of heat, with the result that a surface air temperature maximum occurs over the Bay. Warmest wind directions for the three stations in Figure 5-1 are in each case off the Bay.

Cold air, skirting the southwest edge of the Bay, travels little modified into central Ontario, where November and December temperatures are lower than much farther directly north, over the Bay. December temperatures higher than 10 deg. F over southeastern parts of the Bay quickly disappear, however, as the ice cover forms and the isotherm positions shift again to January's pattern.

### 5.3 VAPOUR PRESSURE

Charts of monthly mean surface air vapour pressure were constructed using data from 1942 to 1966 for most of the same stations as in the air temperature study, as well as weather reports from oceanographic vessels. As mentioned in Chapter 2, the procedure was to find the monthly mean relative humidity from data in the Monthly Record series, then to use monthly mean temperature and relative humidity to arrive at vapour pressure through Equation (2-15).

Vapour pressures for air below freezing were based upon saturation vapour pressure with respect to ice.

At temperatures far below freezing (below 0 deg. F), relative humidity measurements are unreliable, if made at all. Hare and Orvig (1958, p. 170) state "Malmgren found that the winter air over the Arctic Ocean was, as a rule, saturated with water vapour".

In any case the saturation vapour pressure is so small at low temperatures that small errors in relative humidity are unimportant. For the present study, all air temperatures below 0 deg. F were assumed to imply 100% relative humidity (with respect to ice).

The "Theta" oceanographic research vessel reported dry-bulb and wet-bulb temperatures at 129 stations in Hudson Bay during July and August, 1961 (C.O.D.C., 1964). As would be expected, this information implied very high humidity for open water in July and August. Mean wet-bulb depression for 44 July observations was 0.9 deg. C; for 85 August observations, 0.7 deg C.

Figures 5-3 show vapour pressure distributions for Hudson Bay, based on the above data. Maps for January through April are not included, as they are identical in pattern to temperature maps for those months.

In May a tendency appears for higher vapour pressures over the Bay than over surrounding land, especially in southern portions. Both Great Whale River and Port Harrison show values slightly higher than their west-coast counterparts (Winisk and Churchill).

Vapour pressure in June, July and August is lower over Hudson Bay than over surrounding land. This oddity results from the fact that the water (and ice) surface is much cooler than unmodified air beginning to cross the Bay. The air is cooled to saturation and below, thereby losing water vapour through condensation. Mean vapour

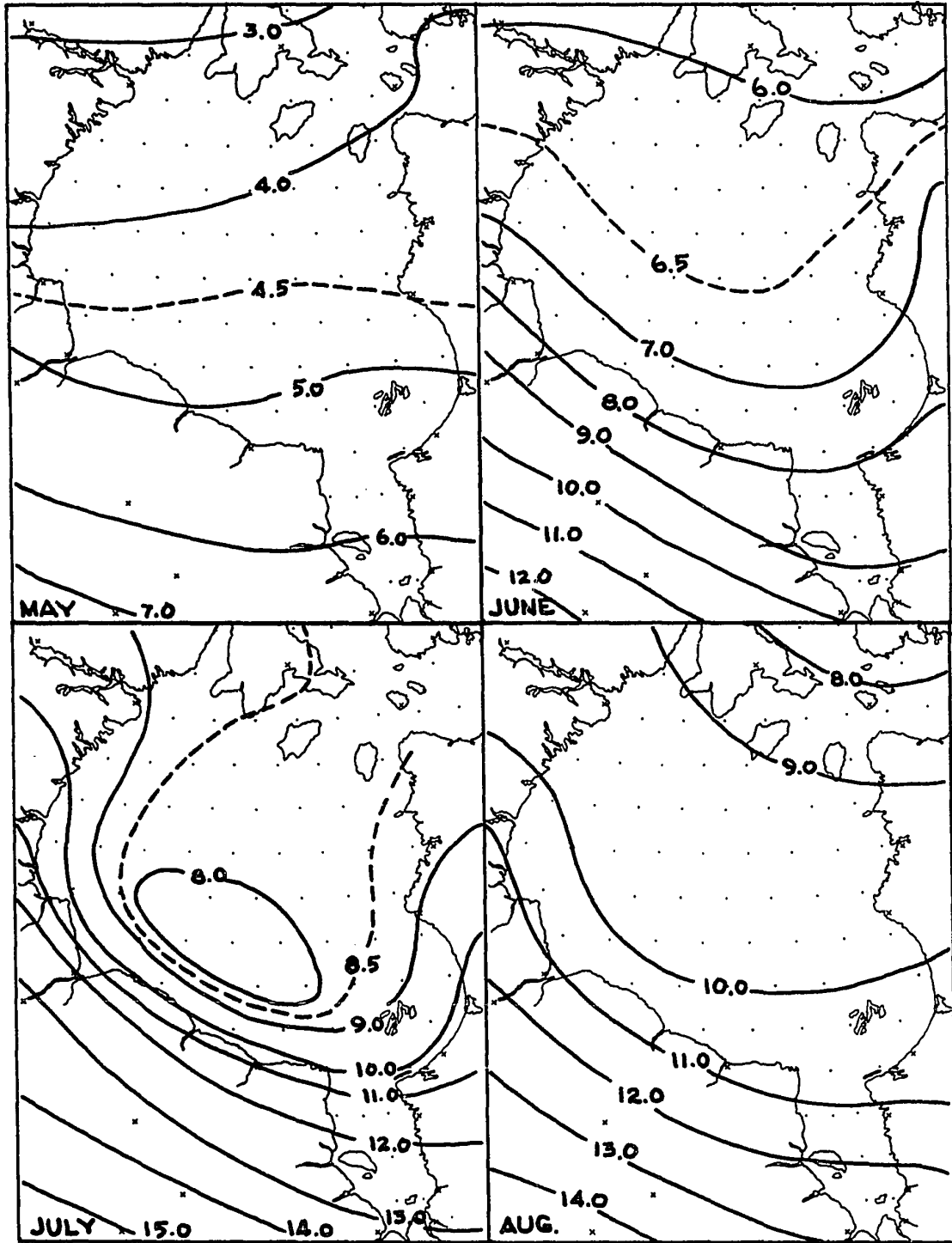


Figure 5-3. Monthly mean surface air vapour pressure (millibars).

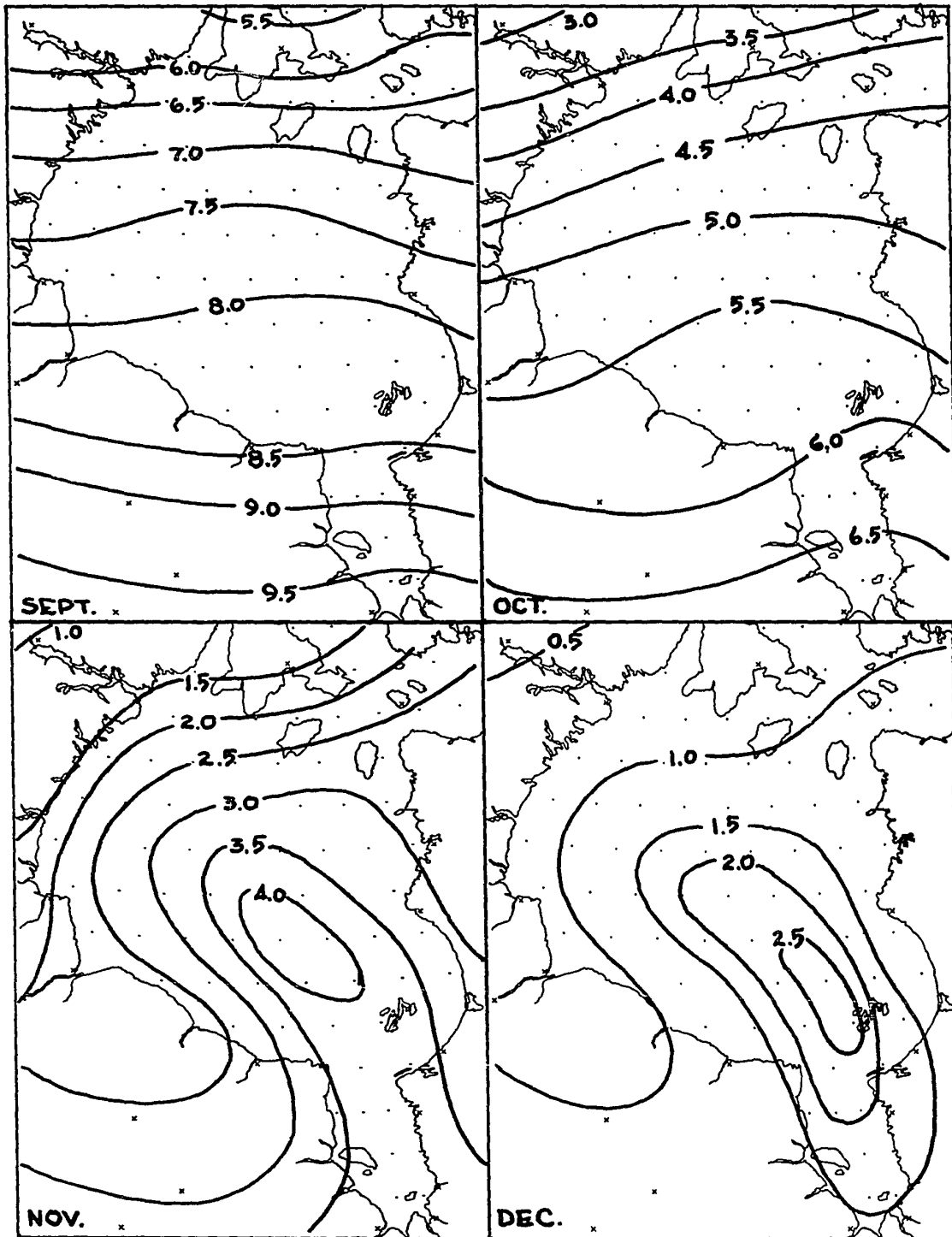


Fig. 5-3 cont'd. Monthly mean surface air vapour pressure (millibars).

pressure at Churchill from June through August is 1.2 mb higher than at Port Harrison, and higher than at Great Whale River in July and August. The similarity between summer vapour pressure and temperature patterns over Hudson Bay is a striking example of thermally influenced moisture conditions.

In September, mid-Bay vapour pressure appears to be slightly higher than inland. This tendency becomes an intense maximum in November and December, as cold air crossing the open Bay absorbs large amounts of heat and moisture. Once again, resemblance between temperature and vapour patterns for these months reflects the dependence of the latter on the former.

#### 5.4 SURFACE WIND

Information pertaining to surface winds on Hudson Bay is of three forms: observed winds at costal stations, wind reports from ships, and geostrophic winds inferred from isobaric charts. Each of these sources was used in the present study.

Surface winds observed at coastal stations often suffer serious bias due to local exposure. Climatological records at different stations are based on records made with anemovanes at different heights above varying kinds of ground cover, in different sorts of terrain. Surface winds respond so quickly to these variations that a station a few hundred yards inland from Hudson Bay may not record typical over-water winds, even during periods with wind-flow directly off the Bay. As a result, attempts

to draw monthly mean wind speed charts based on coastal reports showed little or no spatial continuity.

Ships' weather reports, including those from oceanographic vessels, give wind speed based on the Beaufort scale. The limited number of these reports further restricts their usefulness. Nevertheless, wind speed reports from the "Theta" (C.O.D.C., 1964) and the "MacDonald" (C.O.D.C., 1966) were examined in the following manner.

Each ship observation made within three hours of 0000 GMT was compared with (1) wind speeds reported at nearby coastal stations at 0000 GMT, and (2) geostrophic wind speed determined at 0000 GMT from Deutscher Wetter Bericht series. In all, forty-one reports from July and August 1961 and September 1962 were used.

Mean geostrophic wind speed for the 41 observations was 15.1 kts. Mean speed for ships' reports was 68% of geostrophic, while mean coastal station wind speed was 59% of geostrophic. This limited information suggested that wind speeds over Hudson Bay in summer were somewhere in value between those coastally observed and geostrophic. Accordingly, a closer look was taken at geostrophic speeds.

For the years 1959-1961, geostrophic wind speed was measured each day at 1200 GMT over Chesterfield Inlet and Great Whale River, on the Daily Series, Synoptic Weather Maps (U.S.W.B., 1964-1966). The method followed was that of Walmsley (1966). Measurements were made directly at the stations for purposes of comparing geostrophic and observed surface speed. Selection of the two stations was made more

or less at random; their positions on opposite sides of the Bay, and the availability of surface data, were the only considerations.

The geostrophic speeds obtained were averaged at each station by month. Due to the shortness of the period (3 years), a further smoothing seemed advisable, and was accomplished by taking overlapping monthly means. The mean monthly geostrophic speed  $\bar{V}_i$  was weighted with the speed for the previous month ( $\bar{V}_{i-1}$ ) and the following month ( $\bar{V}_{i+1}$ ) according to

$$\bar{V}_i' = \frac{1}{2}\bar{V}_i + \frac{1}{4}(\bar{V}_{i-1} + \bar{V}_{i+1})$$

where  $\bar{V}_i'$  is the new weighted mean monthly speed.

Results are summarized in Figure 5-4. The upper two dashed curves are  $\bar{V}_i'$ , the 3-monthly running mean for each station. The lower two dashed curves are 15-year monthly mean surface wind speeds for the two stations, taken from Climatic Summaries, Vol. II (1959).

It is interesting to observe that geostrophic wind speeds at Great Whale River are stronger than those at Chesterfield in every month, while, with the exception of July, the reverse is true of observed surface winds. As a result, annual mean surface winds at Chesterfield are 74% of geostrophic, while at Great Whale the figure is only 56.5%. This is probably attributable to local exposure differences, for Chesterfield lies on flat barrens, while Great Whale River is in an area of greater relief, with hills 1000 feet high a few miles northeast. In addition, anemovane height at Chesterfield is 45 feet, at Great Whale, 30 feet (Climatic Summaries, Vol. II, 1954).

Since the geostrophic and observed winds give contradictory indications as to where the wind is strongest, it seemed safest to combine SE and NW values into a single geostrophic and a single observed speed for each month. These values appear in Figure 5-4 as solid lines.

Walmsley (1966) compared observed and geostrophic wind speeds at ship "B" (56.5 deg. N, 51 deg. W) for winter months and found that monthly mean observed speeds ranged from 82% to 106% of geostrophic, averaging 91%. Sheppard, et al, (1952) performed the same calculation under slightly unstable conditions in the eastern Atlantic and obtained a figure of 88%. Their values, as well as Hudson Bay ship reports, suggest that mean speeds appropriate for the Bay should be less than geostrophic, but more than observed at coastal stations. As a first approximation, a value halfway between observed and geostrophic was taken for each station, each month. This speed is indicated by the dotted line in Figure 5-4; it varies in magnitude from 78% to 85% of geostrophic. Since these percentages seem to suggest a fair compromise of the various information, the curve, labelled  $\bar{V}_f$ , was accepted as representing mean monthly surface winds over Hudson Bay. These speeds are listed below.

TABLE 5-2

MEAN MONTHLY SURFACE WIND SPEED OVER HUDSON BAY												
MONTH	J	F	M	A	M	J	J	A	S	O	N	D
SPEED (Meters per second)	7.9	7.2	7.1	7.4	7.1	6.5	6.9	7.8	8.8	8.9	8.6	8.5
PERCENT OF MEAN GEOSTROPHIC	85	83	83	82	83	80	79	78	82	84	83	84

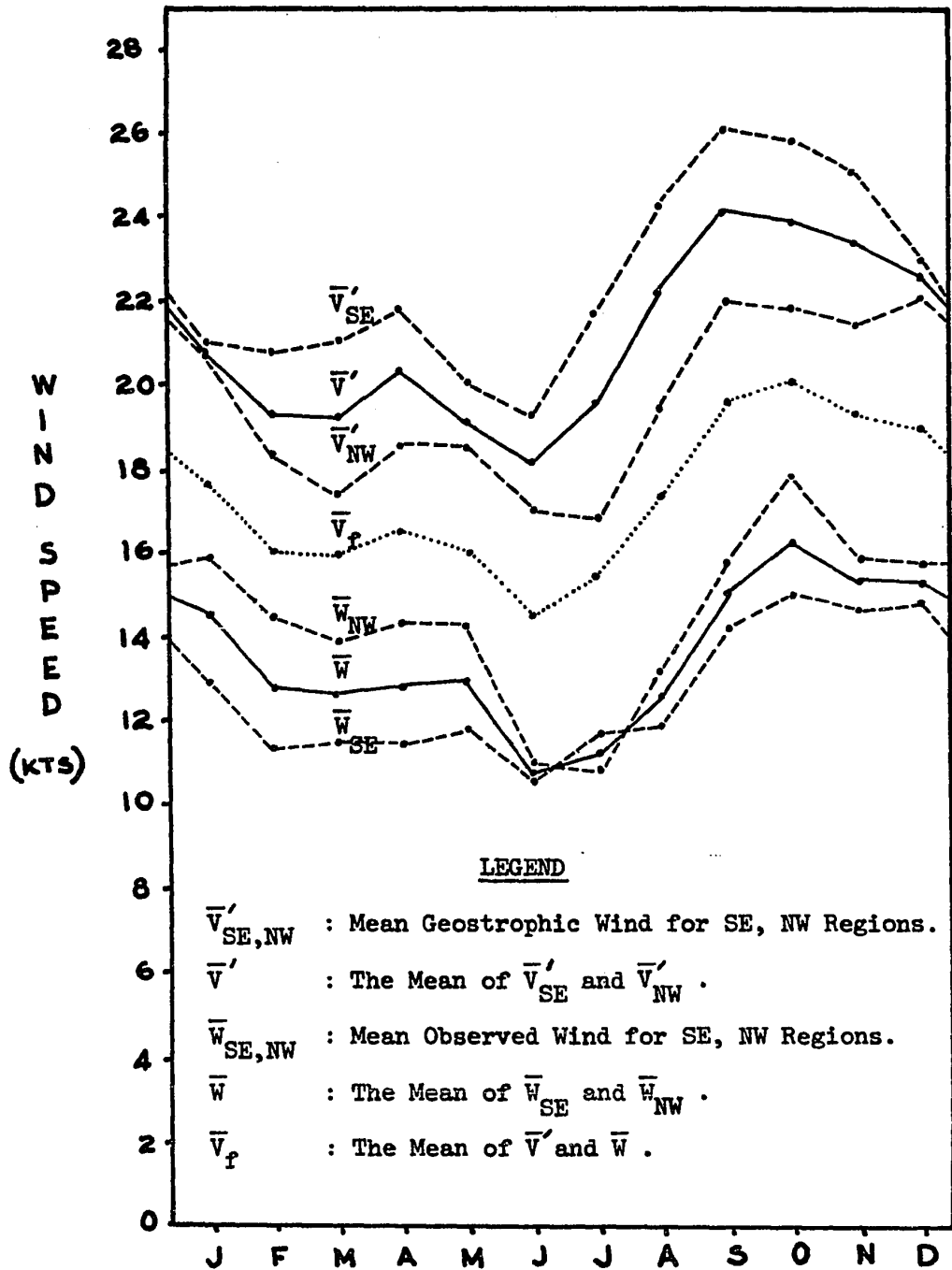


Figure 5-4. Mean Surface Winds over Hudson Bay: Geostrophic and Observed.

It is regrettable that all spatial variation of wind speed was lost by using one figure for each month, but under the circumstances it seemed the wisest course.

The shapes of the annual wind curves are worthy of note. Maxima of both geostrophic and observed speeds appear in fall, the result perhaps of vigorous cyclonic activity stimulated by diabatic heating. Similarly, minima appear in June and July, when surface cooling would hamper cyclogenesis and encourage high-pressure dominance (see Johnson, 1948). Observed wind speeds are the greatest percentage of geostrophic during the autumn months, where instability encourages mixing. Lowest percentages appear in June, July, and August, when low levels are stably stratified.

#### 5.5 TEMPERATURE AND HUMIDITY ALOFT

Six radiosonde stations (Baker Lake, Churchill, Trout Lake, Moosonee, Port Harrison and Coral Harbour) ring Hudson Bay, giving that area better coverage than most arctic regions. The basic source for this data was Titus' (1965, 1967) maps and tabulations for the years 1951-1960.

Mean monthly temperatures for 850, 700, 500, and 300 mb at each grid point were read directly from Titus' charts. As mentioned in Section 2.3 the months of April, July, and August required the use of 950 mb temperatures as well; those charts were constructed from the tabulations.

Titus' tabulations of humidity aloft for each radiosonde station were used to arrive at specific humidity at each station for

each month, at (950), 850, 700, 500, and 300 mb. With these data specific humidity charts were drawn for each level and each month. Precipitable water (W) for each layer ( $\Delta p$ ) was then determined at each point by

$$W = \bar{q} \frac{\Delta p}{1000}$$

where  $\bar{q}$  = mean layer specific humidity.

As discussed in Section 2.3, mean moisture data was reduced 15% for cloud-free calculations.

Maps of temperature and humidity aloft were not included in the present paper, as they are available in identical or similar form in Titus (1967).

## 5.6 CLOUDINESS

Cloudiness is probably the most complex meteorological variable to consider. In attempting to determine representative values for heights, amounts, and frequencies of occurrences of different cloud types, many difficulties arise associated with inadequate data. As a result, various approximate procedures must be invoked.

"Monthly mean total cloudiness" is the fraction of the mean monthly sky hidden by clouds or obscurations such as fog, precipitation, and blowing snow. Data for this parameter were obtained for 27 stations around Hudson Bay by extraction from 10 years (1956-1965) of the Monthly Record series. In addition, observations made from oceanographic ships "Theta" and "MacDonald" in 1961 and 1962 were used. Results are presented in Figure 5-5 and will be discussed shortly.

For the present study, monthly mean amounts of different cloud types had to be found. Since no information of this sort exists in comprehensive yet convenient form, the following methods were employed.

In the General Summaries of Hourly Weather Observations in Canada are tabulations of "Number of Hours With Various Cloud Forms" for each station in Canada, for each month of the year. Cloud forms were grouped into the following categories:

<u>CLOUD TYPE</u>	<u>CLOUD FORMS</u>
(1) Stratus	: Obscurations, Stratus, Fractostratus, and Nimbostratus.
(2) Stratocumulus	: Stratocumulus, Cumulus, Fractocumulus, Cumulonimbus, and Heavy Cumulus.
(3) Middle Clouds	: Altostratus, Altocumulus, and Altocumulus Castellanus.
(4) Cirriform Clouds	: Cirrus and Cirrostratus. Cirrocumulus was not included since other cirriform clouds must be present before Cirrocumulus may be reported.

The number of hours recorded for all cloud forms comprising a given type were added together, giving the total numbers of hours associated with each cloud type for the month. The monthly coverage of each cloud type was assumed to be proportional to the sum of the hours of the component forms. Thus monthly mean cloudiness could be partitioned into cloud cover by type. This procedure was followed for five years of data (1957-1961), for 8 stations on the coast of Hudson Bay (Chesterfield, Coral Harbour, Nottingham Island, Port Harrison, Great Whale River, Moosonee, Winisk, and Churchill).

Although some correlation is certainly to be expected between the number of hours a cloud type is reported and its mean coverage, there is no reason that the linear proportionality assumed above should hold. When two or more cloud forms appear in one hour, all are reported. Thus the sum of a cloud type's component hours is nearly always larger than the amount of time in a month the type was present; in fact it is quite possible for the sum of component hours to exceed the number of hours in a month. Since the observations are more discriminating of low clouds, with more forms in the low cloud types than in middle and high clouds, the low clouds would seem to be overestimated by the proportionality assumption.

On the other hand, high and middle clouds will be partly hidden by lower clouds at times. This would suggest that straight proportionality between cloud hours and amounts would underestimate low cloud amounts.

Data of Kendrew and Currie (1955, p. 105) provided a rough and limited check on the validity of the proportionality assumption. They present "mean monthly duration (hours) of Low Cloud (in tenths of sky covered), and of Sky Obscured (by fog, precipitation, smoke)" for Churchill from 1946 to 1950. The data are grouped by coverage of 0 to 2/10, 3 to 7/10, 8 to 10/10 and sky obscured. Assuming that the center of each range adequately represents the group allowed a simple determination of mean low cloud coverage for each month. Results appear in line (1) of Table 5-3.

TABLE 5-3

## MEAN LOW CLOUD COVERAGE AT CHURCHILL (% OF SKY)

MONTH	J	F	M	A	M	J	J	A	S	O	N	D
FROM KENDREW AND CURRIE	29	18	23	34	56	36	37	34	46	62	45	30
(St & Sc)	22	17	21	33	50	45	33	38	47	61	52	31
WEIGHTED (St & Sc)	25	20	24	39	61	55	41	46	57	72	61	36

Line (2) shows the sum of stratus and stratocumulus types determined from the proportionality assumption. Line (3) shows the sum of stratus and stratocumulus when higher clouds have been reduced in proportion to low clouds by amounts proportional to lower cloud cover.

Table 5-3 indicates that the proportionality assumption provided a fair estimate of low cloud amounts. No large consistent over- or underestimates appeared, and in six of the months values came to within 2 units (%) of each other. Reduction in high cloud amounts (line 3) consistently overestimated low cloud amounts, especially in months of large low cloud amounts.

In the absence of information to the contrary, therefore, total cloudiness was partitioned into types according to the proportion of hourly observations associated with each type. The resulting data allowed preparation of maps of mean monthly cloud cover for each cloud type. Cloudiness data from the U.S. Naval Climatic Atlas, Vol. VI (1963), relating low cloud frequencies to wind direction for Port Harrison, Churchill, and Chesterfield, aided in map construction.

For long-wave radiation calculations, it is necessary to know the mean height of each cloud type.

Mean height for stratus clouds was determined from cloud height tabulations in the General Summaries for Great Whale River and Churchill, from 1957 to 1961. Tables give the number of times each month that cloud ceilings were observed at 0, 1, 2, 3, 4, 5, 6-7, 8-9, 10-14, 15-29, and 30-79 100's of feet. Assuming that stratus clouds and obscurations were solely responsible for the ceilings below 1500 feet, a mean height of 500 feet was determined. As variations in place or time of year were found to be small, the figure was accepted for all stratus everywhere in Hudson Bay.

Stratocumulus was placed midway between the surface and 850 mb, giving a mean height of approximately 2300 feet. Height groupings described above in the General Summaries precluded detailed study of heights in this range; thus the stratocumulus height was chosen largely for computational convenience. Nonetheless, the mean height of 2300 feet does not seem at variance with the information in the General Summaries.

For middle and high clouds, very few height measurements are available. Cirriform and middle clouds were taken to be at 400 mb and 700 mb respectively (approximately 23,000 and 9500 feet), as more or less traditional heights for these types at Hudson Bay latitudes. It was shown in Chapter 2 that these heights may be somewhat in error without significantly altering radiation income.

Significant features appearing on the monthly mean cloud charts (Figures 5-5, 5-6, and 5-7) will now be discussed. Only those cloud type

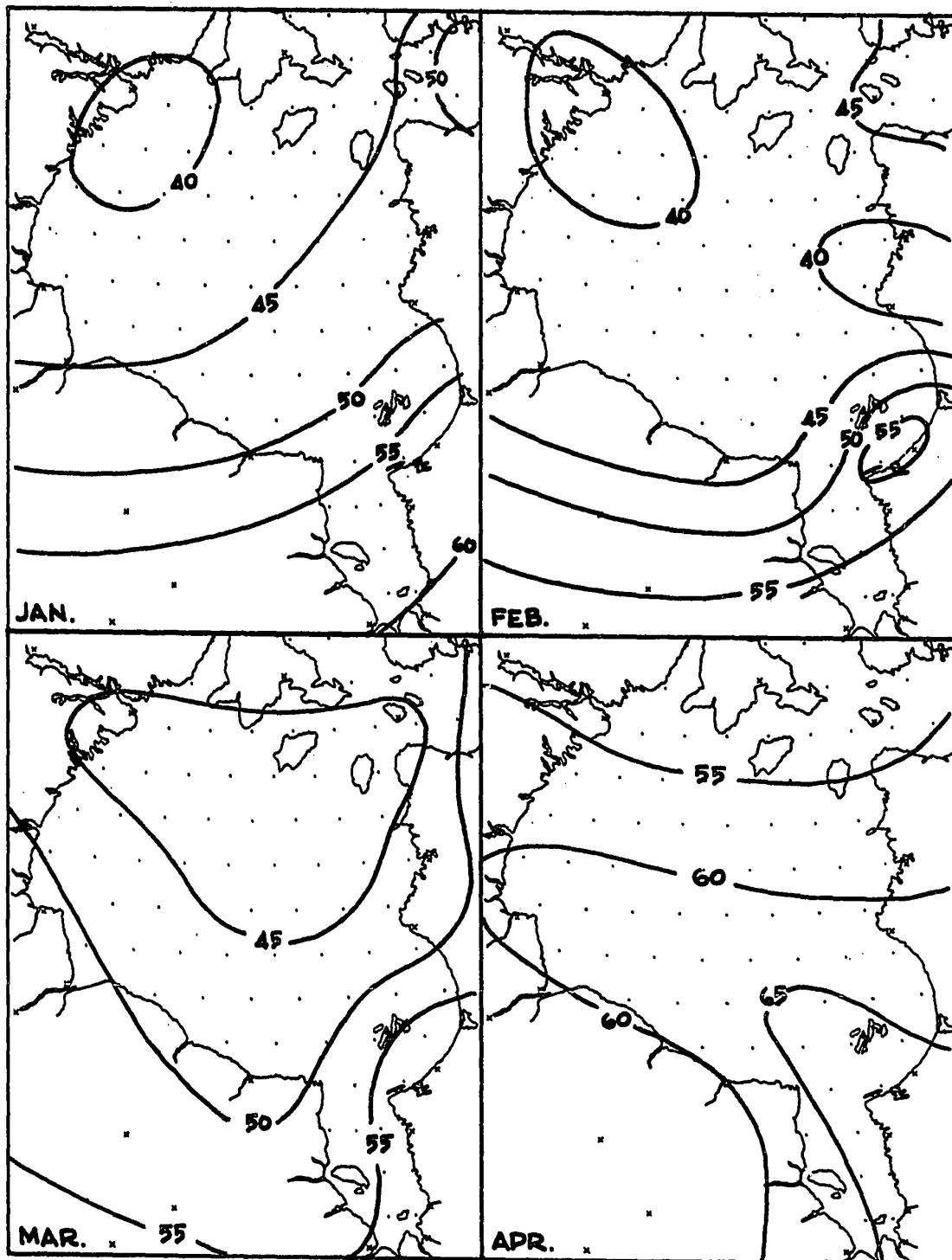


Figure 5-5. Monthly mean total cloud cover (percent of sky covered).

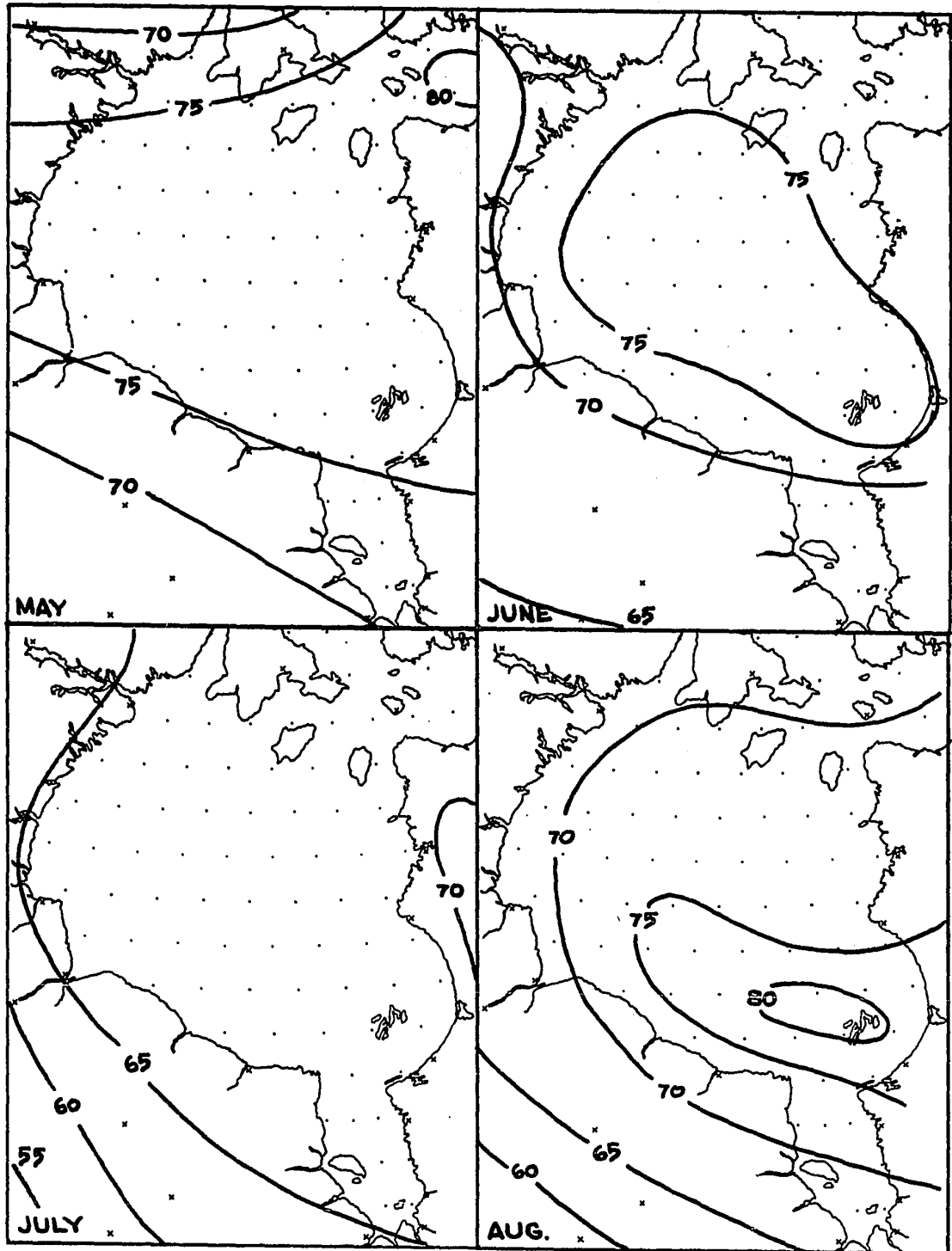


Fig. 5-5 cont'd. Monthly mean total cloud cover (percent of sky covered).

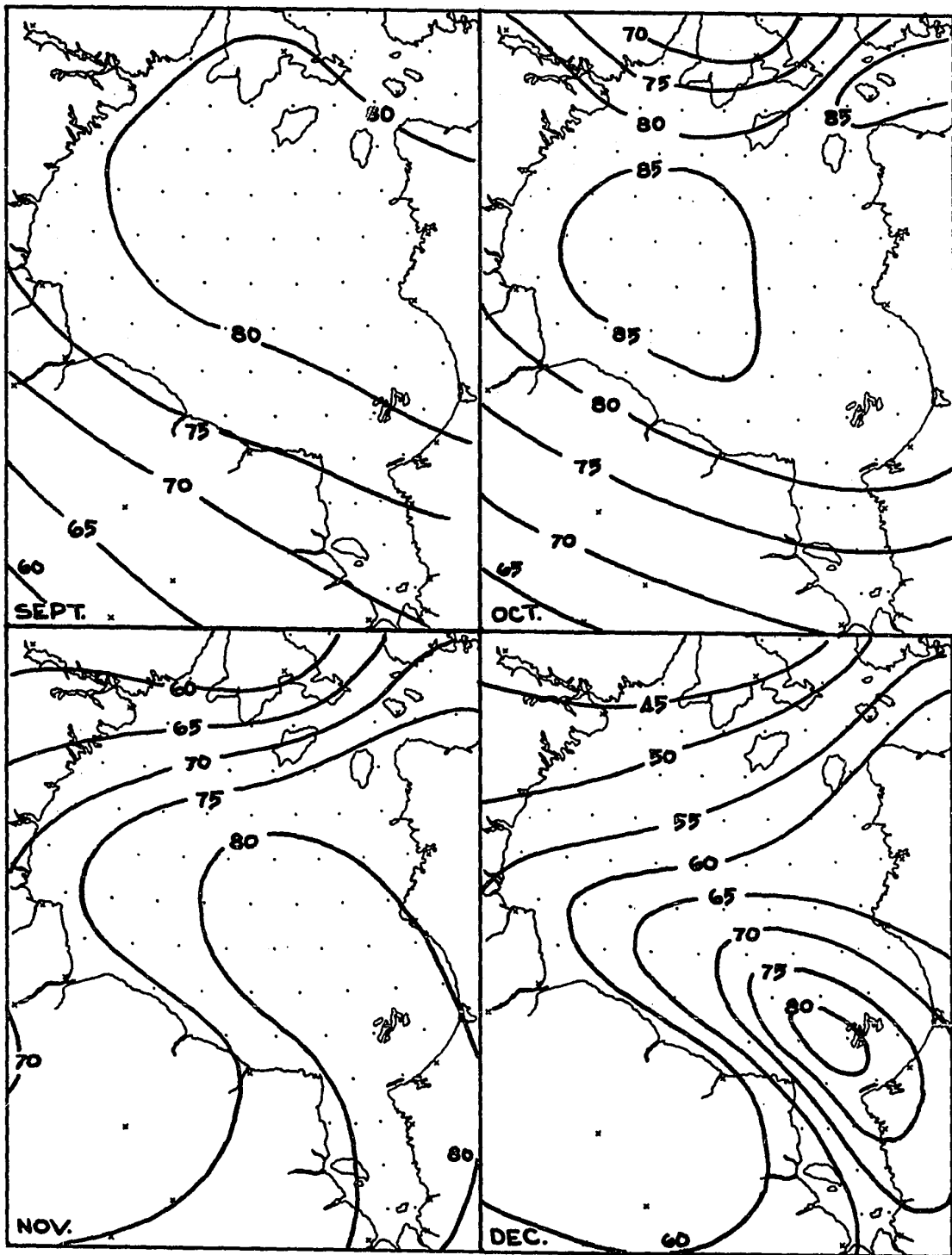


Fig. 5-5 cont'd. Monthly mean total cloud cover (percent of sky covered).

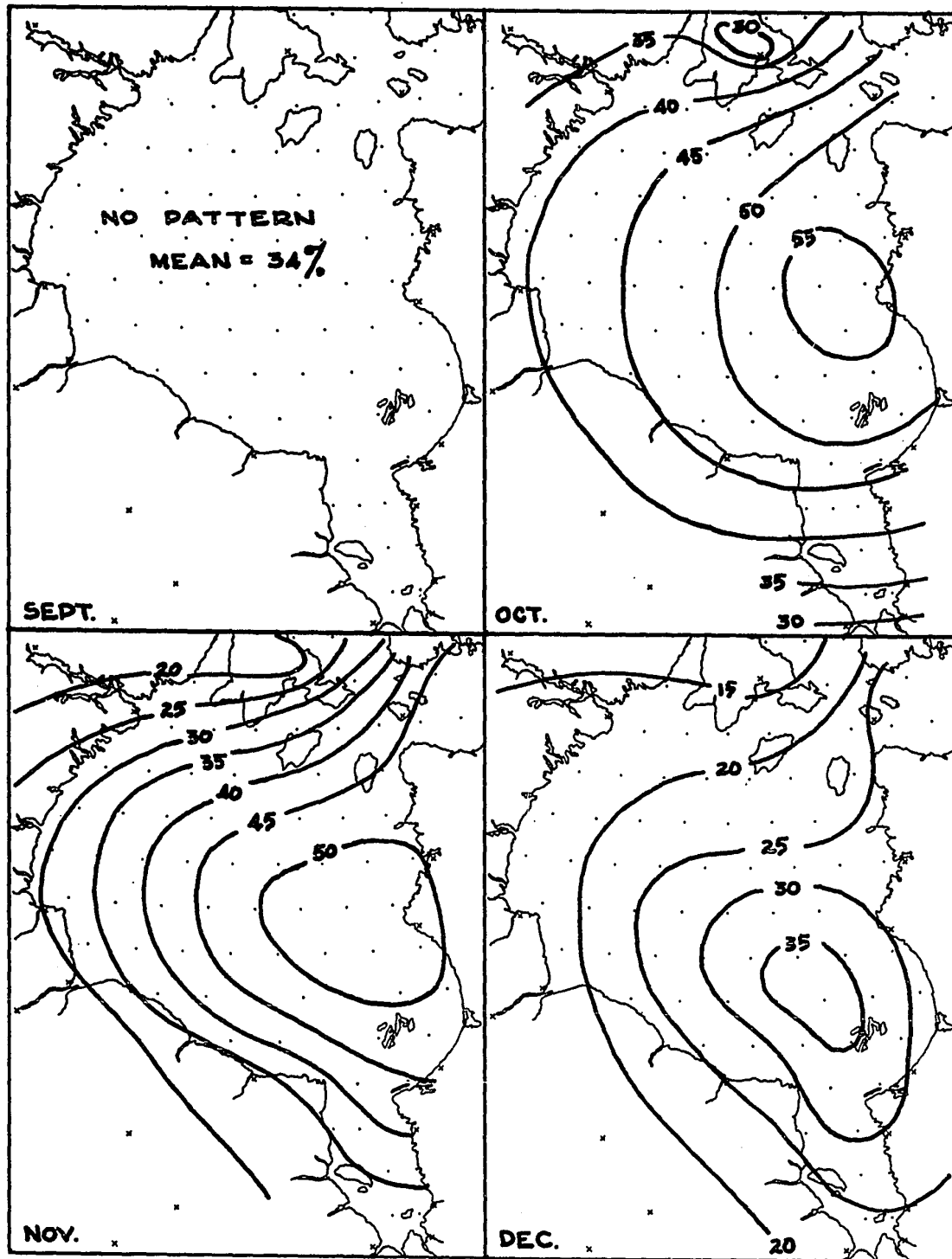


Figure 5-6. Monthly mean stratocumulus cloud cover (percent of sky covered).

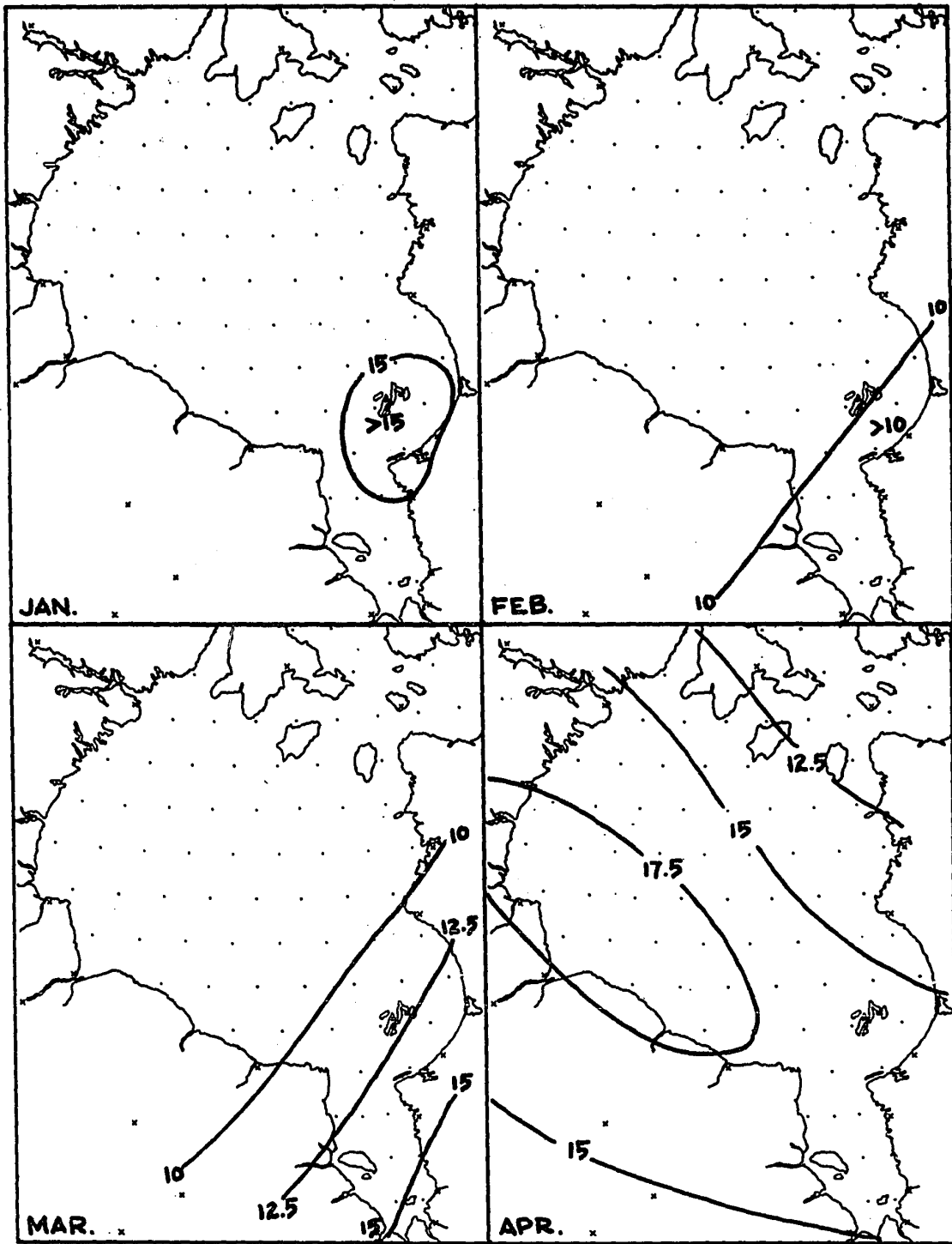


Figure 5-7. Monthly mean stratus cloud cover. (Percent of sky covered.)

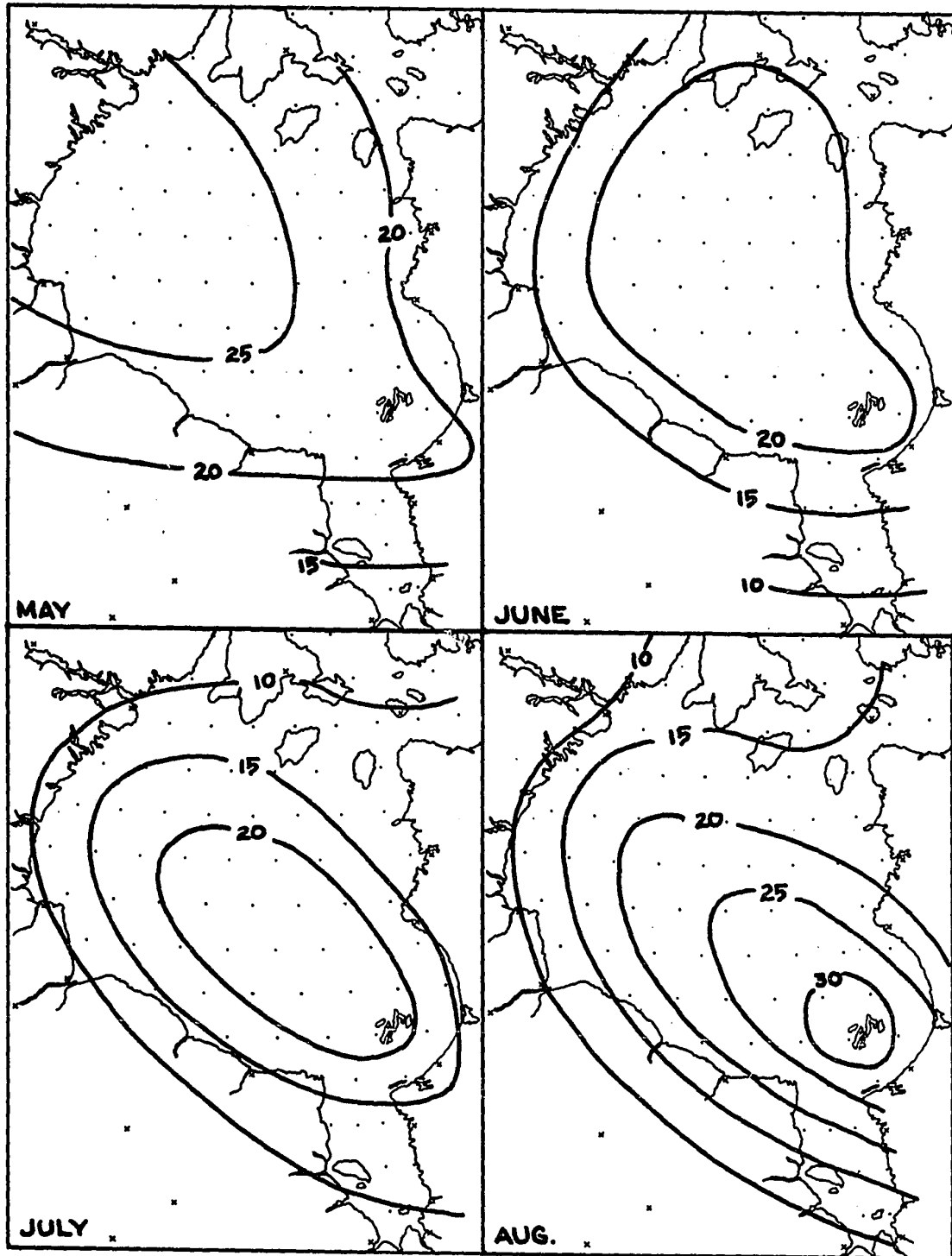


Fig. 5-7 cont'd. Monthly mean stratus cloud cover (percent of sky covered).

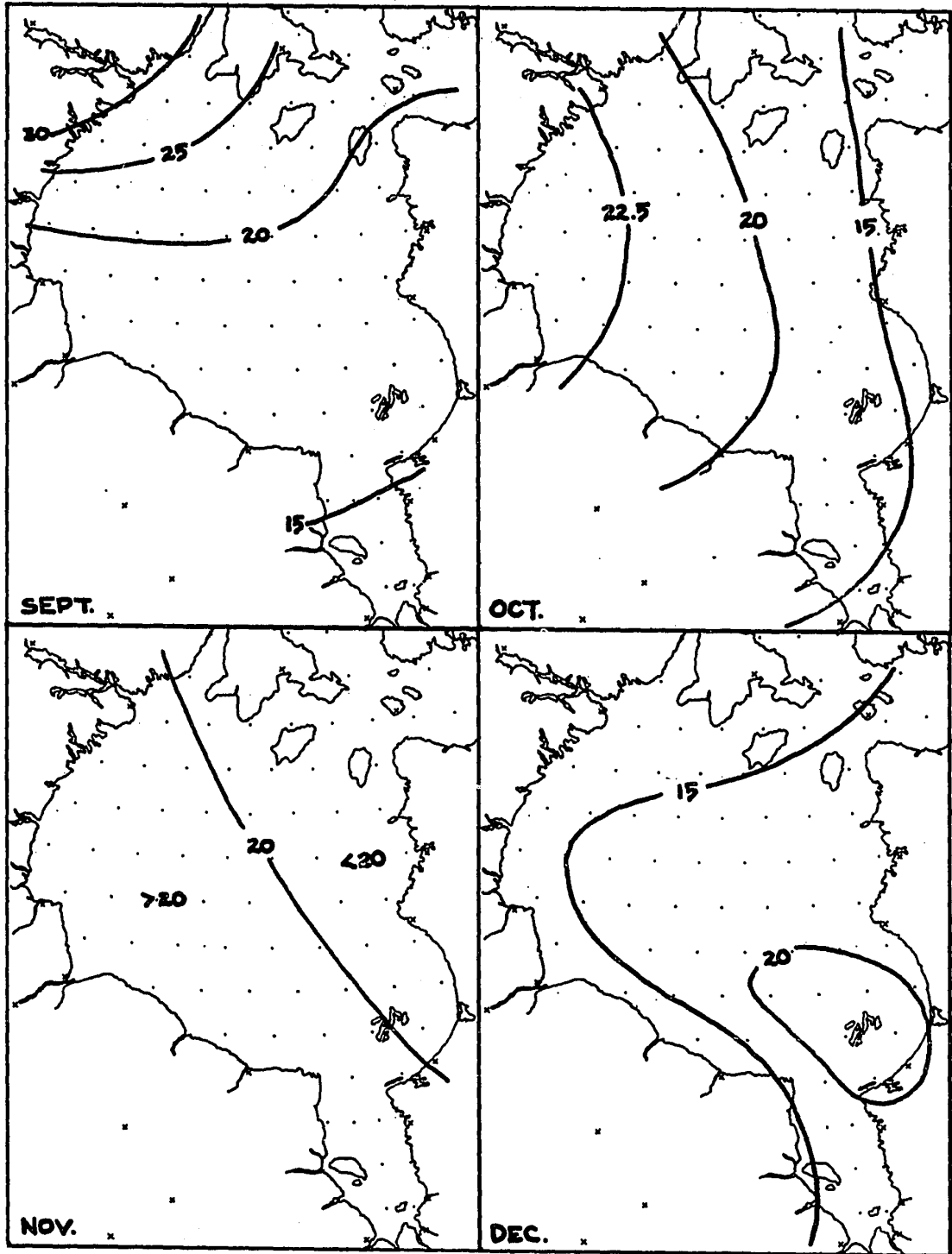


Fig. 5-7 cont'd. Monthly mean stratus cloud cover (percent of sky covered).

maps are included which show significant patterns. In particular, the middle and high cloud maps are largely just reflections of low cloud amounts, and therefore are not shown.

Winter (January-March) total cloud cover shows a minimum over northern portions, and a strong gradient in southern regions as storm track zones and warmer air are approached. High values at Great Whale River may be a combination of more southerly location and local effects such as leads. Minimum cloudiness occurs in February.

By May mean total cloud amounts have nearly doubled from February in the northern half of Hudson Bay, with substantial increases in the south as well. A broad maximum appears over the Bay, a feature present with varying clarity for the following seven months. Strato-cumulus shows no significant spatial variations at this time, but a local maximum of stratus cloud appears over the Bay.

The map of July total cloud cover suggests a slight maximum of cloudiness over Hudson Bay. A much more obvious maximum is over the Ungava plateau, where uplift and surface heating combine to give highest values. Whereas stratocumulus clouds are responsible for the Ungava maximum, however, July's stratus chart shows a pronounced Hudson Bay maximum.

Charts for September through December portray a maximum of total cloud cover passing southward, following the open water. In these months stratocumulus is by far the most important cloud type, reaching values of over 50% mean coverage in some places. With the completion of freeze-up, cloudiness falls sharply to January conditions.

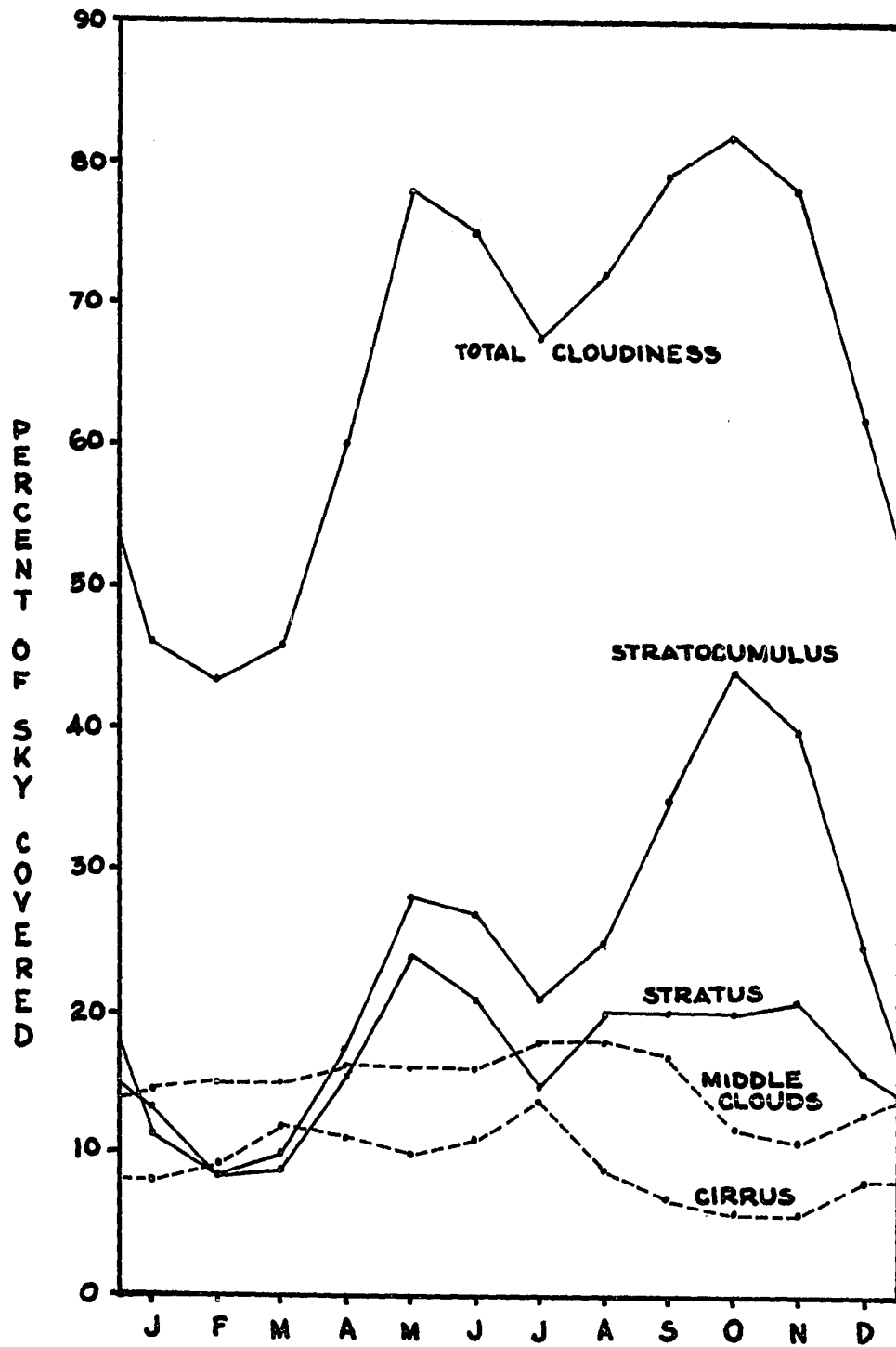


Figure 5-8. Areal Mean Cloud Cover for Hudson Bay.

Figure 5-8 depicts seasonal variations in mean total cloud cover and cloud cover by type, averaged across the Hudson Bay surface. Total cloudiness reaches a maximum in the autumn, obviously a result of surface instability, as the stratocumulus curve for fall indicates. The secondary maximum in May and June is more puzzling. Both stratus and stratocumulus clouds are seen to be the cause. Data from Thompson (1965) indicate a spring maximum to be the general rule in the Canadian Arctic: of the 18 stations for which he presents cloud information, 13 show a maximum in May or June. This feature may be explainable by heat budget fluxes, as will be seen in the next chapter.

This concludes the presentation of basic hydrometeorological information. These data, processed by the methods described in Chapter 2, form the basis of the energy budget computations presented in the next chapter.

## CHAPTER 6

### THE ENERGY BUDGET

#### 6.1 INTRODUCTION

The following sections are devoted to presentation and discussion of the Hudson Bay surface heat fluxes. Much of the information is in map form. On all maps, positive fluxes are downward ones, negative upward.

Many of the charts depict fluxes whose range of values over the Bay is less than the estimated error or uncertainty of individual calculations. If the uncertainties were random in nature from place to place, then maps of flux distribution would be of no value. The flux patterns, however, are the results of patterns in hydrometeorological variables, which were seen in earlier chapters to be mutually consistent. As a result, flux patterns may have a greater validity than local values which may suffer systematic or "zero-point" errors.

On the other hand, it should be remembered that large-scale features, not local details, are the subject of the present study. The depiction of heat losses from leads is a problem in this respect. Because leads are of smaller dimensions than the grid point spacing used, heat fluxes from leads (although generally occurring close to shore) have been spread evenly across Hudson Bay in the map portrayals. Obviously, winter-time charts would give incorrect results if applied on a scale of shore leads' dimensions, near shore.

Figures 6-1 are maps of solar energy absorbed at the Hudson Bay surface.

From January through April, isopleths of energy absorbed closely follow latitude circles. The decrease of solar elevation and (in January to March) length of day with increasing latitude is responsible for this pattern, along with the absence of important east-west variations in albedo, atmospheric moisture content, or cloudiness. A northward decrease of cloudiness in these months (Figure 5-5) acts to reduce the gradient of the isopleths in the southern half of the Bay.

The May chart shows an abrupt departure from the latitudinal pattern. The minimum of energy received in central and southwestern portions is a result primarily of variations in ice cover, and therefore albedo. Comparison with Figure 4-2, p. 77, depicting May ice conditions, illustrates the dominating influence of ice on the distribution of absorbed solar radiation at this time of year.

Albedo variations continue to dominate solar energy distributions in June and July, with areas of minimum absorbed energy coinciding with regions of greatest ice concentration. As a result, northern parts of Hudson Bay, which clear of ice relatively early in the season, absorb considerably more energy from the sun in May, June and July than the southwest quarter of the Bay. In June this north-south gradient is the largest, when northern waters absorb nearly 100 ly per day more than southern portions, or 2850 ly more over the entire month.

Dissipation of ice cover in August results in the virtual

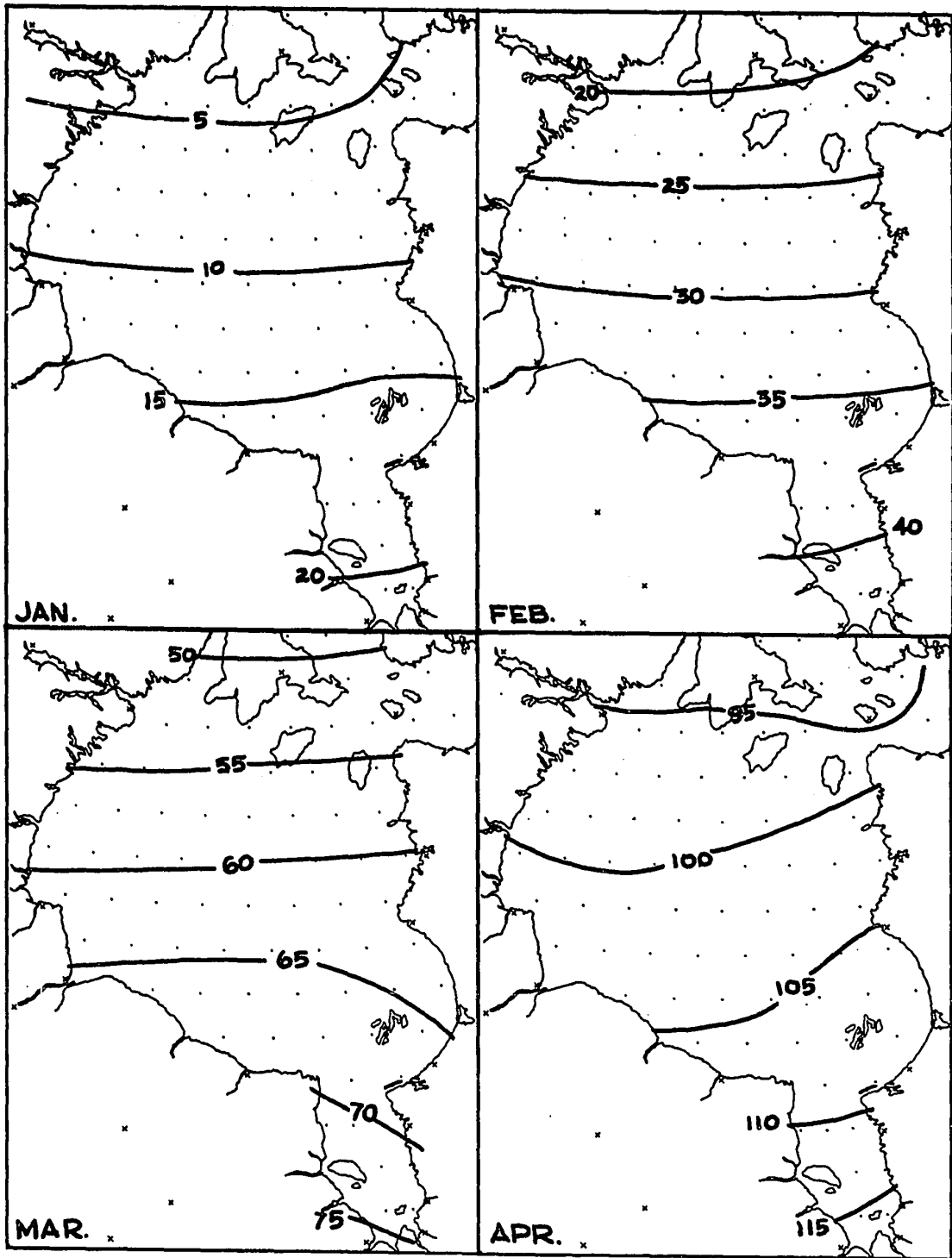


Fig. 6-1. Monthly mean solar radiation absorbed at surface (ly/day).

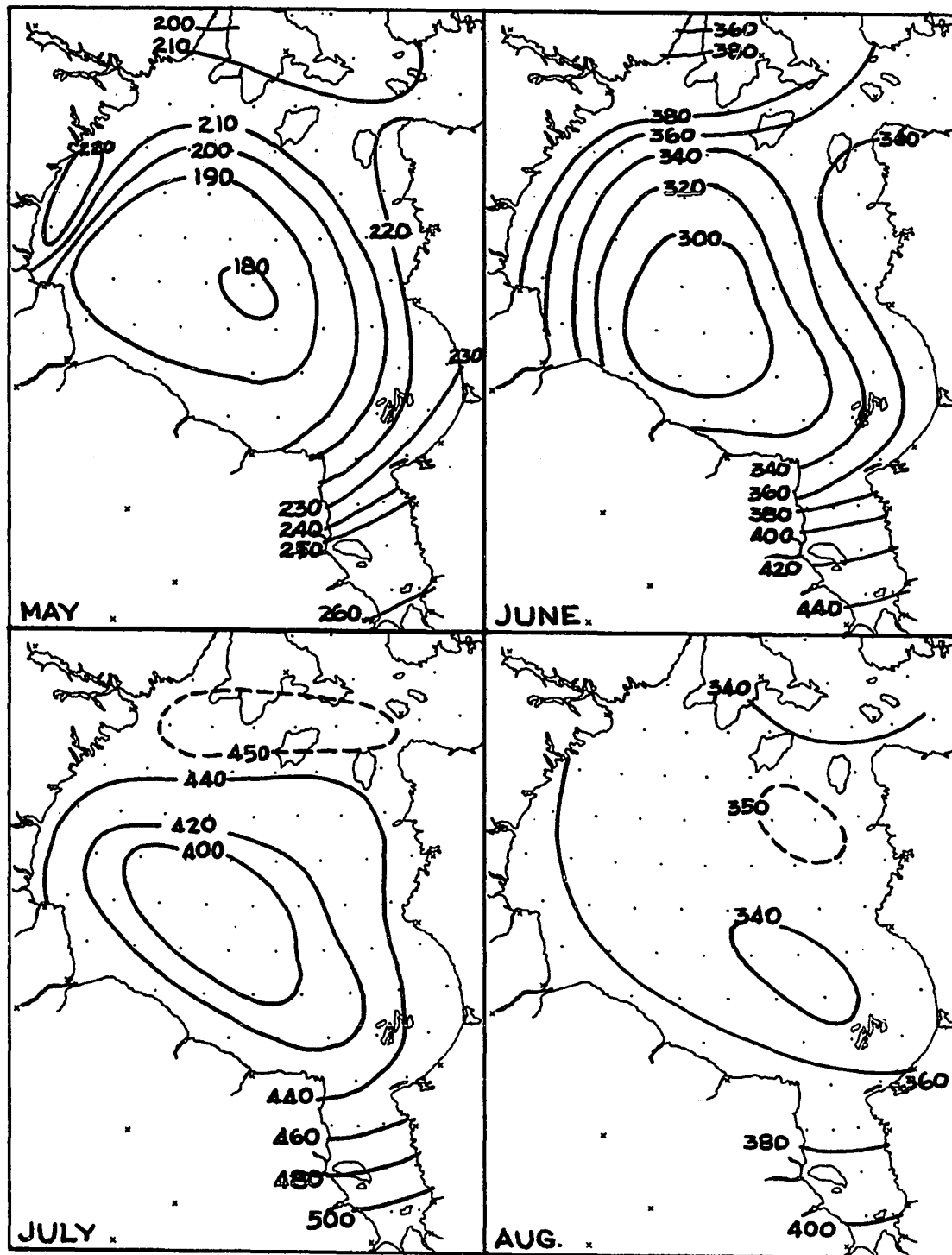


Fig. 6-1 cont'd. Monthly mean solar radiation absorbed at surface (ly/day).

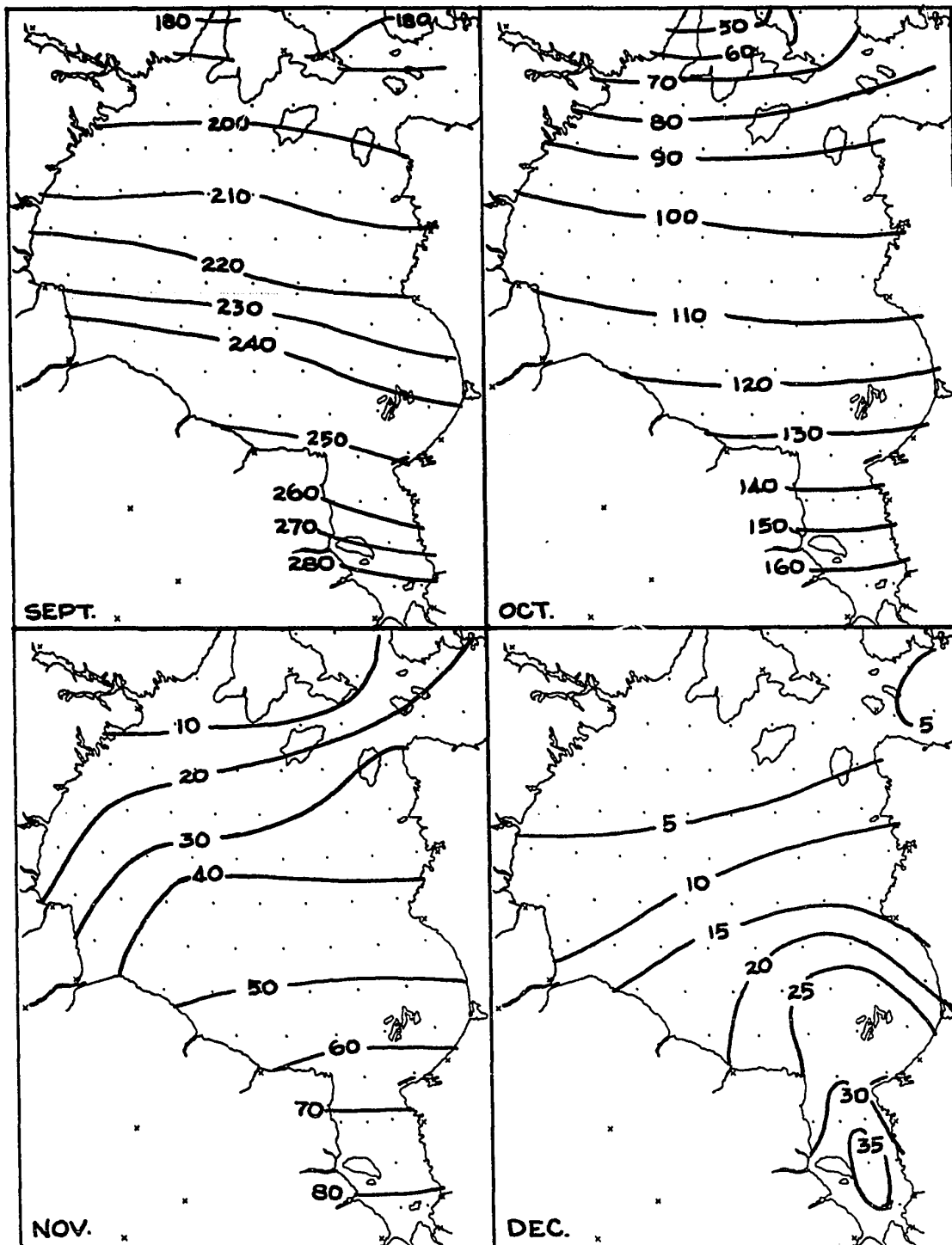


Fig. 6-1 cont'd. Monthly mean solar radiation absorbed at sfc. (ly/day).

disappearance of the solar energy minimum in that month. In September and October, generally open water months, solar energy absorption shows a latitudinal control similar to that of the winter months. October freeze-up results in higher albedoes for the very northernmost regions, which intensifies the north-south gradient there.

November and December distributions reveal distortions of latitudinal solar income patterns in the vicinity of local ice formation. In November isopleths of absorbed solar energy run east-west, except where ice is forming in the northern part of Hudson Bay. In December, open water in southeastern parts results in a local maximum of energy absorbed, in spite of the fact that cloudiness and atmospheric water vapour, both depletors of sunshine, are much greater in that area.

The distribution of annual absorbed solar energy (Figure 6-6a, p. 159) reflects the predominating influences of spring ice cover, and latitude. Southern James Bay, where solar elevation is greatest and spring ice cover dissipates early, absorbs by far the greatest amount of sunshine per unit area. The minimum over southwest-central Hudson Bay is mainly a result of high springtime albedo associated with ice.

### 6.3 MONTHLY MEAN LONG WAVE RADIATION

The surface long wave radiation balance (LD-LU) is presented in Figure 6-2.

From January through April, greatest long wave heat loss occurs in eastern Hudson Bay, the result of slightly warmer surface temperatures (see Section 5.2 and Figure 5-2). Hudson Strait also experiences a large

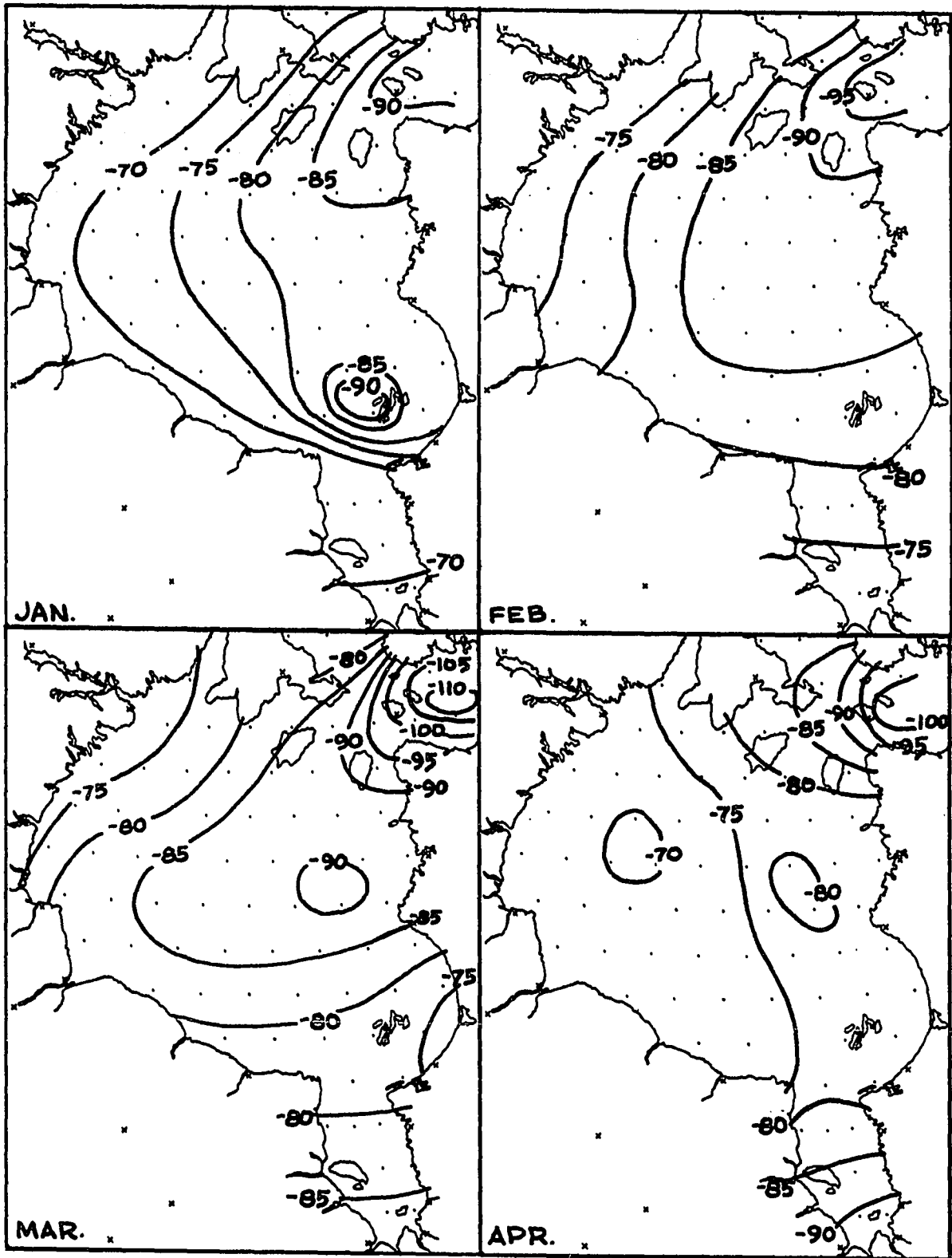


Fig. 6-2. Monthly mean net long wave radiative flux (ly/day).

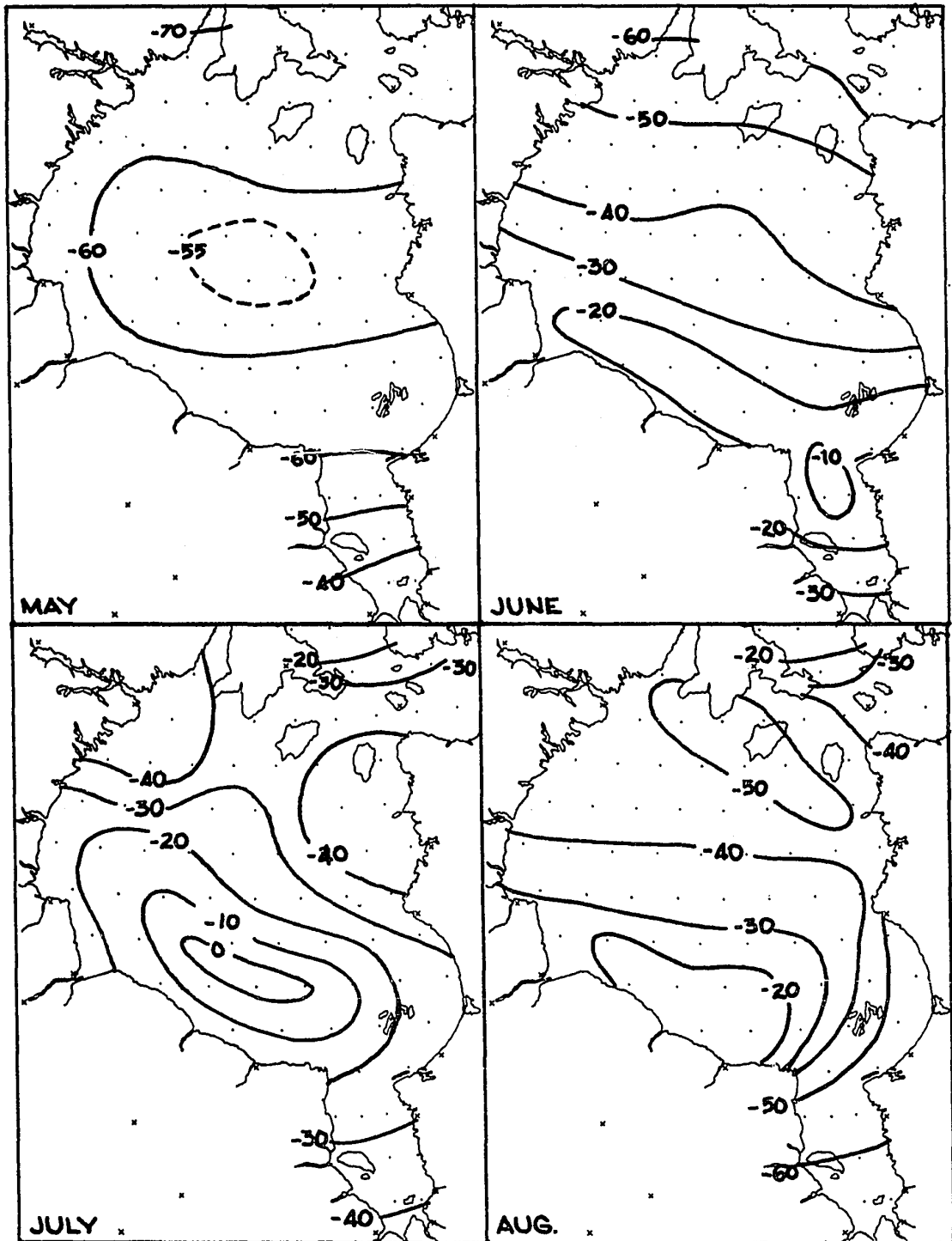


Fig. 6-2 cont'd. Monthly mean net long wave radiative flux (ly/day).

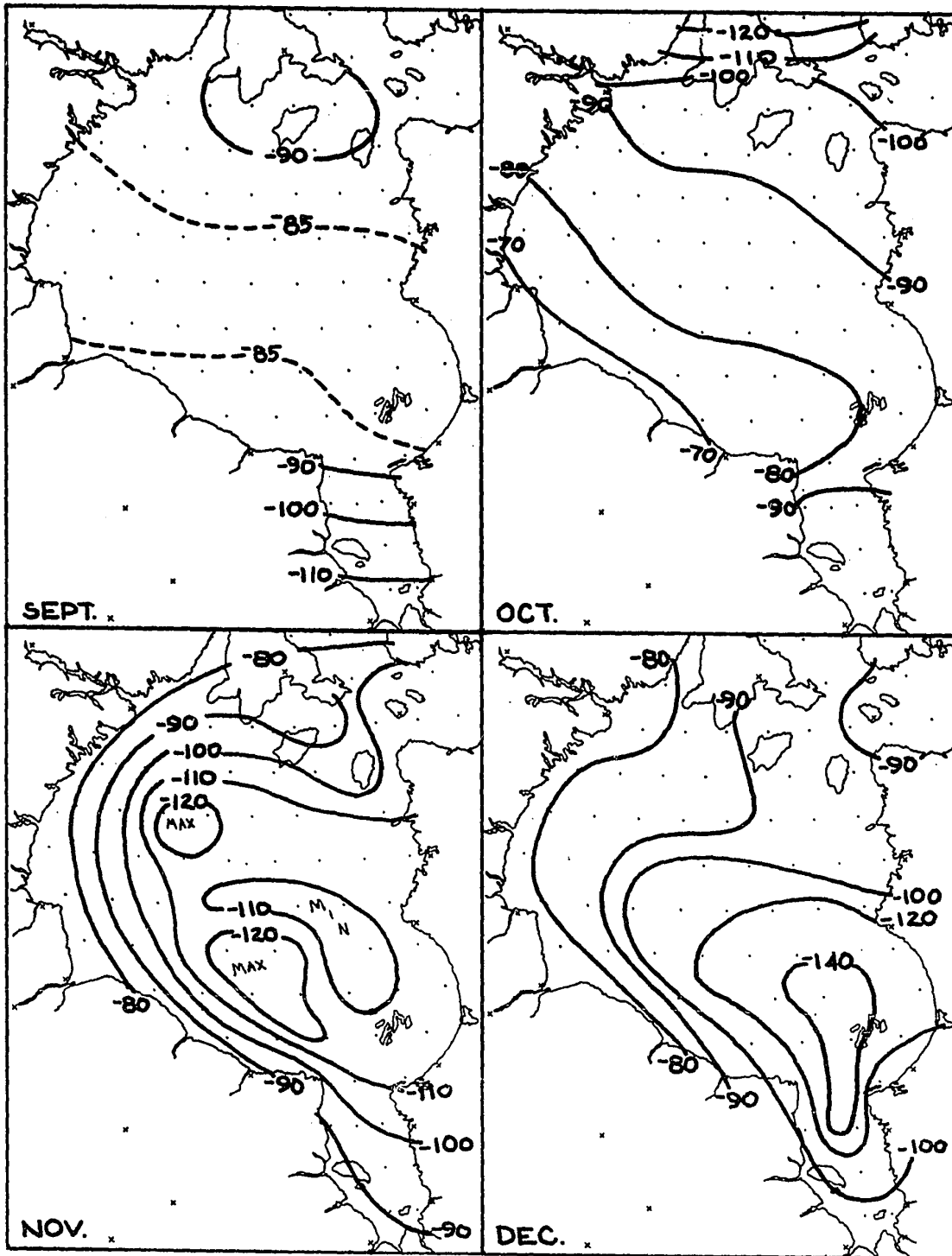


Fig. 6-2 cont'd. Monthly mean net long wave radiative flux (ly/day).

heat deficit, due to a relatively high percentage (10%) of open water there. Although the patterns over Hudson Bay show greater heat loss in the east in each of these months, the difference between eastern and western regions is only about 15 ly per day.

In the thaw months, the cold Hudson Bay surface reduces long wave heat loss to its annual minimum. Smallest deficits appear in extreme southwestern Hudson Bay, the region of heavy ice concentrations and relatively warm air advection from land. Formation of stratus clouds as the air cools further improves the long wave balance.\* July's chart indicates a small region of positive long wave radiation balance. This rare occurrence (especially for monthly mean conditions) may be said to result directly from large air-sea temperature contrasts maintained by a lingering ice cover in continental surroundings.

From September through December, greatest heat deficits appear in regions of maximum sea-air temperature differences. The warm James Bay surface experiences large heat losses. In Hudson Bay, maximum heat loss in fall proceeds southwards in advance of ice formation, with greatest deficits just beyond the ice pack edge; farther out into open water, turbulent sea-air energy transfer works toward equalizing sea and air surface temperatures and encourages instability cloud formation, lessening radiative heat loss. December long wave heat loss west of the Belcher Islands is over 140 ly per day, the greatest deficit in this component

---

\* Following common practice in heat budget discussions, the word "balance" is used for the sum of two or more fluxes which at least partially cancel each other. In this context the "balance" does not necessarily equal zero. If the balance becomes more positive (or less negative) it is said to "improve".

appearing in any month over the Hudson Bay surface.

Annual long wave deficits appear in Figure 6-6b, p. 159 . The difference between maximum heat loss in the northeast and minimum in the southwest amounts to about 14 ly per day or about 5000 ly per year.

#### 6.4 MONTHLY MEAN RADIATION BALANCE

Figure 6-3 portrays the monthly radiation balance, the sum of solar and long wave radiation.

In January, February, and March, the long wave component controls the patterns of the radiation balance, with greatest deficits appearing in the east. From March to April the balance shifts from negative to positive at all points across Hudson Bay, as solar energy begins to control the radiation budget.

May, June, and July radiation patterns show the importance of solar radiation, influenced by albedo. Locally the presence or absence of ice acts in opposite ways for the different (long and short wave) components of the radiation balance: maximum ice cover results in a minimum of absorbed solar radiation, but a maximum of long wave radiation (or minimum deficit). Therefore the distribution of radiation in May, June, or July, although the same pattern essentially as that of solar radiation, exhibits less intense gradients than the short wave component alone (Figure 6-1.).

With the disappearance of ice during August, the radiation balance becomes more latitudinally aligned and minimum radiation values occur in northern Hudson Bay, where they remain through October. For most

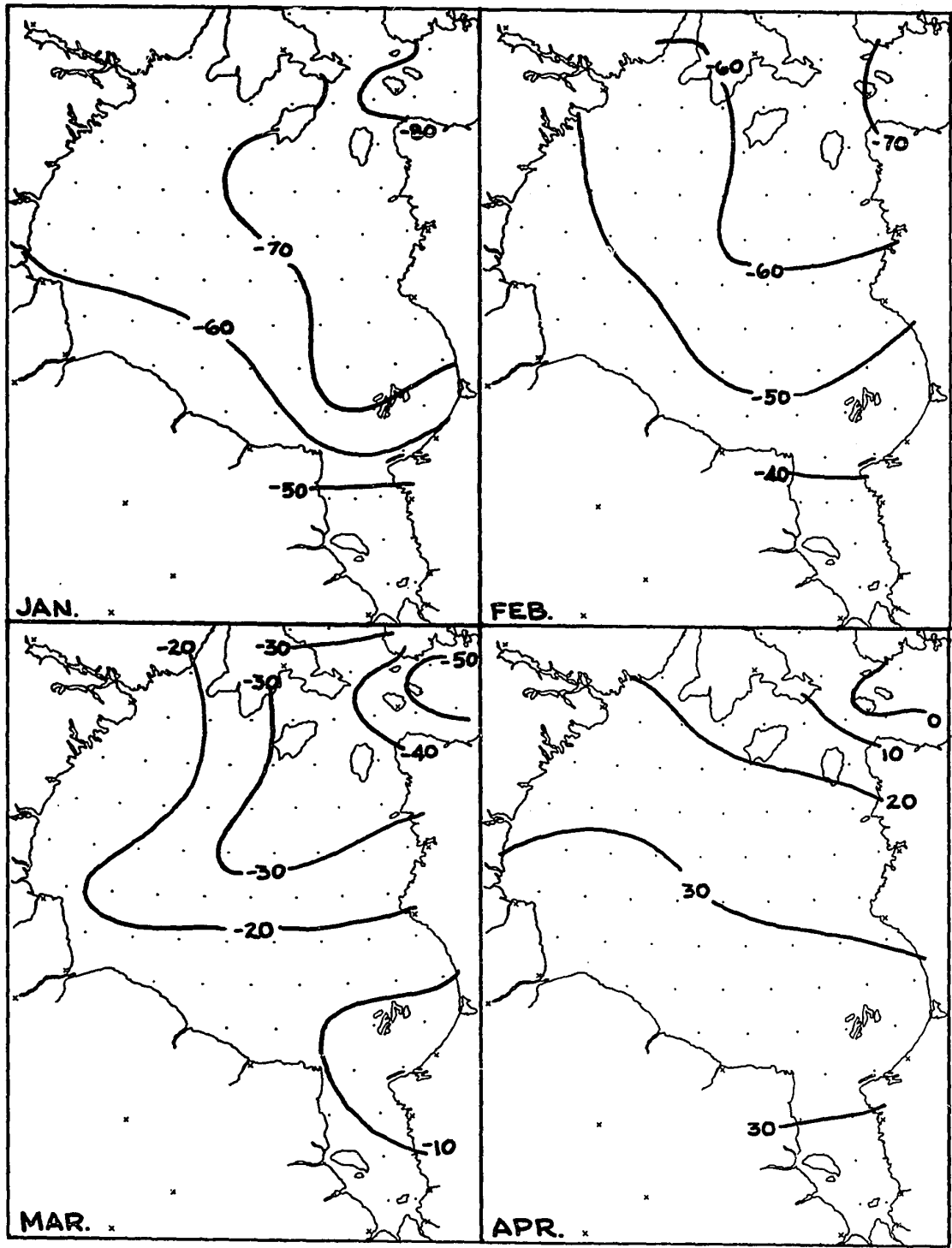


Fig. 6-3. Monthly mean surface radiation balance (ly/day).

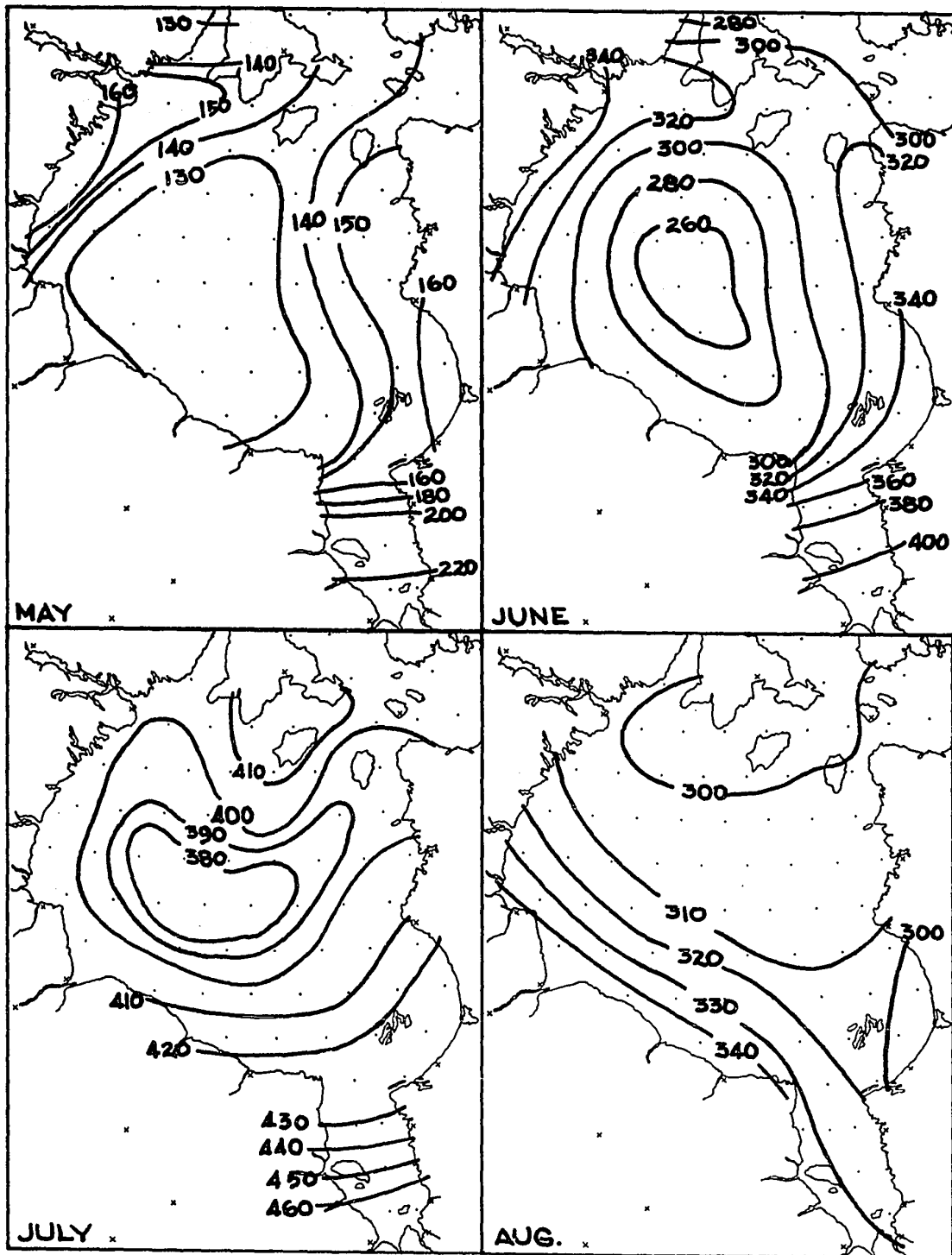


Fig. 6-3 cont'd. Monthly mean surface radiation balance (ly/day).

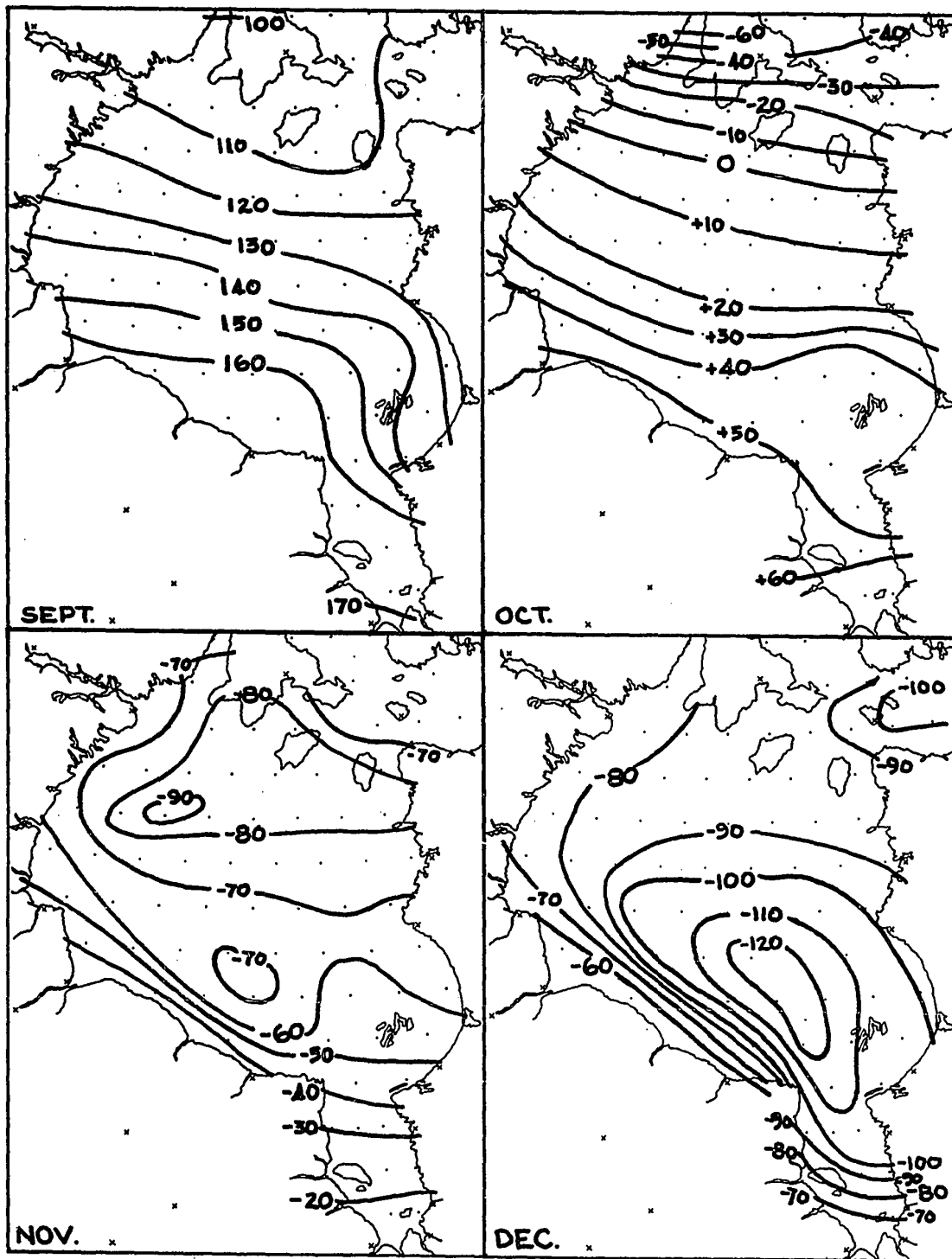


Fig. 6-3 cont'd. Monthly mean surface radiation balance (ly/day).

parts of the Bay, the transition from positive to negative radiation balance occurs in October.

The long wave component dominates November and December radiation balance patterns. The correlation of greater solar income with greater long wave deficits tends to diminish the amount of local variation in the radiation balance, however.

The annual radiation balance (Figure 6-6c, p. 159) is strongly positive everywhere. Greatest income is in southern James Bay, and along the Hudson Bay perimeter. Smallest values are in the north, and in central or south-central parts of the Bay. Many factors contribute significantly to the pattern; however, the main feature, the central minimum, derives most directly from the high albedo of the ice pack in spring and summer.

#### 6.5 MONTHLY MEAN TURBULENT HEAT FLUXES

Maps of monthly mean evaporative and sensible heat flux appear in Figure 6-4.

January, February, and March distributions are rather featureless except in the extreme northeast, where the higher percentage of open water allows much more vigorous turbulent heat transfer. Part of the flatness of the pattern over Hudson Bay is artificial, arising from the method of representing heat loss from leads (see Section 6-1). Thus in reality the wintertime turbulent heat loss is concentrated along shore, with fluxes close to zero in mid-Bay.

Through April, May, and June a maximum of convective heat loss

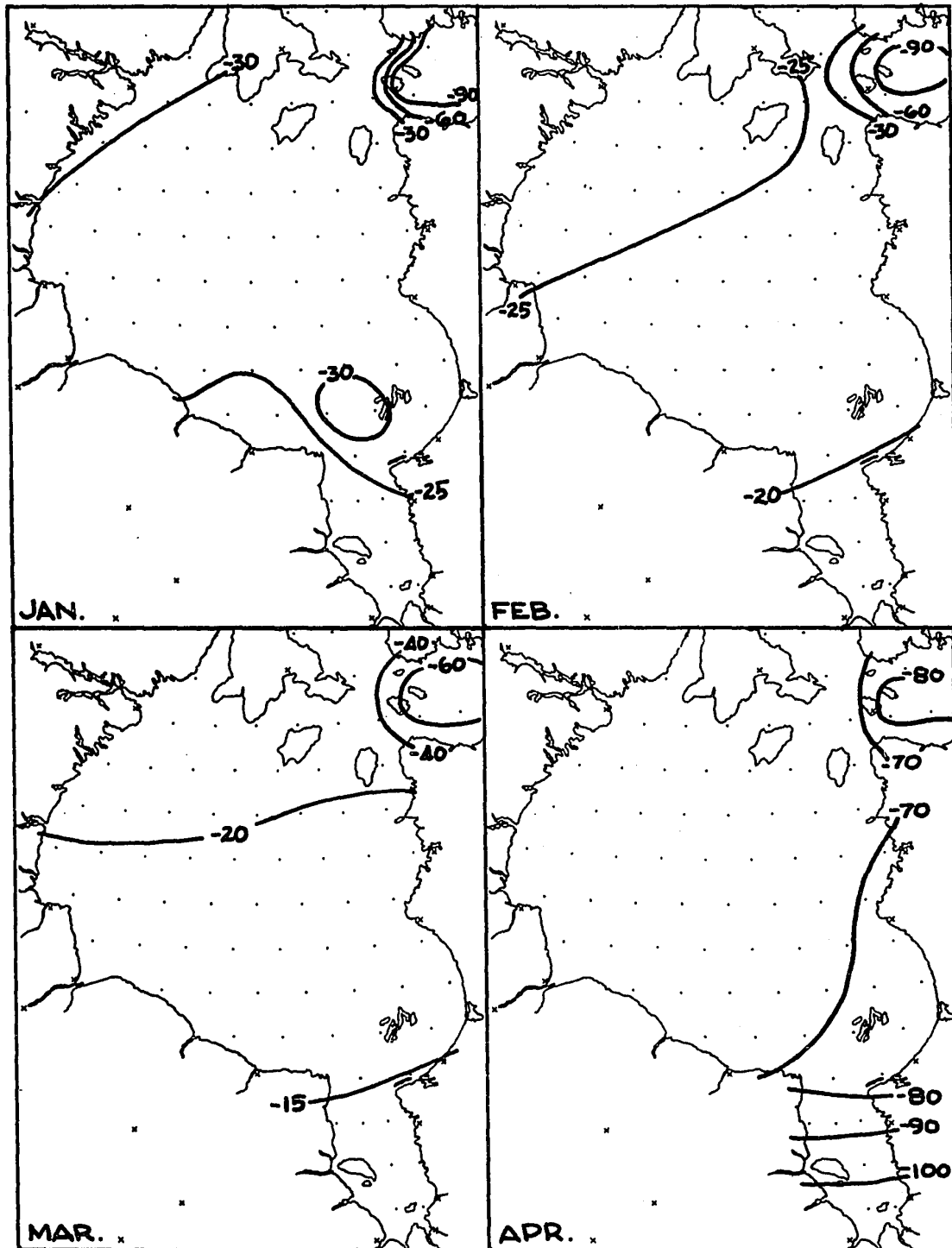


Fig.6-4. Monthly mean turbulent heat fluxes: evaporative plus sensible. (ly/day).

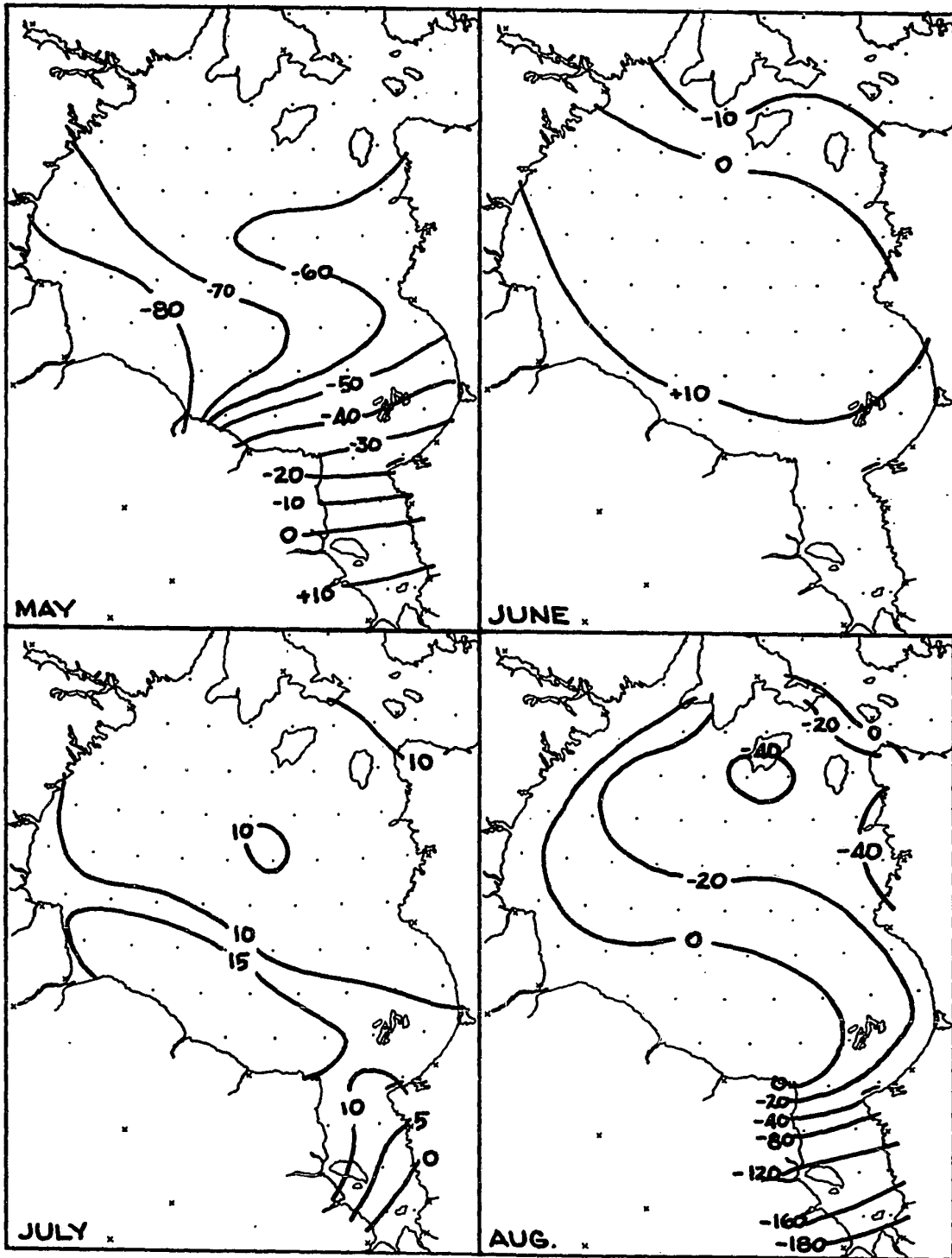


Fig. 6-4 cont'd. Monthly mean turbulent heat fluxes: evaporative plus sensible (ly/day).

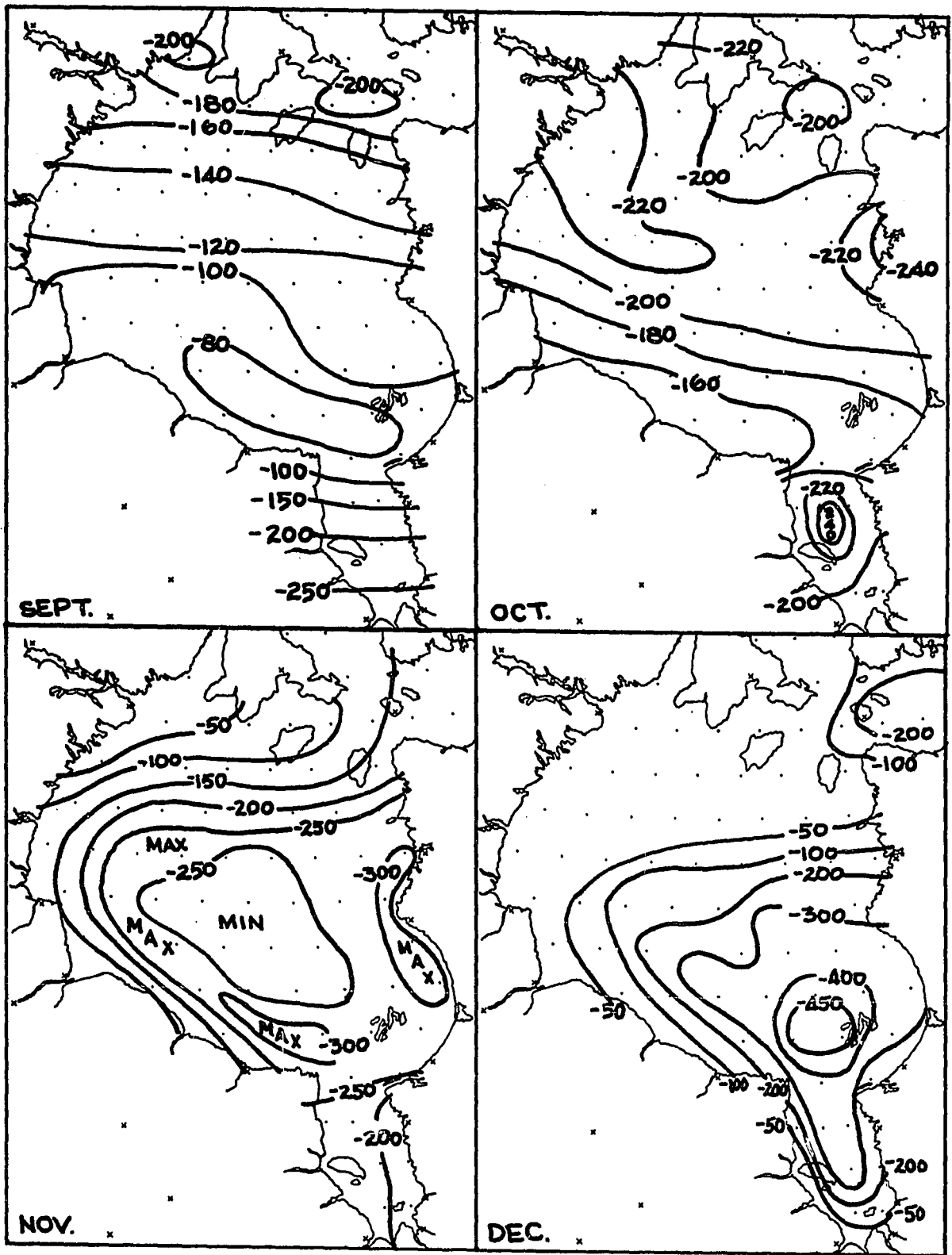


Fig. 6-4 cont'd. Monthly mean turbulent heat fluxes: evaporative plus sensible (ly/day).

moves northward across Hudson Bay. Locally, the maximum appears under the following circumstances: (1) the radiation balance has become positive, allowing the ice surface to become warmer than the overlying air, thus encouraging convection; (2) air and ice surface temperatures have increased from mid-winter values, permitting greater vapour pressures and larger air-ice differences of vapour pressure; (3) the air surface temperature has not yet reached 0 degrees C, the occurrence of which marks the onset of stable summer conditions. Vowinckel and Taylor (1965), in a study of turbulent fluxes over the Arctic Ocean, found a similar springtime maximum under like circumstances.

This period of greater convection may cause the springtime maximum in cloudiness observed at many arctic stations, and pointed out in Section 5.5. With the snow or ice surface acting as a source of heat and moisture, both the property for transfer (moisture) and the mechanism for transfer (convection) are present. The result is increased amounts of cloud, especially stratocumulus (see Figure 5-8).

Downward turbulent heat fluxes occur in June, July, and August, as the overlying air generally is warmer and of higher vapour pressure than the water or ice surface. Due to pronounced atmospheric stability, however, summer fluxes are small. Greatest downward fluxes appear along the south coast, where the late spring and summer ice causes maximum air-sea temperature and moisture gradients.

From September through December, turbulent heat exchange is negative (upward) across the entire Hudson Bay surface. Greatest heat losses occur just beyond the edge of the ice pack, where relatively

unmodified cold air passes over much warmer water, creating strongly unstable conditions.

The map of mean annual heat exchange by convection (Figure 6.6d, p. 159) is mostly a reflection of autumnal patterns, when heat loss is very high. Greatest deficits appear in the southeast, due to late freeze-up there. Western regions, although most exposed to the cold, dry winds which promote turbulent heat transfer, lose less heat convectively than any other part of the Bay. The reason may be found in the observation of Hare (1950, p.272) that "the shallow, shelving west coast freezes very quickly". Thus shallow waters, holding less heat than deep waters at the same temperature, reach zero heat storage early in the autumn and freeze, thereby insulating themselves from large additional losses.

#### 6.6 MONTHLY MEAN SURFACE HEAT BUDGET

Figure 6-5 portrays monthly distributions of radiative plus convective fluxes, the surface heat budget. The flux at each point must be matched by an equal amount of advective and/or storage change in the waters below (see Equation 1-2).

From January through April the energy balance is everywhere negative. Greatest surface heat losses occur in the east and north. Heat advection by currents is very small during these months, since the waters are well-mixed vertically and close to the freezing point everywhere (Dunbar, 1958, p.195). Thus the energy deficits must result in local ice formation, the only remaining storage change possible.

Larger heat losses in the north imply greater ice growth there,

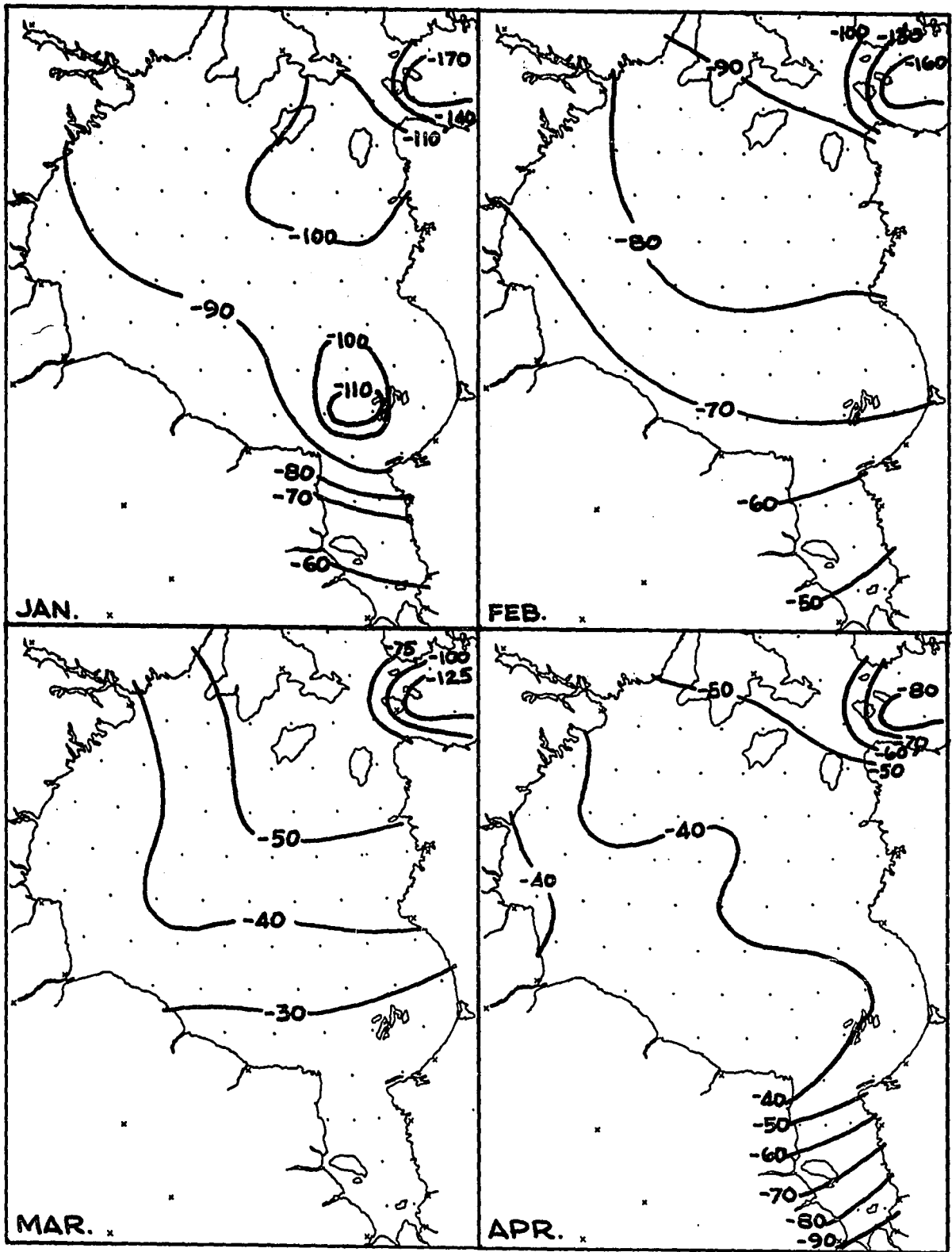


Fig. 6-5. Monthly mean surface heat budget (ly/day).

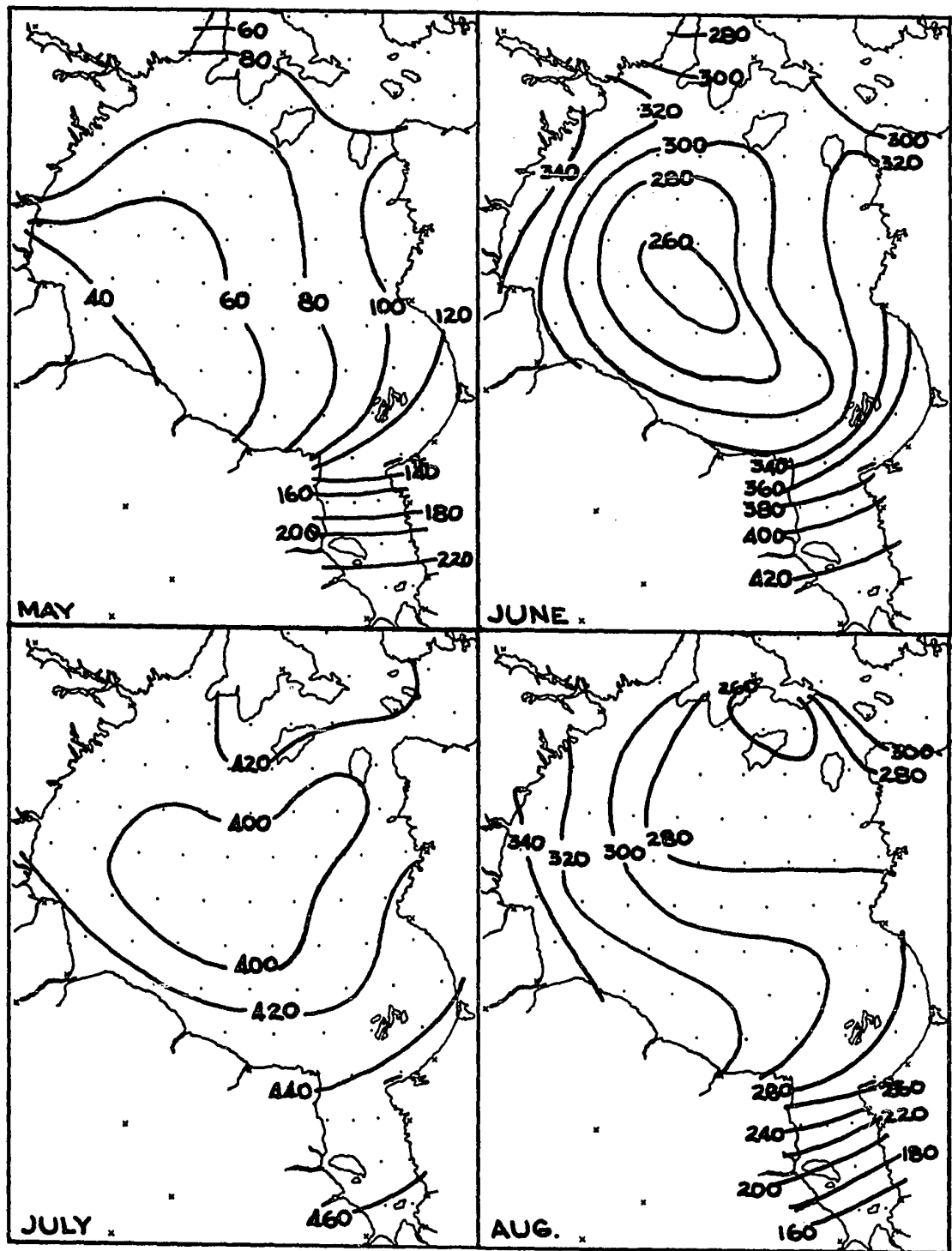


Fig. 6-5 cont'd. Monthly mean surface heat budget (ly/day).

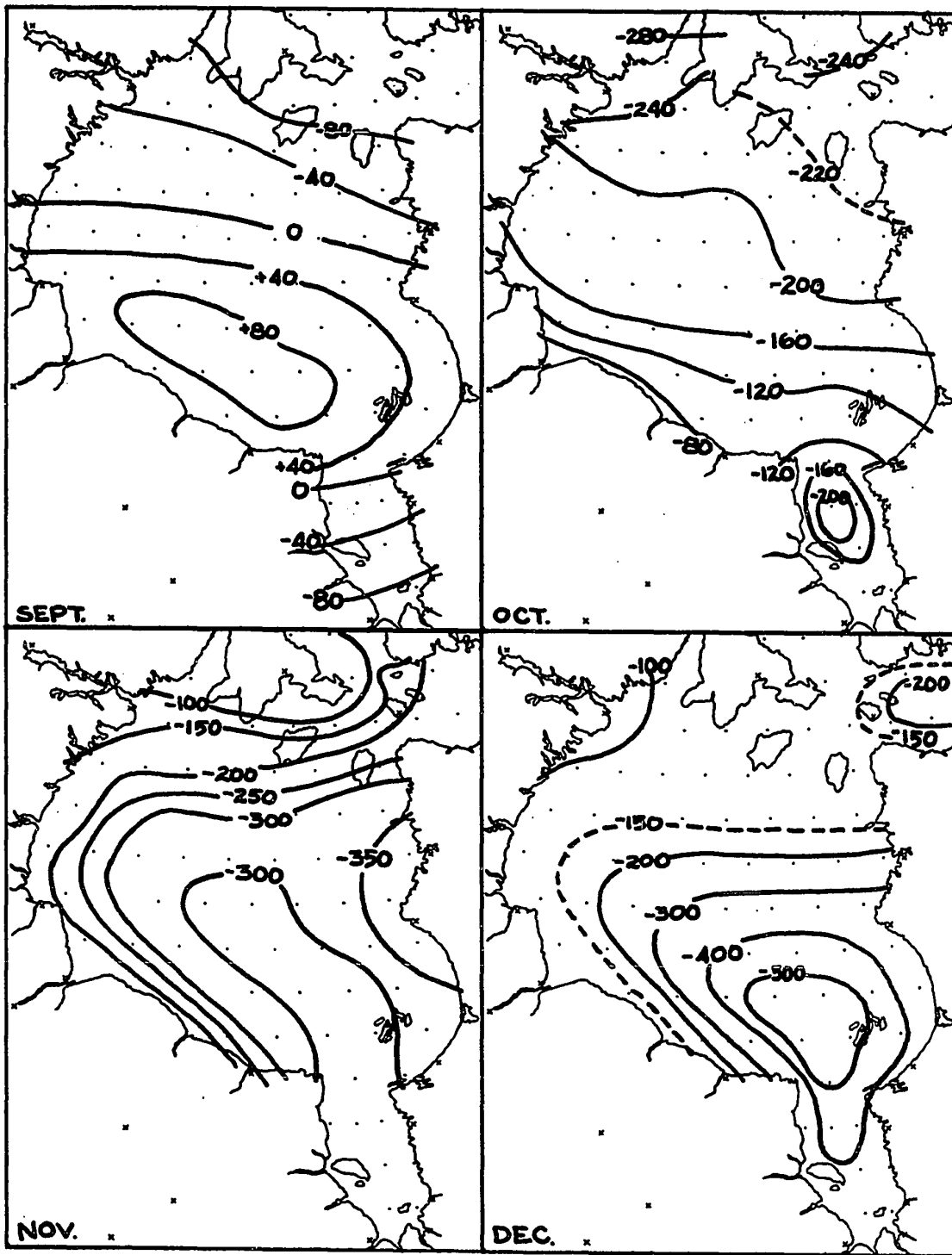


Fig. 6-5 cont'd. Monthly mean surface heat budget (ly/day).

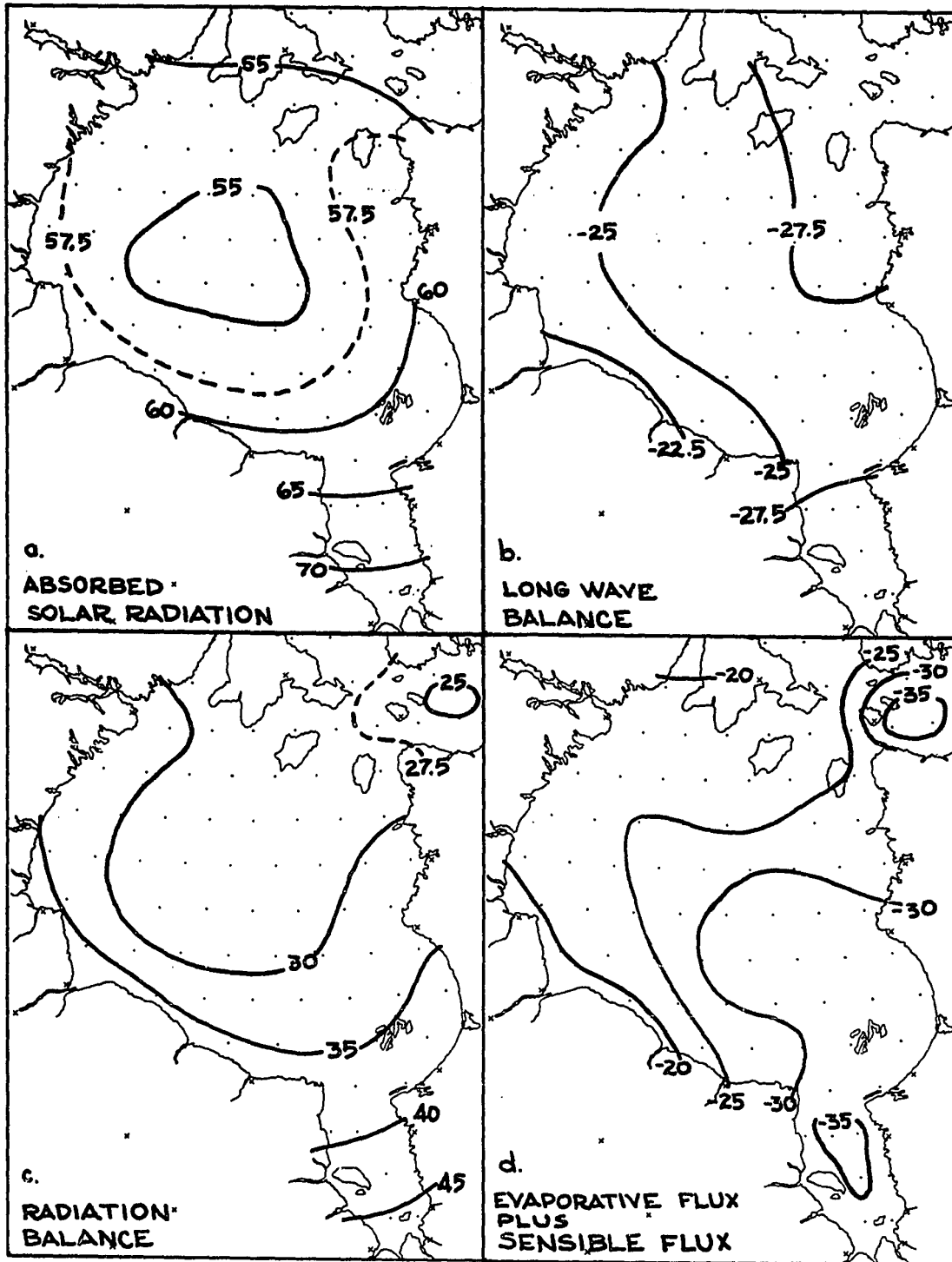


Fig. 6-6. Annual mean heat budget components (thousands of ly/year).

which is borne out by observation. Likewise greater losses in the east require more ice growth during these months than in the west. As discussed in Section 4.9 , the larger winter heat losses in eastern Hudson Bay may be explained by faster ice growth due to later freeze-up than in the west.

From April to May, Hudson Bay's energy budget everywhere shifts from negative to positive, the result of increasing amounts of solar radiation. It seems remarkable that thawing and loosening of the ice cover do not begin at quite different times in different quarters of the Bay, but rather start almost simultaneously over the whole ice pack. Prevailing northwesterly surface wind flow re-consolidates the pack by compressing it to the south as it thaws, with the result that extensive open water appears first in spring off the northwestern coast. Thus the large-scale break-up patterns are the result of general thawing over all of Hudson Bay, combined with a preferred wind direction.

Solar radiation dominates the heat budget patterns from May through August. It is interesting that minimum energy surplus through these months coincides with areas of ice pack; regions with the greatest heat deficit (the southwest) also have the least amount of energy available to erase the deficit. The result, as indicated in Section 3.7, is that southwestern waters develop the smallest summer heat storage surplus.

September energy fluxes lead toward an equalization of storage across Hudson Bay. In the southwest, ice at last has disappeared, allowing solar energy to be absorbed efficiently. Surface water temperature is relatively low, so that evaporative, sensible, and long wave heat

losses all occur at rates lower than elsewhere. The result is a pronounced September maximum of heat gain in the southwest. In the north and in James Bay, September turbulent heat fluxes have a marked influence on the surface budget, which they completely dominate in the following months. Heat fluxes are strongly negative (upward) everywhere from October through December. Greatest total losses, as in the case of turbulent transfers, occur at the land-water or ice-water boundary.

It is seen in the next section that, considering advection into and out of Hudson Bay, an excess of about 4200 ly per year exists in the calculated annual mean surface energy budget. Figure 6-7 represents the local annual heat surplus or deficit, corrected for the imbalance, which was accomplished simply by subtracting 4200 ly per year from the annual sum of heat fluxes at each point. Local annual energy excesses and deficits in Figure 6-7 must be brought to zero by advection within and across Hudson Bay's boundaries.

Figure 6-7 indicates that the mean annual total heat flux is negative in central Hudson Bay, positive elsewhere. Greatest surpluses appear along the western coasts. The implication is that central regions must receive heat through advection by currents, while the remainder of the Bay must lose energy by the same process.

Clearly, advection's main task is to move energy excesses eastward. The slow counterclockwise circulation from western waters, through southern and into eastern regions, must help to redistribute the heat. The southward movement of ice in spring, under the influence of currents and wind, constitutes a positive advection to waters cleared

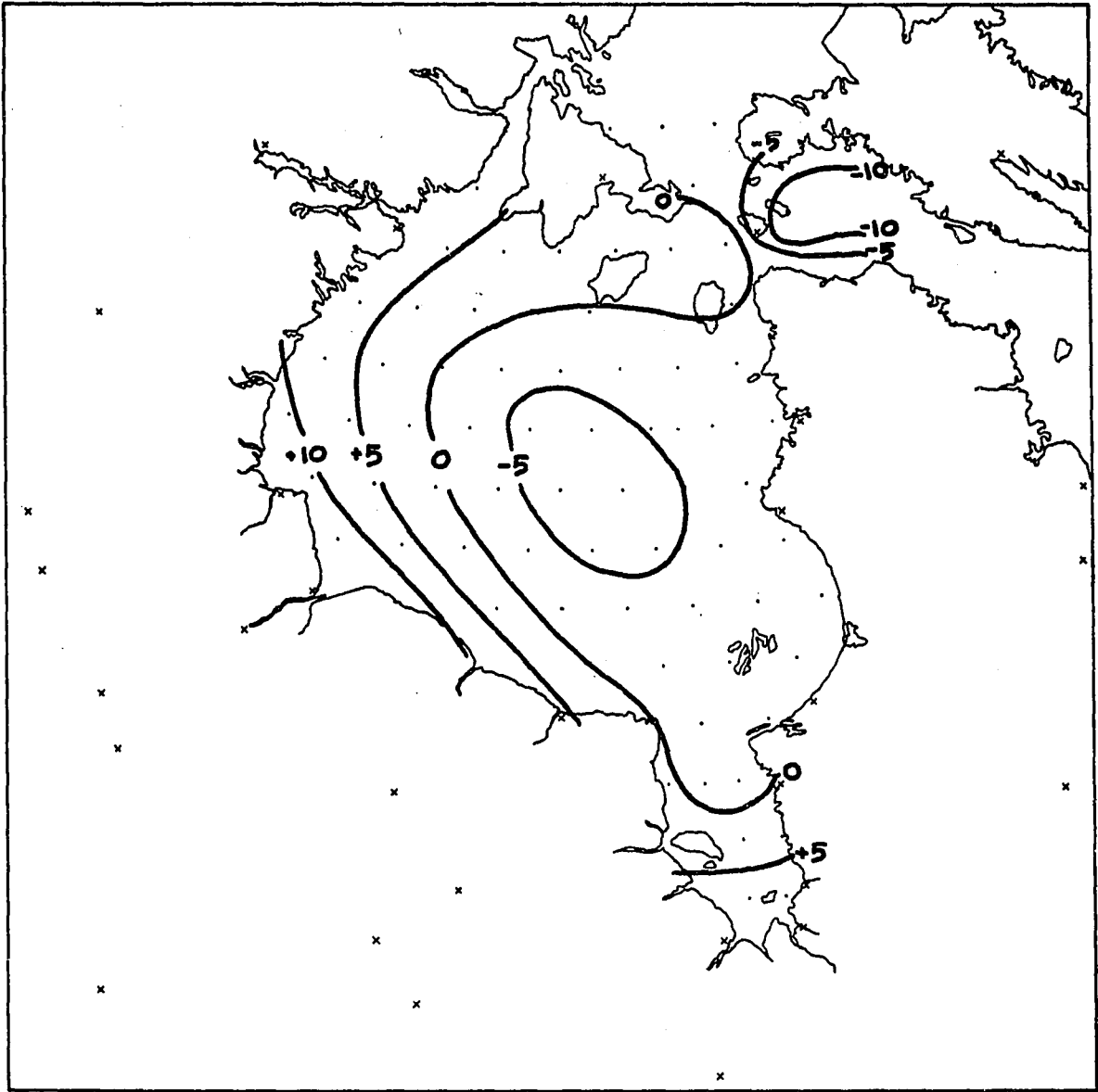


Fig. 6-7. Annual mean net surface heat flux (thousands of ly/year).

of ice, and negative advection to waters receiving it.

Another vehicle of heat transport may be upwelling. Barber (1967) has given evidence suggesting its presence along western Hudson Bay shores. Since the deep, upwelling water is colder than the surface water it replaces, the process may be considered cold advection for the western coastal waters.

Thus although the mean annual heat budget, unadjusted, was in error by approximately 4200 ly per year, the distribution of surpluses and deficits given by Figure 6-7 is consistent in broad scale with advection patterns within the Bay.

#### 6.7 AREAL AVERAGES OF HEAT BUDGET FLUXES

Figures 6-8 and 6-9 depict areal means of the heat budget components, and certain combinations of components, by month.

Solar energy fluxes are represented by the solid lines in Figure 6-8. The topmost solid curve is clear sky insolation; the June peak and December minimum are in phase with solar declination variations, indicating astronomical control of this flux. Absorbed clear sky radiation (curve SCA) is far less than clear sky insolation in the first half of the year, due to the high albedo of ice and snow, but nearly equal to curve SC in the latter half, when the surface state is mostly liquid. Curve SA is the solar energy absorbed under normally cloudy skies. It is evident that high surface albedo is the greatest depletor of solar energy from December to June, whereas in August through October cloudiness is most important. Albedo distributions are responsible for

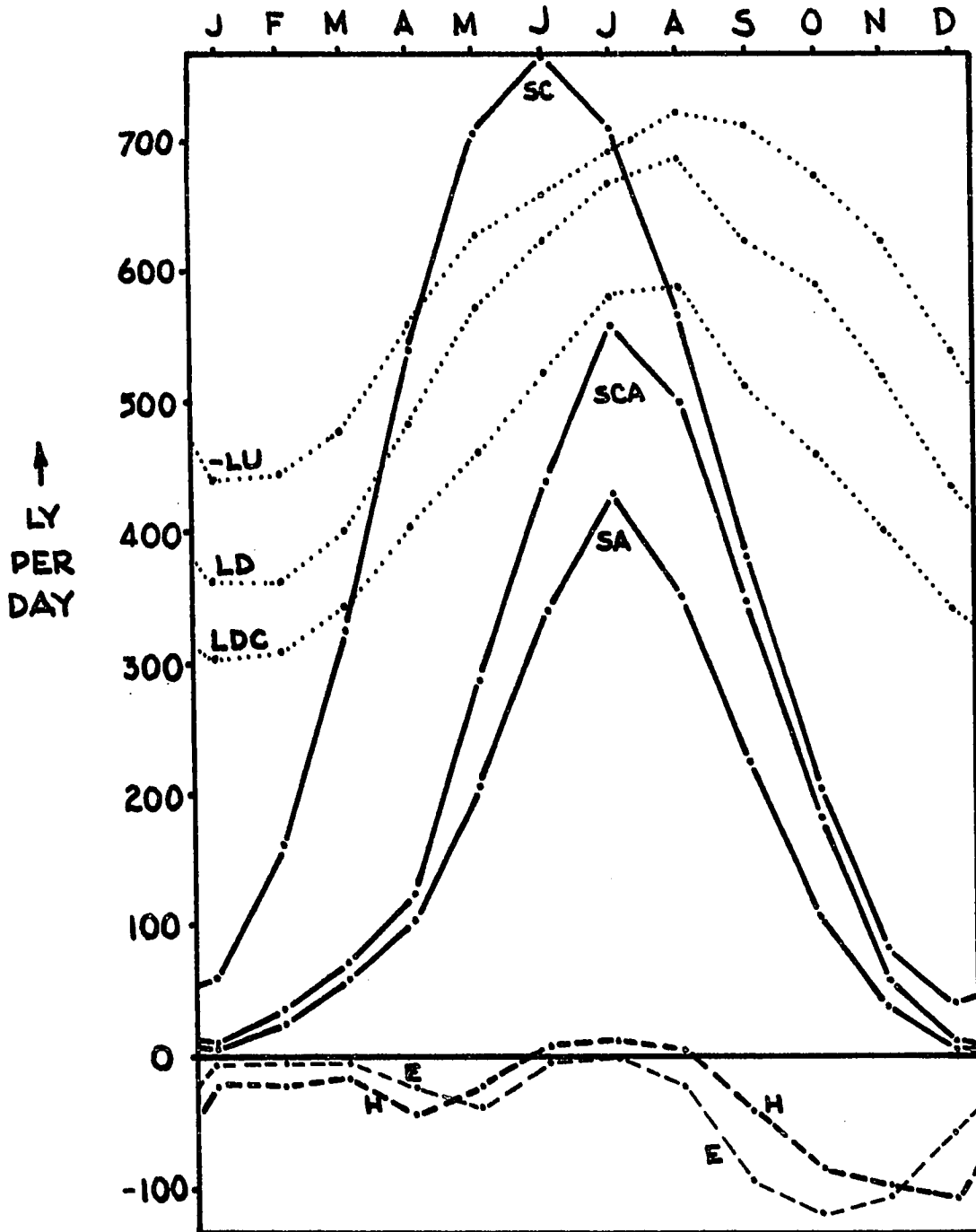


Fig. 6-8. Areal averages of heat budget components (I).

- SC: Incoming solar radiation under clear skies;
- SCA: Absorbed solar radiation under clear skies;
- SA: Absorbed solar radiation under normally cloudy skies;
- LU: Long wave radiation from surface (graphed in negative, for convenience);
- LDC: Clear sky downward atmospheric long wave flux;
- LD: Downward atmospheric longwave flux for normally cloudy skies;
- E: Evaporative flux;
- H: Sensible flux.

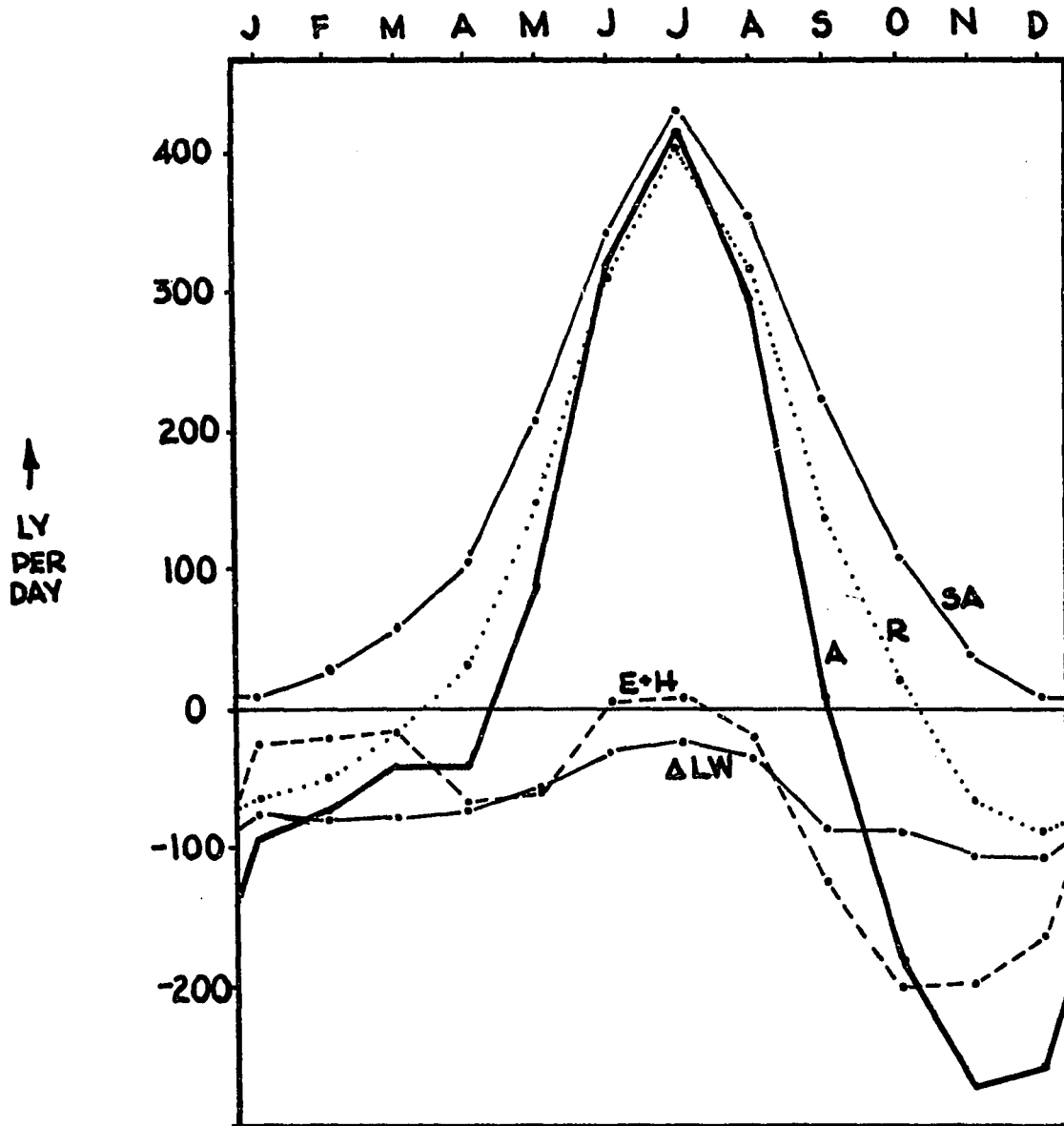


Fig. 6-9. Areal averages of heat budget components (II).

- SA: Absorbed solar radiation;
- LW: Long wave balance;
- R: Radiation balance;
- E+H: Evaporative plus sensible heat flux;
- A: The surface heat budget.

the occurrence of maximum absorbed solar energy in July rather than in June. In spite of the large amounts of energy lost by reflection and cloudiness, however, solar radiation income was seen (Section 6.6) to dominate the surface heat budget from May to August.

Long wave radiative fluxes upward (LU) and downward (LD and LDC) in Figure 6-8 are seen to be nearly mirror images of each other, whose sum is much smaller than either flux alone. The curves LDC and LD are atmospheric downward radiation under clear and normally cloudy skies, respectively. Clouds are seen to exert least influence in winter, most in May and June and autumn. Comparing LDC and LD with SCA and SA, it is seen that clouds act to improve the energy balance all months except July, August, and September. Annually, the overall effect of clouds is to increase the radiation budget by nearly 11,000 ly.

Figures 6-8 and 6-9 indicate that smallest annual long wave deficits ( $\Delta LW$ ) occur in June, July, and August, when the sea surface is colder than the overlying air. Greatest deficits appear in late autumn, when the water surface is much warmer than the air.

Evaporative (E) and sensible (H) heat fluxes are graphed in Figures 6-8 and 6-9. These fluxes are rather unimportant during the first eight months of the year (except perhaps briefly during April or May), but become highly significant from September through December. The evaporative heat loss reaches its greatest rate in October (Figure 6-8), whereas sensible heat flux is seen to be highest in December. The two-month difference appears because of saturation vapour pressure's exponential dependence on temperature; at low temperatures, vapour pressures

themselves are small, and large air-sea vapour pressure differences cannot occur. Sensible heat flux, however, is linearly dependent upon the air-sea temperature difference; hence the coldest month with large amounts of open water, December, shows the greatest sensible heat loss.

Curve A in Figure 6-9 represents the mean surface heat budget, the sum of (SA+LD+LU+E+H). The annual oscillation has been seen to be caused by spring and summer solar heating, and autumnal convective cooling. Although the budget is positive in only five months out of twelve, the large amplitude of the solar heating curve makes the annual budget positive.

Comparing the times of ice cover change (Figure 4-9, p. 96) with the times of greatest radiative and convective fluxes, it may be said that the radiation balance (especially the solar term) is the ice dissipating agent, whereas turbulent heat fluxes are responsible for ice formation. This conclusion is compatible with the nature of the processes involved; for surface radiative heat gain occurs independently of atmospheric stability conditions, while turbulent transfer is very sensitive to stability variations. As long as significant amounts of ice remain, the sea surface temperature will not rise above 0 degrees C during thaw. Thus stable atmospheric stratification is assured during the ice melt period. Convective heat transfer is small, and radiative heating must melt the ice. In autumn, the surface water is warm and slow to cool, so that instability is the rule, and convective transport operates efficiently.

These considerations are applicable to large water bodies in

general, and help to explain why spring break-up dates often show poor correlation with air temperature anomalies around break-up, whereas fall freeze-up dates can be predicted by formulae involving temperature departures from average. (For example, Hare (1950) states on p. 276 "...the date of closing of harbours is closely correlated with the course of daily mean temperature," but, on pp. 283-4, indicates the lack of a similar correlation for break-up time.) Springtime anomalies in cloudiness may have a much greater effect than the surface temperature variations on spring break-up dates.

The mean annual contribution by each heat budget term is shown in Figure 6-10. Solar energy absorption is seen to be the only positive term, averaging 161 ly per day. Over the year, evaporative and sensible heat losses combined approximately equal the long wave loss. Oceanic advection is small and negative.

Since mean storage change over the whole year was assumed to be zero (implying no year-to-year warming or cooling), the annual heat budget for Hudson Bay may be written

$$SA + LU + LD + H + E + O = 0, \quad (6-1)$$

where  $O$ , on the left hand side of the expression, is the oceanic advection term. Because each heat budget component was calculated independently of the others, and was subject to certain errors, Equation (6-1) cannot be expected to balance perfectly. In the present study, the sum of the fluxes amounts to +11.5 ly per day, or about 4200 ly per year. From Tables 2-4 through 2-8, and 4-1, the annual mean estimated error for the sum of the components was found to be  $\pm 45$  ly per day; thus the error is well within the expected error magnitude. The relative

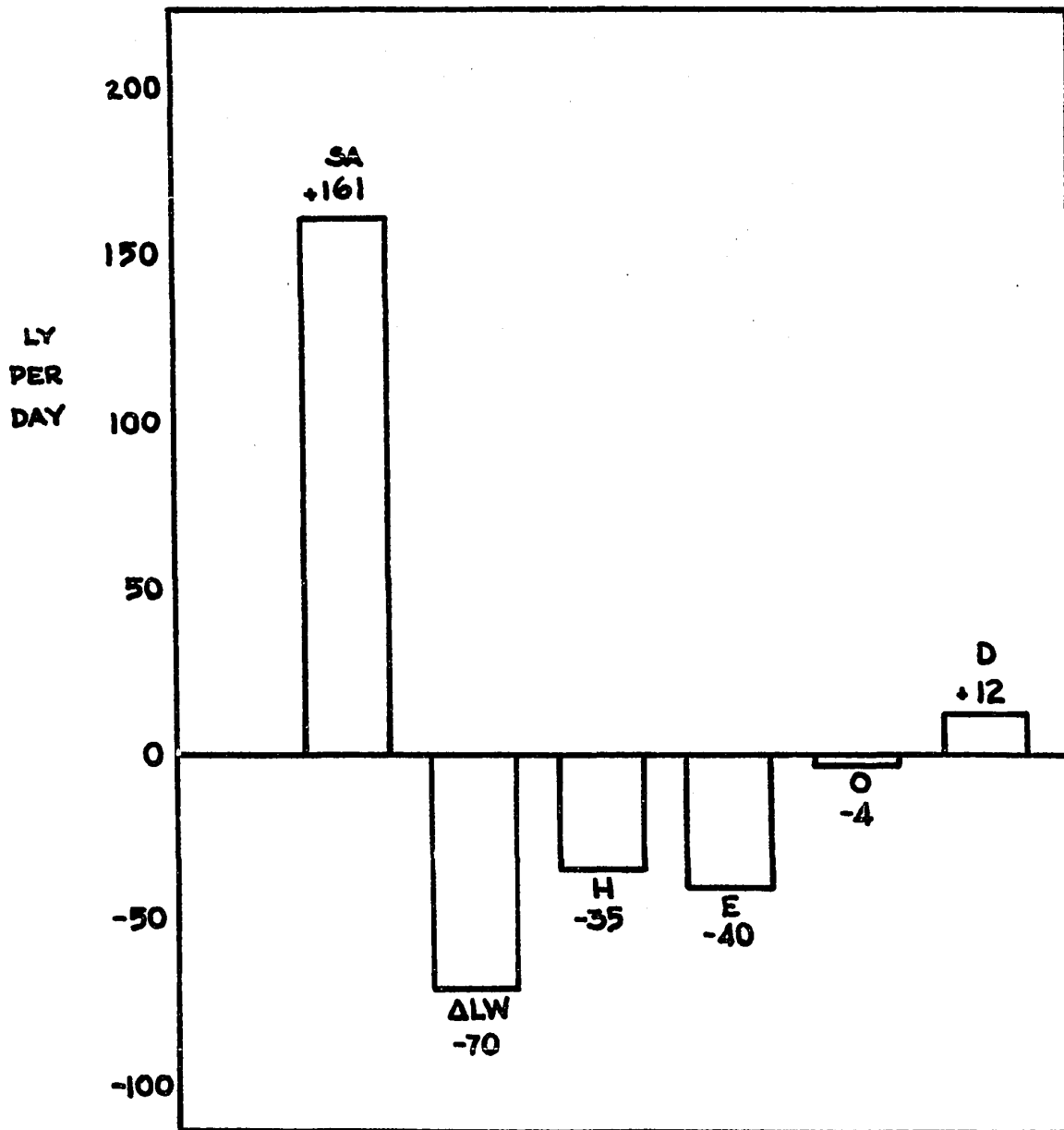


Fig. 6-10. Areal mean of annual heat budget components.

SA: Absorbed solar radiation;

LW: Long wave balance;

H: Sensible heat flux;

E: Evaporative flux;

O: Advection by water;

D: Difference (error) term.

magnitude of the discrepancy, labelled D, may be seen in Figure 6-10, where it is graphed along with the heat budget components.

Although D appears to be small in comparison with the heat budget fluxes, its very magnitude indicates it cannot be interpreted as a year-to-year storage change. An annual energy excess of 4200 ly implies an annual warming of 0.4 deg C throughout all of Hudson Bay, a rate far too large to go undetected for more than a few years. In fact, such a warming would require rather sudden adjustments in ice cover, air temperature, and heat flux distributions.

Integration of the area between the heat budget curve A and the zero line in Figure 6-9 gives computed storage and advective changes during the course of the year. In the following table, these calculations are compared with observations of storage and advective changes from Table 4-1, p. 101, for periods of heat storage gain (April to September) and loss (September to April).

TABLE 6-1

COMPUTED vs. OBSERVED VALUES OF HEAT STORAGE  
PLUS ADVECTION IN HUDSON BAY (IN LY).

PERIOD	APRIL-SEPT.	SEPT.-APRIL
COMPUTED CHANGE	+36,400±3600	-30,900±4300
OBSERVED CHANGE	+31,400±4100	-30,000±3600
COMPUTED MINUS OBSERVED:	+5000±6300	-900±5600

The agreement between calculated and observed figures is reasonably close; the difference in each case is less than the associated

error estimate. The discrepancy is much larger in the April to September period; as the estimated errors in these months are much higher for solar radiation than for long wave or convective fluxes (Tables 2-3 to 2-8) the short wave energy term is probably the major source of error.

#### 6.8 COMPARISON OF RESULTS WITH THOSE OF OTHER AUTHORS

Section 1.3 contained a brief summary of work by other authors on various aspects of Hudson Bay's heat budget. In the following pages their results are compared with those of the present work, in order to check the validity of the different methods and conclusions.

Burbidge (1949) studied transformations of air masses crossing Hudson Bay. For the months of November and December he determined mean modification figures which allow estimates of the energy fluxes involved. In November, he found that air mass modification (in the form of moistening and warming) took place to an average height of 6250 feet, or 785 mb. Mean surface temperature increased by 7 deg C, surface humidity by 1.0 gm/kg. The usual length of time for transformation was 24 hours.

From these data, it is possible to estimate associated heat fluxes. If the amount of modification decreases linearly with height to zero at 6250 feet (a convenient assumption, which is sufficiently accurate for an approximate calculation), then heat fluxes appearing as temperature rises in the atmosphere amount to 189 calories per  $\text{cm}^2$  column of air per day. This figure includes gains by

sensible heat flux, heat of condensation, and radiation. From Bryson and Kuhn (1962) the radiative flux divergence for such a column of air is 17 calories per day (negative). Therefore sensible heat flux plus condensation warm the column by 206 calories per day. Water vapour increase gives an additional heat gain (latent) of 67 calories per day, resulting in a mean total convective heat gain of 273 calories per  $\text{cm}^2$  column of air per day in November. Since the air under study crossed Hudson Bay generally in 24 hours, it may also be said that the mean surface convective heat loss along the trajectory was 273 ly per day.

This figure may be expected to be a sizeable overestimate of mean surface turbulent fluxes for all November days, for the following reason. To facilitate trajectory analysis, Burbidge selected for study those days with well-defined, generally vigorous circulation patterns. Periods with light or calm winds were avoided; at these times, however, turbulent heat exchange decreases, as air-sea property differences are diminished by the transfer itself and little advection of unmodified air occurs.

Comparison of the flux derived from Burbidge's data, 273 ly per day, with the mean November turbulent flux from the present study, 199 ly per day, shows the former value indeed exceeds the latter, by about 40%. On the basis of the above argument, however, the two fluxes appear to be compatible.

For December, Burbidge found a mean modification height of 3500 feet, a mean surface temperature rise of 8 deg C, and a mean

specific humidity increase of 0.6 gm/kg. The resulting convective heat gain is calculated to be 183 ly/day. This is greater by 12% than the corresponding mean December heat flux of 164 ly/day, from the present paper.

The diminishing difference (40% to 12%) between the two methods from November to December is understandable at least qualitatively. Burbidge studied trajectories which, for the most part, crossed central Hudson Bay. Greatest December turbulent heat loss (Figure 6-4) is concentrated in the southeastern regions, out of reach of trajectories across the central Bay. Thus data from Burbidge's trajectory studies give fluxes less in excess of the areal mean in December than in November.

In summary, the flux estimates based on Burbidge's modification figures seem consistent with those of the present study.

Bryson and Kuhn (1962) also studied air trajectories and modification. Part of their work concerned determination of monthly mean atmospheric heat budget values for a trajectory from Churchill to Port Harrison. Months studied were April, July, and December. The method followed was to find, from radiosonde observations, the change in mean atmospheric heat and moisture content from the starting point (Churchill) to the end point (Port Harrison); to subtract radiative flux divergence (determined from an Elsasser chart) from the heat gain, giving sensible heat flux; and to evaluate evaporative flux from water vapour increase.

Atmospheric heat budget components thus determined are

given in the following table, along with the mean monthly heat fluxes derived earlier in the present work.

TABLE 6-2

COMPARISON OF ATMOSPHERIC HEAT BUDGET FLUXES OF BRYSON AND KUHN (1962) WITH SURFACE FLUXES FROM FIGURE 6-9.  
Units: ly/ day, positive upward.

	APRIL		JULY		DECEMBER	
	Bryson & Kuhn	from Fig.6-9	Bryson & Kuhn	from Fig.6-9	Bryson & Kuhn	from Fig.6-9
Sensible heat flux H	- 48	+ 43	-140	- 9	+ 74	+104
Latent heat flux E	- 52	+ 26	-280	(0)	+ 23	+ 60
H + E	-100	+ 69	-420	(-9)	+ 97	+164

The method seems to suffer from several shortcomings. Churchill and Port Harrison are at very nearly the same latitude, and, as indicated in Chapter 5, mean wind flow over Hudson Bay is northwesterly at all times and altitudes. Consequently, a mean trajectory through Churchill passes well south of Port Harrison. As a result, positive modification (increase of temperature and moisture) from Churchill to Port Harrison is substantially underestimated, negative modification exaggerated, by the assumption that the two stations lie on the same trajectory.

Another difficulty lies in the method of partitioning latent and sensible heat fluxes. Surely some latent heat is released as recently evaporated moisture condenses, as evidenced, for instance, by heavy October to December snowfalls on eastern shores.

Assuming that the final temperature (minus radiative effects) and moisture profile changes faithfully reflect the true proportions of surface evaporative and sensible heat fluxes leads to an overestimate of sensible heat flux, at the expense of latent flux.

The two sets of figures in Table 6-2 are not directly comparable, due to the fact that changes along a single trajectory cannot be expected to give results the same as an areal mean. In April and July, however, the values from Bryson and Kuhn and those from Figure 6-9 are totally dissimilar and imply the inadequacy of one or the other method.

The main reason for this irreconcilability probably is the failure of mean trajectories to pass through both Churchill and Port Harrison, which, it was pointed out, exaggerates the amount of atmospheric heat loss. The April and July surface turbulent heat gains implied by Bryson and Kuhn's figures are of the same order of magnitude as the solar radiation fluxes for those months, and would cause a very large annual energy surplus. As they point out, their computed July turbulent heat fluxes alone are large enough to melt 1.5 m of ice. In Section 4.18 it was seen that 1.5 m represents the annual maximum ice thickness. It seems that these downward fluxes are too large.

Morrissey (1964) calculated the atmospheric moisture budget for January, April, July, and October, 1962, for a hexagonal region covering Hudson Bay. Making twice-daily evaluations of the geostrophic flux of moisture through the volume, he found a monthly

mean moisture divergence D (gm/month, >0 for convergence). In this fashion Morrissey determined the "total transport". By computing the flux from monthly means of wind and moisture he found the "time mean" flux; this subtracted from the total transport gave the "time eddy" flux. Assuming that vapor divergence resulting from cloud formation or dissipation within the volume is negligible, then

$$D = P - E \quad , \quad (6-2)$$

where P = precipitation (gm/month) and  
E = evaporation (gm/month).

Estimating P from monthly precipitation charts allowed evaporation to be determined from Morrissey's data and Equation 6-2. Converting evaporation mass to energy flux, the following results were obtained.

TABLE 6-3  
EVAPORATIVE FLUXES DERIVED FROM DATA OF MORRISSEY (1964)  
COMPARED WITH VALUES FROM FIGURE 6-9.  
(Units: ly/day)

	JANUARY	APRIL	JULY	OCTOBER
Evaporation for 1962, Based on data from Morrissey:	32	23	60	100
Evaporation from Fig. 6-9 :	6	26	0	119

Agreement with values computed in the present study appears to be satisfactory for April and October. The January discrep-

ancy may be explained by meteorological anomalies. From the Monthly Record, the November, 1961, mean surface air temperatures over Hudson Bay were found to be above normal; December temperatures were far above normal. As a result, considerable open water doubtless existed into January, 1962, allowing abnormally large amounts of evaporation in that month, before freeze-up.

July evaporation of 60 ly/day is more difficult to understand. Temperature and moisture anomalies for July, 1962, are not the cause. In the lowest layer (surface to 850 mb) Morrissey found the time mean flux to be zero, while the time eddy flux was negative. This suggests that evaporation in the rear of travelling cyclones (the "time eddies") exceeds precipitation from the lowest layer during cyclone passage. Thus evaporation appears when variance (eddies) about mean conditions is considered.

Evaporation may not be the only July moisture source. Some of the necessary moisture may come from convergence of liquid cloud droplets, which are undetectable in advection terms, but appear as precipitation. However, a good reason is lacking for such convergence in July; thus the explanation must be found elsewhere.

In summary, Morrissey's study provides reasonable confirmation of evaporative fluxes for January, April, and October. His July data suggest that variance considerations lead to negative heat fluxes from the Hudson Bay surface in summer months. A July evaporative heat flux of 60 ly/day would significantly reduce the

calculated annual energy excess of 4200 ly. Extended to June and August, and to sensible heat flux, which may be expected to be affected similarly by the inclusion of variance, the energy involved could conceivably amount to 4000 ly/year.

Schwerdtfeger (1962) recorded surface heat fluxes at a micrometeorological station on Button Bay, a portion of Hudson Bay near Churchill. His daily observations cover most of the period from late January to mid-April, 1961, and include measured radiative fluxes, conductive fluxes through the ice, and changes in ice thickness and temperature. Turbulent fluxes were based upon wind speed measurements at two levels, and calculated by Halstead's (1954) formulae.

Agreement between Schwerdtfeger's figures and those of the present study is satisfactory for the most part, in spite of the fact that Schwerdtfeger's data represent conditions for only a few days, which well may have differed from average conditions in any of several important respects.

Radiative fluxes in sum averaged about -30 ly/day in late February and mid-March, according to Schwerdtfeger; by early April, the radiation balance was approximately +30 ly/day. The present study gives radiative fluxes of -38 ly/day and -20 ly/day in late February and mid-March, becoming +25 ly/day by early April. These figures apply to the grid point closest to Button Bay.

Schwerdtfeger found sensible and latent heat fluxes to be small (generally <10 ly/day ) throughout his period of observation,

a result similar (disregarding fluxes from leads) to that computed in this study, for February and March. Figure 6-9, however, gives April convective losses of 30 ly/day for sensible and 16 ly/day for latent heat. Even subtracting the contribution from leads results in a figure considerably larger than Schwerdtfeger's. However, his April fluxes do not balance with observed heat storage changes in the ice; the discrepancy he attributes primarily to underestimation of turbulent heat flux by the Halstead equations, which neglect buoyant convection under calm winds.

Thus the overall correspondence between the fluxes of Schwerdtfeger and those of the present work seems acceptable.

Barber (1967), in the most comprehensive study of the subject to date, performed monthly heat budget computations for "the sea in the vicinity of Churchill for 1961" (quoted from the title).

Solar radiation was taken from Mateer (1955a) for clear skies, which was corrected to cloudy sky income by empirical formulae by Anderson (1954). Long wave radiation flux was also computed from an empirical formula of Anderson. Barber does not describe his method of arriving at evaporative flux, other than saying that it was calculated, but the Bowen ratio was employed to find sensible heat flux from evaporation.

Table 6-4, on the following page, gives Barber's fluxes, along with those for the grid point nearest to Churchill (59N, 93W) representing the calculations presented earlier in this study.

TABLE 6-4

MONTHLY ENERGY FLUXES FROM BARBER (1967, p.46)  
 COMPARED WITH MONTHLY MEAN FLUXES FROM FIGURES 6-1 THROUGH 6-5,  
 FOR GRID POINT AT 59N, 93W.  
 Units: ly/day (lines a. and b.), and fluxes at 59N 93W as a % of those  
 of Barber.

	JAN	FEB	MAR	APR	MAY	JUN	JUL	AUG	SEP	OCT	NOV	DEC	
<u>ABSORBED</u>													
<u>SOLAR RAD.</u>													
a. 59N 93W :	11	30	62	103	190	346	428	367	228	106	25	6	ly
b. Barber :	20	42	64	116	256	306	409	326	199	102	26	9	ly
(a./b.)×100:	55	71	97	89	74	113	104	112	114	104	96	67	%
<u>LONG WAVE</u>													
<u>BALANCE</u>													
a. 59N 93W :	-72	-75	-82	-72	-62	-27	-21	-33	-83	-76	-79	-74	ly
b. Barber :	-87	-96	-93	-103	-112	-122	-100	-80	-77	-116	-166	-77	ly
(a./b.)×100:	83	77	88	70	55	22	21	24	107	66	48	96	%
<u>RADIATION</u>													
<u>BALANCE</u>													
a. 59N 93W :	-61	-45	-20	33	128	319	408	333	145	30	-54	-68	ly
b. Barber :	-87	-54	-30	13	144	185	309	246	182	-14	-140	-68	ly
(a./b.)×100:	70	83	67	253	89	172	132	135	77	--	39	100	%
<u>EVAPORATIVE</u>													
<u>FLUX</u>													
a. 59N 93W :	-5	-5	-4	-16	-64	0	0	0	-86	-109	-58	-19	ly
b. Barber :	-4	-7	-10	-12	-28	-20	-23	-62	-74	-90	-99	-6	ly
(a./b.)×100:	120	72	40	125	228	0	0	0	116	121	58	317	%
<u>SENSIBLE</u>													
<u>HEAT FLUX</u>													
a. 59N 93W :	-20	-19	-14	-30	-31	11	11	8	-12	-82	-95	-23	ly
b. Barber :	0	0	0	0	-6	-7	16	-19	-24	-112	-189	0	ly
(a./b.)×100:	--	--	--	--	517	--	69	--	50	73	50	--	%
<u>BUDGET:</u>													
<u>SUM OF FLUXES</u>													
a. 59N 93W :	-89	-69	-38	-43	33	331	418	341	52	-161	-208	-109	ly
b. Barber :	-90	-78	-51	-11	109	157	302	165	24	-216	-428	-89	ly
(a./b.)×100:	99	89	75	391	30	211	138	207	216	74	49	123	%
<u>ANNUAL TOTAL:</u>													
a. 59N 93W :	+14,500 ly												
b. Barber :	- 715 ly												

Solar radiation figures show fair correspondence. Systematic percentage variations between the two studies indicate the same seasonal dichotomy (percentages less than 100 in winter, greater in summer) as the figures in Table 2-2; this is to be expected since Barber's values are based on Mateer's, which are based on the same Churchill observations as those in Table 2-2. Annually, solar income at 59N 93W is 1800 ly more than Barber's figure, a relatively minor difference. It must be remembered that Barber's study applies to only a single year, so that in general, exact numerical agreement between the two studies is not to be expected.

Long wave radiation shows the poorest correspondence of fluxes. Barber's heat losses are considerably higher in all but the winter months and September. The large heat losses from May through August are difficult to believe, as the sea surface is colder than the air in these months, and cloud cover is great. The unreasonably high fluxes perhaps indicate that Anderson's empirical formula for Lake Hefner, Oklahoma, is not applicable to conditions over Hudson Bay. The formula involves only surface air properties, thus tacitly assuming some certain temperature and moisture profiles, and stability. With radical departures from near-neutral conditions, as during late spring and autumn over Hudson Bay, the resulting long wave flux calculations will likely be in error. Indeed, these times of year show the greatest departures from the values at 59N 93 W, which were computed as separate upward and downward fluxes. Annually, the difference between Barber's long wave calculations and those for

59N 93W amounts to about 14,000 ly.

Turbulent heat fluxes show very poor percentage agreement, but actual energy discrepancies are small in most months. The greatest differences occur in November, when Barber's computations indicate much higher heat loss. How much of the differences can be ascribed to conditions peculiar to 1961 is not known. Over the year, convective heat loss at 59N 93W is 3300 ly less than in Barber's computation.

The annual sum of all heat budget terms gives a heat gain of 14,500 ly at 59N 93W, while Barber's calculations yield a heat loss of 715 ly per year. As was seen, by far the major part of this difference arises from long wave discrepancies, which are significant to the point of indicating the non-validity of one method or the other. Other terms show a fair correspondence, and in this respect serve as an effective reminder that the computed fluxes are estimates only. This reminder applies to all of the results presented in this section.

## 6.9 SUMMARY OF RESULTS

The charts, figures and discussions presented throughout this chapter are themselves the result of this study, and further numerical or graphical summarization would seem to be of no special value. However, a descriptive summary of the main results and their implications may be useful for reference.

Winter heat fluxes are small, dominated by the long wave radiation loss. Turbulent heat fluxes are near zero except over leads, where they are very large.

During April and May, solar radiation income increases sharply, in spite of the high albedo of the ice surface. Initially, solar heating gains are nullified to large extent by increased turbulent transfer. As the surface approaches the melting point, however, turbulent transfer decreases to nearly zero.

Solar radiation dominates the heat budget from May through August, although the high surface albedo sharply restricts total income. Long wave heat loss is at a minimum at this time due to the occurrence of warm air over the ice and cold water surface. Near-surface air is hydrostatically stable, keeping turbulent transfer to a minimum through these months. High concentrations of ice in the southwest are responsible for a minimum of energy absorbed there. Total income is more than enough, however, to melt the entire ice pack.

September sees the appearance of the autumnal heat budget characteristics. Solar heating has begun to be much less important, in spite of low albedo everywhere. Long wave and turbulent heat losses become dominant. The convective fluxes can be said to remove summer heat from Hudson Bay, and force ice formation. Rather earlier freeze-up in western waters results in smaller convective heat losses there. By January, the Bay is frozen once more; long wave losses continue through the winter, allowing ice to reach its greatest thickness

in April. The amplitude of the seasonal variations in heat storage is remarkably large, amounting to 30,000 ly from the April minimum to the September maximum.

Annually, Hudson Bay receives a slight surplus of heat from above the surface, which must be removed by currents. Greatest annual heat surpluses appear in western waters, while deficits are the rule in the east. Local non-balances must be corrected by heat advection within and across the boundaries. Solar radiation constitutes the only mean annual heat gain; all other fluxes (long wave balance, turbulent and advective) remove heat from Hudson Bay waters.

Work by others on different aspects of Hudson Bay's heat budget for the most part is not at variance with these results.

Perhaps the most general conclusion of the present study concerns the central role of ice cover in the heat budget computations. The nature of the surface affects heat fluxes in two basic ways:

(1) Thermal diffusivity is much lower for ice than for water or air. As a result, ice acts as an insulator whose upper surface becomes nearly equal to the surface air temperature. Water distributes surface heat gains or losses to depth more efficiently, allowing the water surface temperature to be more representative of the water below than of the air above. Because the long wave radiation balance, the evaporative flux, and the sensible heat flux all depend on the magnitude of air-interface differences, the state of

the surface is critically important.

(2) The albedoes of ice (or snow-covered ice) and water are very different. Albedo differences were seen to be the greatest contributors to space and time variations of solar energy absorption during the spring and summer months.

These physical characteristics of ice and water, it has been seen, make the nature of the surface by far the most important variable for heat budget computations over Hudson Bay.

No object or physical condition acts solely as an influence, unaffected by external events. So it is with ice cover; its presence or absence is the result of earlier processes, which were affected, but not completely controlled, by the state of the surface at those earlier times. Thus to say that all surface heat fluxes ultimately are determined by the nature of the surface is a great oversimplification.

On the other hand, some parameters certainly may be recognized as being much more influential than others. In this respect, the evidence presented in this study indicates that the state of the surface is the most critical and basic hydrometeorological variable affecting Hudson Bay's surface heat budget.

## CHAPTER 7

### CONCLUSION

In preceeding chapters, monthly mean hydrometeorological data were presented. This information, processed by the methods described in Chapter 2, gave estimates of monthly mean heat budget components for the Hudson Bay surface.

The computed annual mean budget showed a reasonably close balance. Flux distributions were seen to be compatible with attendant hydrometeorological conditions: patterns of temperature, moisture, ice cover, cloudiness, stability, and radiative and turbulent fluxes were mutually consistent. In addition, flux rates generally agreed acceptably with calculations by other authors. All of these facts tend to confirm the general validity of the methods and results of Chapters 1-6. Thus the present study is believed to be a fair representation of Hudson Bay's surface and near-surface climatology in large scale.

As has been mentioned, this work has dealt with only the gross aspects of Hudson Bay's heat budget. Although the study appears to have yielded a number of interesting results, surely a myriad of details have escaped discovery. To add detail to the broad outline presented here, the first logical step would seem to require repeating the analysis on shorter scales of space and time, following the widely held belief that an increasingly dense network of local observations and calculations is the key to extending knowledge of regional

conditions. Accordingly, the density of the observation network always looms as the barrier to greater understanding.

Over Hudson Bay, observations are so sparse that the present study probably represents the practical limit to large-scale analysis of regional variations. Thus the observational barrier mentioned above has already been reached. It is by no means necessary, however, to suspend study of the region for what probably will be the very long time until general data coverage of Hudson Bay improves. By choosing an appropriate "degenerate observational network" of one or a few stations, each with detailed data records, many small-scale features doubtless will come to light. The studies of Burbidge, Bryson and Kuhn, Morrissey, Schwerdtfeger, and Barber discussed in Section 6.8 are but a few examples of alternative methods for more detailed exploration of Hudson Bay's geophysics. It is hoped that the present work may be useful as a first estimate, a large-scale description of surface conditions and fluxes, for general reference.

## BIBLIOGRAPHY

- Anderson, E.R., 1954: "Energy Budget Studies." Water-Loss Investigation: Lake Hefner Studies. U.S. Geol. Survey, Prof. Papers, 269, pp. 71-119.
- Arctic Meteorology Research Group, 1960: Temperature and Wind Frequency Tables for North America and Greenland, Vol. I and II. Pubs. in Met., No. 24 and 25, McGill Univ., Montreal. 275 pp.
- Barber, F.G., 1967: A Contribution to the Oceanography of Hudson Bay. Manuscript Report Series No. 4, Marine Sciences Branch, Dept. of Energy, Mines and Resources. Ottawa. 69pp.
- Barber, F.G., and C.J. Glennie, 1964: On the Oceanography of Hudson Bay, an Atlas Presentation of Data Obtained in 1961. Manuscript Report Series No. 1, Marine Sciences Branch, Dept. of Mines and Tech. Surveys. Ottawa. 10pp. + 88 pp. maps and figures.
- Barry, R.G., 1966: "Meteorological Aspects of the Glacial History of Labrador-Ungava With Special Reference to Atmospheric Water Vapour Transport." Geogr. Bull. Vol. 8, No.4. pp. 319-40.
- Beaton, A.P., and W.E. Markham, 1964: Ice Summary for Hudson Bay, Hudson Strait and Adjacent Waters, May-Oct. 1963. Met. Branch, Dept. of Transport, CIR 4088, Toronto.
- Bennett, P.M., 1940: "The British- Canadian Arctic Expedition." Geogr. J. Vol. 95, pp.109-120.
- Binney, Sir George, 1929: "Hudson Bay in 1928." Geogr. J. Vol. 74, pp. 1-27.
- Birkit-Smith, K., 1931: "Geographical Notes on the Barren Lands." Report of the 5th Thule Expedition, 1921-24, Vol.1, No. 4. Copenhagen.
- Bryson, R.A., and P.M. Kuhn, 1962: "Some Regional Heat Budget Values for Northern Canada." Geogr. Bull. Vol. 17, pp. 57-65.
- Budyko, M.I., 1956: The Heat Balance of the Earth's Surface. (Translated from Russian by N.A. Stepanova.) U.S. Dept. of Commerce, Washington, D.C. 259 pp.

- Burbidge, F.E., 1949: The Modification of Polar Continental Air over Hudson Bay. Unpub. M. Sc. Thesis, McGill Univ., Montreal. 253pp.
- Campbell, N.J., 1958: The Oceanography of Hudson Strait. Canada, Fisheries Research Board. Manuscript Report Series, Oceanographic and Limnological, No. 12. Ottawa. 60 pp. and figures.
- , 1959: Some Oceanographic Features of Northern Hudson Bay, Foxe Channel, and Hudson Strait. Canada, Fisheries Research Board, Manuscript Report Series, Oceanographic and Limnological. No. 46. Ottawa. 29 pp.
- Canada, Dept. of Transport, 1930-1961: Navigation Conditions on the Hudson Bay Route. (Published by the Dept. of Marine until 1936.) Toronto.
- Canada, Geographical Branch, Dept. of Mines and Tech. Surveys, 1957: Atlas of Canada. Ottawa.
- Canada, Hydrographic Service, 1965: Labrador and Hudson Bay Pilot. Marine Sciences Branch, Dept. of Mines and Tech. Surveys. Ottawa. 552 pp.
- Canada, Meteorological Branch, Dept. of Transport, 1942-1966: Monthly Record. Toronto.
- , 1946-1961: General Summaries of Hourly Weather Observations in Canada. Toronto.
- , 1947, 1956, 1959: Climatic Summaries for Selected Meteorological Stations in Canada. Toronto.
- , 1957-1963: Aerial Ice Observing and Reconnaissance. The Hudson Bay Route. Circulars 3254, 3569, 3710, 3896, 3951, 4432, 4509. Toronto.
- , 1966, and 1967: Ice Summary and Analysis, 1964 and 1965. Hudson Bay and Approaches. Toronto.
- , 1958-1965: Ice Thickness Data for Selected Canadian Stations. Circulars 3537, 3711, 3918, 4153, 4372, 4529. Toronto.
- , 1960-1967: Monthly Radiation Summary. Toronto.

- Canadian Oceanographic Data Center, 1964: 1964 Data Record Series, No. 1 and No. 12. Hudson Bay Project-1961. Ottawa.
- , 1966: 1966 Data Record Series, No. 4. Arctic, Hudson Bay and Hudson Strait. Ottawa.
- Cavadias, G.S., 1961: "Evaporation Applications In Watershed Yield Determination." Proc. of Hydrology Symp. No. 2. Evaporation. Dept. of Northern Affairs and Natural Resources, Water Resources Branch. The Queen's Printer. Ottawa. pp.170-178.
- Collin, A.E., 1966: "Hudson Bay and Approaches." The Encyclopedia of Oceanography, Reinhold Publ. Co., New York. pp. 357-59.
- Craddock, J.M., 1951: "The Warming of Arctic Airmasses over the Eastern North Atlantic." Quart. J., Royal Met. Soc., Vol. 77, pp. 355-64.
- Derecki, J.A., 1964: Variation of Lake Erie Evaporation and its Causes. Pub. No. 11, Great Lakes Research Division, Univ. of Michigan, Ann Arbor. pp. 217-77.
- Deutscher Wetterdienst, 1958-1967: Täglicher Wetterbericht. Offenbach.
- Donovan, F.P., 1957: A Preliminary Report on Ice Conditions on Salt and Fresh Water Bodies in the Vicinity of Fort Churchill. Canada, Defense Research Northern Laboratory. Tech. Mem. No. 1/57. 3pp. and figures and maps.
- Dunbar, M.J., 1951: Eastern Arctic Waters. Bulletin No. 88, Fisheries Research Board of Canada. Ottawa. 131 pp.
- , 1958: Physical Oceanographic Results of the "Calanus" Expeditions, 1949-1955. J. of Fisheries Research Board of Canada, Vol. 15(2). pp. 155-201.
- , 1959: Fisheries Research Board Manuscript Report Series, Oceanographic and Limnological, No. 56. Ottawa.
- , 1966: "The Sea Waters Surrounding the Quebec-Labrador Peninsula." Cahiers de Geogr. de Que., Vol. 10, No. 19, pp. 13-35.
- Dunbar, Moira, 1954: "The Pattern of Ice Distribution in Canadian Arctic Seas." Royal Soc. of Canada Transactions, Third Series, Vol. 48, Oceanographic Session, pp. 9-18.

- Flaherty, R.J., 1918: "The Belcher Islands of Hudson Bay." Geogr. Rev.  
Vol. 5, June 1918, pp. 433-58.
- Fletcher, J.O., 1955: The Heat Budget of the Arctic Ocean and its  
Relation to Climate. The Rand Corp. Santa Monica. 179 pp.
- Forward, C.N., 1956: "Sea Ice Conditions Along the Hudson Bay Route."  
Geogr. Bull. Vol. 8, pp. 22-50.
- Fritz, S. 1949: "Average Solar Radiation in the United States."  
Heating and Ventil. Vol. 46, No. 7, pp. 61-64.
- Gagnon, R.M., 1964: Types of Winter Energy Budgets Over the Norwegian  
Sea. Publ. in Met. No. 64, McGill Univ., Montreal. 56 pp.
- Grainger, E.H., 1960: Some Physical Oceanographic Features of South-  
east Hudson Bay and James Bay. Canada, Fisheries  
Research Board. Manuscript Report Series, Oceanographic  
and Limnological, No. 71. 40 pp.
- Hachey, H.B., 1935: "The Circulation of Hudson Bay Waters as Indicated  
by Drift Bottles." Science, Sept. 20, 1935. Vol. 82,  
No. 2125. pp. 275-76.
- , 1954: "The Hydrology of Hudson Bay." Royal Soc. of Canada  
Transactions, Third Series, Vol. 48, Oceanographic  
Session, pp. 19-23.
- Halstead, M.H., 1954: The Fluxes of Momentum, Heat and Water Vapour  
in Micrometeorology. Johns Hopkins Univ. Pub. in  
Climatology VII, No. 2.
- Hanson, W.J., 1949: Ice Conditions and Other Factors Relating to the  
Opening and Closing of Navigation on the Hudson Bay Route.  
Regina.
- Hare, F.K., 1950: The Climate of the East Canadian Arctic and Sub-  
Arctic, and its Influence on Accessibility. Unpub.  
Ph.D. Thesis, Universite de Montreal. 440 pp.
- , 1951: "Some Climatological Problems of the Arctic and  
Sub-Arctic." Compendium of Meteorology, (T. Malone,  
ed.) Amer. Met. Soc. Boston, Mass. pp. 953-64.
- , 1966: "Recent Climatological Research in Labrador-Ungava."  
Cahiers de Geogr. de Que. Vol. 10, No. 19. pp. 5-12.

- , and M.R. Montgomery, 1949: "Ice, Open Water, and Winter Climate in the Eastern Arctic of North America." Arctic, Vol. 2, pp. 79-89, pp. 149-164.
- , and S. Orvig, 1958: The Arctic Circulation. Pub. in Met. No. 12, McGill Univ., Montreal. 211 pp.
- Houghton, H.G., 1954: "On the Annual Heat Balance of the Northern Hemisphere." J. Met., Vol. 11, pp. 3-9.
- Jacobs, W.C., 1951: "Large Scale Aspects of Energy Transformation over the Oceans." Compendium of Meteorology (T. Malone, ed.), Amer. Met. Soc., Boston, Mass. pp. 1057-70.
- Johnson, C.B., 1948: "Anticyclogenesis in Eastern Canada During Spring." Amer. Met. Soc. Bull., Vol. 29, pp. 47-55.
- Kendrew, W.G., and B.W. Currie, 1955: The Climate of Central Canada. The Queen's Printer, Ottawa. 194 pp.
- Kniskern, F.E., and G.J. Potocsky, 1965: Frost Degree Day, Related Ice Thickness Curves, and Harbor Freezep and Breakup Days for Selected Canadian Stations. U.S. Naval Hydro. Office Tech. Report, July 1965. 123 pp.
- Kraus, E.B., and R.E. Morrison, 1966: "Local Interactions Between the Sea and the Air at Monthly and Annual Time Scales." Quart. J., Royal Met. Soc., Vol. 92(391), pp. 114-27.
- Lambert, R.S., 1963: Mutiny in the Bay. Macmillan. Toronto. 160 pp.
- Lamont, A.H., 1948: Ice Observation Flight over Hudson Bay. Met. Div., Dept. of Transport, Toronto.
- , 1949: "Ice Conditions over Hudson Bay and Related Weather Phenomena." Amer. Met. Soc. Bull., Vol. 30, pp. 288-89.
- Larsson, P. and S. Orvig, 1962: Albedo of Arctic Surfaces. Pub. in Met. No. 54, McGill Univ., Montreal. 42pp.
- Leahey, D.M., 1966: Heat Exchange and Sea Ice Growth in Arctic Canada. Pub. in Met. No. 82, McGill Univ., Montreal. 48 pp.
- London, J., 1957: A Study of the Atmospheric Heat Balance. AFCRC, Project No. 131, AFCRC-TR-57-287. New York Univ.
- McFadden, J.D., 1965: The Interrelationship of Lake Ice and Climate in Central Canada. Dept. of Met., Univ. of Wisconsin, Tech. Report No. 20. 120 pp.

- MacKay, D.K., 1966: "Characteristics of River Discharge and Runoff in Canada." Geogr. Bull. Vol. 8, No. 3, pp. 219-227.
- , and J.R. MacKay, 1965: "Historical Records of Freeze-up and Break-up of the Churchill and Hayes Rivers." Geogr. Bull. Vol. 7, No. 1, pp. 7-16.
- MacKay, G.A., 1952: "The Effect of Protracted Spring Thaws on Ice Conditions in Hudson Bay." Amer. Met. Soc. Bull., Vol. 33, pp. 101-06.
- Malkus, J.S., 1962: "Large Scale Interactions." The Sea (Hill, M.N., ed.), Vol. 1. Interscience. pp. 88-294.
- Manning, T.H., 1943: "The Foxe Basin Coasts of Baffin Island." Geog. J., Vol. 101, p. 228.
- , ca. 1950: Coast 1. South Coast of Hudson Bay. Arctic Institute of North America - Defense Research Board Project Report 5. Unpub.
- Markham, W.E., 1962: Summer Break-up Patterns in the Canadian Arctic. Met. Branch., Dept. of Trans., CIR-3586, TEC-389. Toronto. 8 pp.
- , and R.H.W. Hill, 1962: Sea Ice Distribution in Canadian Arctic Waters: Summer, 1962. Met. Branch, Dept. of Trans., CIR-3824, TEC-463. Toronto. 12 pp. and maps.
- Mateer, C.L., 1955a: "Average Insolation in Canada during Cloudless Days." Canad. J. Tech., Vol. 33, pp. 12-32.
- , 1955b: "A Preliminary Estimate of Average Insolation in Canada." Canad. J. Agr. Sci., Vol. 35, pp. 579-94.
- Matheson, K., 1967: The Meteorological Effect of Ice in the Gulf of St. Lawrence. Pub. in Met. No. 89, McGill Univ., Montreal. 110 pp.
- Mathiasson, T., 1931: "Contribution to the Physiography of Southampton Island." Report of the 5th Thule Expedition, 1921-24, Vol. 1, No. 2. Copenhagen.
- Merrill, G.C., 1949: Ice Reconnaissance of Hudson Bay. Unpub. Manuscript, at Arctic Institute of North America.

- Montgomery, M.R., 1950: "Ice Reconnaissance Flights over Hudson Bay." Arctic Circular, Vol. III, No. 4, pp. 40-46.
- Morrissey, E.G., 1964: A Geostrophic Atmospheric Moisture Budget for Hudson Bay. Met. Branch, Dept. of Trans. CIR-4159, TEC-545. Toronto. 14 pp.
- , 1965: Ocean-Atmosphere Heat Exchange at Station Bravo. Met. Branch, Dept. of Trans. CIR-4301, TEC-579. Toronto. 10 pp.
- Munn, H.T., 1919: "Southampton Island." Geogr. J., Vol. 44, pp. 52-3.
- Munn, R.E., 1966: Descriptive Micrometeorology. Academic Press. New York. 245 pp.
- Potter, J.G. 1965: Snow Cover. Met. Branch, Dept. of Trans., Climatological Studies, No. 3. CIR-4232. Toronto. 25 pp.
- Pounder, E.R., 1965: Physics of Ice. Pergamon Press. London. 151 pp.
- Rae, R.W., 1951: Climate of the Canadian Arctic Archipelago. Met. Branch, Dept. of Trans. Toronto. 90 pp.
- Robinson (ed.), 1966: Solar Radiation. Elsevier Pub. Co., New York.
- Rodgers, C.D., and C.D. Walshaw, 1966: "The Computation of Infrared Cooling Rate in Planetary Atmospheres." Quart. J., Royal Met. Soc., Vol. 92, No. 391. pp. 67-92.
- Schwerdtfeger, P., 1962: Energy Exchange Through an Annual Sea Ice Cover. Unpub. Ph.D. Thesis, McGill Univ., Montreal. 144 pp.
- , 1963: "The Thermal Properties of Sea Ice." J. of Glac. Vol. 4, No. 36, Oct. 1963, pp. 789-807.
- Sellers, W.D., 1965: Physical Climatology. Univ. of Chicago Press. 272 pp.
- Sheppard, P.A., H. Charnock, and J.R.D. Francis, 1952: "Observations of the Westerlies over the Sea." Quart. J., Royal Met. Soc., Vol. 78, pp. 563-82.
- Shuleikin, V.V., 1957: "Molecular Physics of the Sea." Physics of the Sea. Part VIII, pp. 727-86. (U.S.H.O. translation, Washington, D.C., 1957). (Quoted in Vowinckel and Taylor, 1965.)

- Sverdrup, H.U., 1951: "Evaporation from the Oceans." Compendium of Meteorology (T. Malone, ed.), Amer. Met. Soc., Boston, Mass. pp. 1071-1081.
- , M.W. Johnson, and R.H. Fleming, 1942: The Oceans. Prentice-Hall, Inc., Englewood Cliffs, N.J. 1087 pp.
- Thompson, H.A., 1965: The Climate of the Canadian Arctic. Met. Branch, Dept. of Trans., Toronto. 32 pp.
- Titus, R.L., 1965: Upper Air Climate of Canada. Average, Extreme and Standard Deviation Values 1951-1960. Met. Branch, Dept. of Trans., No. T56-2760. Toronto. 70 pp.
- , 1967: Upper Air Climate of Canada. Charts of Monthly Geopotential, Temperature and Humidity 1951-1960. Met. Branch, Dept. of Trans., No. T56-2960. Toronto. 103 pp.
- U.S. Weather Bureau, Dept. of Commerce, 1958-1967: Daily Series, Synoptic Weather Maps. Part I. Washington, D.C.
- , 1959, 1965: World Weather Records 1941-1950, 1951-1960. Washington, D.C.
- U.S. Hydrographic Office, 1946: Sailing Directions for Northern Canada. H.O. 77. Washington, D.C.
- U.S. Navy, 1963: Marine Climatic Atlas of the World. Vol. VI. Washington, D.C.
- Untersteiner, N., 1964: "A Nomograph for Determining Heat Storage in Sea Ice." J. of Glac., Vol. 5, No. 39. Oct. 1964. p. 352.
- Vowinckel, E., 1965: The Energy Balance over the North Atlantic - January, 1963. Part I. Energy Loss at the Surface. Pub. in Met. No. 78, McGill Univ., Montreal. 34 pp.
- , 1967: Evaporation on the Canadian Prairies. Pub. in Met. No. 88, McGill Univ., Montreal. 21 pp. and maps and figs.
- , and S. Orvig, 1962: "Relation Between Solar Radiation Income and Cloud Type in the Arctic." J. Appl. Met., Vol. 1, No. 4. pp. 552-59.

- , and -----, 1964a: "Energy Balance of the Arctic. Incoming and Absorbed Solar Radiation at the Ground in the Arctic." Arkiv Met. Geoph. Biokl. Bd. 13, pp. 352-77.
- , and -----, 1964b: "Energy Balance of the Arctic. Long Wave Radiation and Total Radiation Balance at the Surface in the Arctic." Arkiv Met. Geoph. Biokl. Bd. 13, pp. 451-79.
- , and -----, 1964c: "Energy Balance of the Arctic. Radiation Balance of the Troposphere and of the Earth-Atmosphere System in the Arctic." Arkiv Met. Geoph. Biokl. Bd. 13, pp. 480-502.
- , and -----, 1966: "Energy Balance of the Arctic. The Heat Budget over the Arctic Ocean." Arkiv Met. Geoph. Biokl. Bd. 14, pp. 303-25.
- , and -----, 1967: "Climate Change over the Polar Ocean. I. The Radiation Budget." Arkiv Met. Geoph. Biokl. Bd. 15, pp. 1-23.
- , and B. Taylor, 1965: "Energy Balance of the Arctic. Evaporation and Sensible Heat Flux over the Arctic Ocean." Arkiv Met. Geoph. Biokl. Bd. 14, pp. 36-52.
- Wakeham, W., 1898: Report of the Expedition to Hudson Bay in the S.S. Diana. L.E. Dawson. Ottawa.
- Walmsley, J.L., 1966: Ice Cover and Surface Heat Fluxes in Baffin Bay. Pub. in Met. No. 84, McGill Univ., Montreal. 94 pp.
- Weaver, J.C., (Unpub.): "The Ice of Seas in the North American Arctic." Encyclopedia Arctica. Vol. 7 part 12. Copy at Arctic Institute of North America.
- Wendland, W.M., and R.A. Bryson, 1966: Aerial Survey of Hudson Bay Surface Temperature-1965. Tech. Report No. 28, Dept. of Met., Univ. of Wisconsin. 30 pp.
- , and -----, 1967: Aerial Surveys of Hudson Bay Surface Temperature-1967. Tech. Report No. 36, Dept. of Met., Univ. of Wisconsin. 20 pp.